
[All ETDs from UAB](#)

[UAB Theses & Dissertations](#)

1982

Characterization Of The Insulin Receptor In Isolated Bovine Cerebral And Retinal Microvessels.

Joyce Fehl Haskell
University of Alabama at Birmingham

Follow this and additional works at: <https://digitalcommons.library.uab.edu/etd-collection>

Recommended Citation

Haskell, Joyce Fehl, "Characterization Of The Insulin Receptor In Isolated Bovine Cerebral And Retinal Microvessels." (1982). *All ETDs from UAB*. 4158.
<https://digitalcommons.library.uab.edu/etd-collection/4158>

This content has been accepted for inclusion by an authorized administrator of the UAB Digital Commons, and is provided as a free open access item. All inquiries regarding this item or the UAB Digital Commons should be directed to the [UAB Libraries Office of Scholarly Communication](#).

INFORMATION TO USERS

This reproduction was made from a copy of a document sent to us for microfilming. While the most advanced technology has been used to photograph and reproduce this document, the quality of the reproduction is heavily dependent upon the quality of the material submitted.

The following explanation of techniques is provided to help clarify markings or notations which may appear on this reproduction.

1. The sign or "target" for pages apparently lacking from the document photographed is "Missing Page(s)". If it was possible to obtain the missing page(s) or section, they are spliced into the film along with adjacent pages. This may have necessitated cutting through an image and duplicating adjacent pages to assure complete continuity.
2. When an image on the film is obliterated with a round black mark, it is an indication of either blurred copy because of movement during exposure, duplicate copy, or copyrighted materials that should not have been filmed. For blurred pages, a good image of the page can be found in the adjacent frame. If copyrighted materials were deleted, a target note will appear listing the pages in the adjacent frame.
3. When a map, drawing or chart, etc., is part of the material being photographed, a definite method of "sectioning" the material has been followed. It is customary to begin filming at the upper left hand corner of a large sheet and to continue from left to right in equal sections with small overlaps. If necessary, sectioning is continued again—beginning below the first row and continuing on until complete.
4. For illustrations that cannot be satisfactorily reproduced by xerographic means, photographic prints can be purchased at additional cost and inserted into your xerographic copy. These prints are available upon request from the Dissertations Customer Services Department.
5. Some pages in any document may have indistinct print. In all cases the best available copy has been filmed.

**University
Microfilms
International**

300 N. Zeeb Road
Ann Arbor, MI 48106

8311149

Haskell, Joyce Fehl

CHARACTERIZATION OF THE INSULIN RECEPTOR IN ISOLATED
BOVINE CEREBRAL AND RETINAL MICROVESSELS

The University of Alabama in Birmingham

PH.D. 1982

University
Microfilms
International 300 N. Zeeb Road, Ann Arbor, MI 48106

Copyright 1982

by

Haskell, Joyce Fehl

All Rights Reserved

PLEASE NOTE:

In all cases this material has been filmed in the best possible way from the available copy.
Problems encountered with this document have been identified here with a check mark ✓.

1. Glossy photographs or pages ✓
2. Colored illustrations, paper or print _____
3. Photographs with dark background ✓
4. Illustrations are poor copy _____
5. Pages with black marks, not original copy _____
6. Print shows through as there is text on both sides of page _____
7. Indistinct, broken or small print on several pages ✓
8. Print exceeds margin requirements _____
9. Tightly bound copy with print lost in spine _____
10. Computer printout pages with indistinct print _____
11. Page(s) _____ lacking when material received, and not available from school or author.
12. Page(s) _____ seem to be missing in numbering only as text follows.
13. Two pages numbered _____. Text follows.
14. Curling and wrinkled pages _____
15. Other _____

University
Microfilms
International

CHARACTERIZATION OF THE INSULIN RECEPTOR IN
ISOLATED BOVINE CEREBRAL AND RETINAL MICROVESSELS

by
JOYCE FEHL HASKELL

A DISSERTATION

Submitted in partial fulfillment of the requirements for the degree of
Doctor of Philosophy in the Department of Biochemistry
in The Graduate School, University of Alabama in Birmingham

BIRMINGHAM, ALABAMA

1982

ABSTRACT OF DISSERTATION
GRADUATE SCHOOL, UNIVERSITY OF ALABAMA IN BIRMINGHAM

Degree Doctor of Philosophy Major Subject Biochemistry
Name of Candidate Joyce Fehl Haskell
Title Characterization of the Insulin Receptor in Isolated Bovine
Cerebral and Retinal Microvessels

The high incidence of microvascular disease as a long-term complication of diabetes mellitus may be related to a derangement in the metabolic control of vascular tissue by insulin. Binding of [125 I]-insulin to isolated bovine cerebral, bovine retinal, and porcine cerebral microvessels was measured at 22°C for 75 minutes in the presence and absence of excess unlabeled hormone. Inhibition of insulin binding was observed with various concentrations of unlabeled insulin and Scatchard analysis of the data yielded a curvilinear plot similar to that obtained with other tissues. A particulate fraction prepared from isolated bovine retinal microvessels was crosslinked to [125 I]-insulin using disuccinimidyl suberate, yielding a specifically labeled subunit with a molecular weight of approximately 125,000 daltons. These data verify the existence of a high affinity insulin receptor in cerebral and retinal microvessels and demonstrate that this hormone receptor is similar in its binding characteristics to receptors found on well-characterized insulin-sensitive organs.

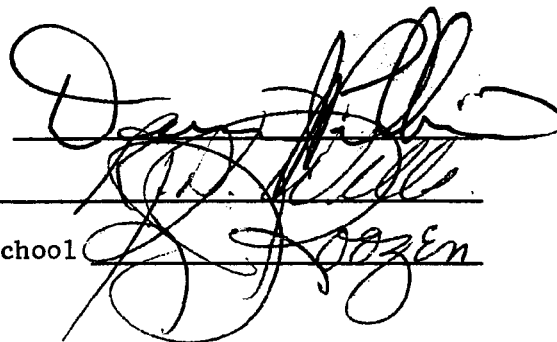
Abstract Approved by: Committee Chairman

Program Director

Date

12/3/82

Dean of Graduate School



DEDICATION

I would like to dedicate this dissertation
to my children, Jennie Elizabeth and Connie Guion Haskell,
to my husband, Alexander Cheves Haskell III, and
to my parents, Andrew Theodore and Earline Knight Fehl.

ACKNOWLEDGMENTS

I am most grateful to my able advisor, Dr. Dennis J. Pillion, for his guidance, patience, and instruction during my graduate education. I would like to thank the Graduate School for the financial support that made it possible to perform the work. I would also like to express my gratitude to Dr. Elias Meezan for his expert guidance and encouragement. I would like to thank my graduate committee, Dr. John McKibbin, Dr. Kenneth Taylor, Dr. Gerald Becker, Dr. Caroline Pace and Dr. Geraldine Emerson. I would like to acknowledge the role Dr. Vinod Bhalla and the late Dr. William J. Reddy played in my graduate education. Finally, I would like to thank all who assisted me in tissue preparation and especially Glenn Roth for his aid and Dr. Fred Harris for the use of his facilities to develop my autoradiographs.

TABLE OF CONTENTS

	<u>Page</u>
ABSTRACT	ii
DEDICATION	iii
ACKNOWLEDGEMENTS	iv
LIST OF FIGURES	vii
LIST OF TABLES	ix
LIST OF ABBREVIATIONS	x
I. INTRODUCTION	1
II. REVIEW OF RELATED LITERATURE	4
Insulin	4
Chemistry of the Insulin Molecule	4
Biological Effects of Insulin	9
Mechanism of Insulin Action	13
Insulin Receptor	15
Definition of Receptor	15
Binding	16
Insulin Degradation	19
Isolation of the Insulin Receptor	21
Microvascular Tissue	25
The Blood-Brain Barrier	25
Isolated Microvessels	26
Insulin in Microvascular Tissue	30
Vascular Complications in Diabetes Mellitus	34
III. MATERIALS AND METHODS	40
Animals	40
Chemicals	40
Tissue Isolation	41
Membrane Preparation	42
[¹²⁵ I]-Insulin Binding Assay	42
Degradation	43
Protein Determination	43

TABLE OF CONTENTS

	<u>Page</u>
Deoxyribonucleic Acid Determination	44
[¹⁴ C]-Inulin Space Determination	44
Dissociation Experiments	45
Crosslinking Experiments	46
SDS-Polyacrylamide Gel Electrophoresis	47
Determination of Molecular Weight	47
Autoradiography	47
 IV. RESULTS	 48
Isolation of Microvessels	48
Insulin Binding to Isolated Microvascular Tissue	55
[¹²⁵ I]-Insulin Binding Assay	55
Effect of Protein Concentration	58
Effect of Time and Temperature	61
Characterization of Insulin Binding	64
[¹⁴ C]-Inulin Trapping in Microvessels	70
Insulin Degradation in Microvessels	72
Competitive Displacement Experiments	75
Dissociation of [¹²⁵ I]-Insulin	93
Bovine Cerebral Microvessels	93
Bovine Retinal Microvessels	95
Identification of the Microvascular Insulin Receptor	100
Crosslinking Procedure	100
Isolation of the Insulin Receptor	107
 V. DISCUSSION	 113
Tissue Isolation	113
Insulin Binding	114
Scatchard Analysis	116
Dissociation of [¹²⁵ I]-Insulin	117
Isolation of the Insulin Receptor	118
 VI. SUMMARY	 121
 VII. BIBLIOGRAPHY	 122

LIST OF FIGURES

Figure	<u>Page</u>
1. Structure of the Insulin Molecule	5
2. Procedure for Isolation of Microvascular Tissue	49
3. Phase Contrast Micrograph of Isolated Microvascular Tissue	52
4. Insulin Binding Assay	56
5. [¹²⁵ I]-Insulin Binding to Retinal Microvessels as a Function of Protein Concentration	59
6. Effect of Incubation Time and Temperature on Specific Binding of [¹²⁵ I]-Insulin to Bovine Cerebral Microvessels	62
7. Effect of Variable Concentrations of [¹²⁵ I]-Insulin on Insulin Binding to Neonatal Porcine Cerebral Microvessels	65
8. Inhibition of Specific [¹²⁵ I]-Insulin Binding to Bovine Cerebral Microvessels	79
9. Scatchard Analysis of [¹²⁵ I]-Insulin Binding to Bovine Cerebral Microvessels	81
10. Inhibition of Specific [¹²⁵ I]-Insulin Binding to Bovine Retinal Microvessels	84
11. Scatchard Analysis of [¹²⁵ I]-Insulin Binding to Bovine Retinal Microvessels	86
12. Inhibition Curve of Specific [¹²⁵ I]-Insulin Binding to Porcine Cerebral Microvessels	88
13. Scatchard Analysis of [¹²⁵ I]-Insulin Binding to Porcine Cerebral Microvessels	90
14. Dissociation of [¹²⁵ I]-Insulin from Bovine Cerebral Microvessels	96

LIST OF FIGURES (Continued)

Figure	<u>Page</u>
15. Dissociation of [¹²⁵ I]-Insulin from Bovine Retinal Microvessels	98
16. Crosslinking Procedure	101
17. Electrophoretic Patterns of Membrane Proteins	105
18. Isolation of the Insulin Receptor in Liver Using Disuccinimidyl Suberate and Reducing and Nonreducing Conditions	109
19. Isolation of the Insulin Receptor of Retinal Microvessels and Liver	111

LIST OF TABLES

Table	<u>Page</u>
1. Wet Weights of Isolated Microvascular Tissues	54
2. [^{125}I]-Insulin Binding to Isolated Microvessels per mg Protein	68
3. [^{125}I]-Insulin Binding to Isolated Microvessels per mg DNA	69
4. [^{14}C]-Inulin Trapping in Tissue Pellets	71
5. [^{125}I]-Insulin Degradation in Bovine Retinal Microvessels: Concentration Curve	73
6. [^{125}I]-Insulin Degradation in Bovine Retinal Microvessels: Time Response	74
7. [^{125}I]-Insulin Binding to Isolated Bovine Cerebral Microvessels	76
8. [^{125}I]-Insulin Binding to Isolated Bovine Retinal Microvessels	77
9. [^{125}I]-Insulin Binding to Isolated Porcine Cerebral Microvessels	78
10. [^{125}I]-Insulin Binding Constants and Binding Capacities	92
11. Effect of Insulin Analogues on [^{125}I]-Insulin Binding	94
12. [^{125}I]-Insulin Binding in Crosslinking Experiments	103
13. Summary of Insulin Receptor Characterization	119

LIST OF ABBREVIATIONS

BSA	Bovine serum albumin
cAMP	Adenosine 3',5'-cyclic monophosphate
CPM	Counts per minute
DSS	Disuccinimidyl suberate
DTT	Dithiothreitol
	Daltons
K _a	Affinity constant
K _d	Dissociation constant
K _m	Michaelis constant
KRP	Krebs-Ringer phosphate
M	Moles per liter
MW	Molecular Weight
NSB	Nonspecific binding
PCA	Perchloric acid
PDE	Phosphodiesterase
PPO	2,5 diphenyloxazole
POPOP	1,4 bis[2-(5-phenyloxazolyl)]-benzene
R _f	Ratio of electrophoretic mobility
SDS-PAGE	Sodium dodecyl sulfate polyacrylamide gel electrophoresis
TCA	Trichloroacetic acid
U	Micro units
xg	Times gravitational force

I. INTRODUCTION

Marked pathophysiology of the microvessels, and particularly the retinal microvessels, is a major complication of long-standing diabetes mellitus. Diabetic retinopathy is the leading cause of adult blindness in the United States today (37). There is an increased incidence and accelerated appearance of diffuse vascular complications, highlighted by thickening of the vascular basement membrane, altered vascular permeability and retinal aneurysms (32,34,37,38,119,130).

The microvessels of the brain, retina and other organs are continuously exposed to the body's circulating insulin. Maturity onset diabetics often have an elevated blood insulin level (38), and juvenile diabetics require a lifetime of insulin injections (14). Since insulin is routinely injected, via pump or syringe, at daily doses sufficient to lower blood glucose levels, the systemic circulation is perfused with very high levels of insulin. In addition, the systemic circulation is exposed to insulin first, instead of the liver, contrary to the normal situation (120).

The biologic effects of insulin, like those of other peptide hormones, are generally believed to begin with the interaction of insulin with its specific receptor on the cell surface. The hormonal effects are then mediated by some still unknown mechanism to regulate carbohydrate, lipid and protein metabolism within the cell (4,25,43,66, 67,69,77,80, 114). Insulin binding and degradation have been extensively studied in vitro in a large number of tissues, and recently,

various methods have been developed to isolate the insulin receptor. Brendel et al. (13) and Meezan et al. (88) presented a method for isolating bovine brain and retinal microvessels by selective sieving. These workers have shown that these vessels are capable of oxidizing a variety of substrates, including D-glucose. A number of investigators have proposed the existence of an insulin receptor in the capillaries of the cerebral cortex. Van Houten and Posner (123) visualized heavy labeling of cerebral microvessels when rat brains were perfused with labeled insulin. Recently, Frank and Pardridge (42) have studied [^{125}I]-insulin binding in isolated bovine cerebral microvessels, and Meezan and Pillion (89) have shown that these isolated vessels respond to insulin by increased [^{14}C]-glucose oxidation to [$^{14}\text{CO}_2$], increased lipogenesis and increased cAMP-phosphodiesterase activity.

If an insulin receptor exists in microvascular tissue, then it is possible that the pathophysiology observed in diabetes mellitus results from a change in the normal interaction between insulin and the receptor. The present study was initiated to determine if there is an insulin receptor in the isolated microvessels of the cerebral cortex and the retina. The objectives of this dissertation are as follows: 1) to characterize the binding and degradation of [^{125}I]-insulin in preparations of microvessels isolated from bovine cerebral cortex, porcine cerebral cortex and bovine retina; 2) to determine whether unlabeled insulin inhibits binding in a dose-dependent manner and whether the results yield a curvilinear Scatchard plot; 3) to determine whether the binding of [^{125}I]-insulin is specific for insulin or whether it can be displaced by insulin analogues or other protein hormones; 4) to compare [^{125}I]-insulin binding in the various microvascular preparations with

preparations with respect to their binding capacity per mg protein and affinity constants; and finally, 5) to covalently crosslink [^{125}I]-insulin to the plasma membrane insulin receptor of isolated retinal microvessels using disuccinimidyl suberate and to isolate the resulting labeled hormone-receptor complex using SDS-polyacrylamide gel electrophoresis.

II. REVIEW OF RELATED LITERATURE

Insulin

Chemistry of the Insulin Molecule

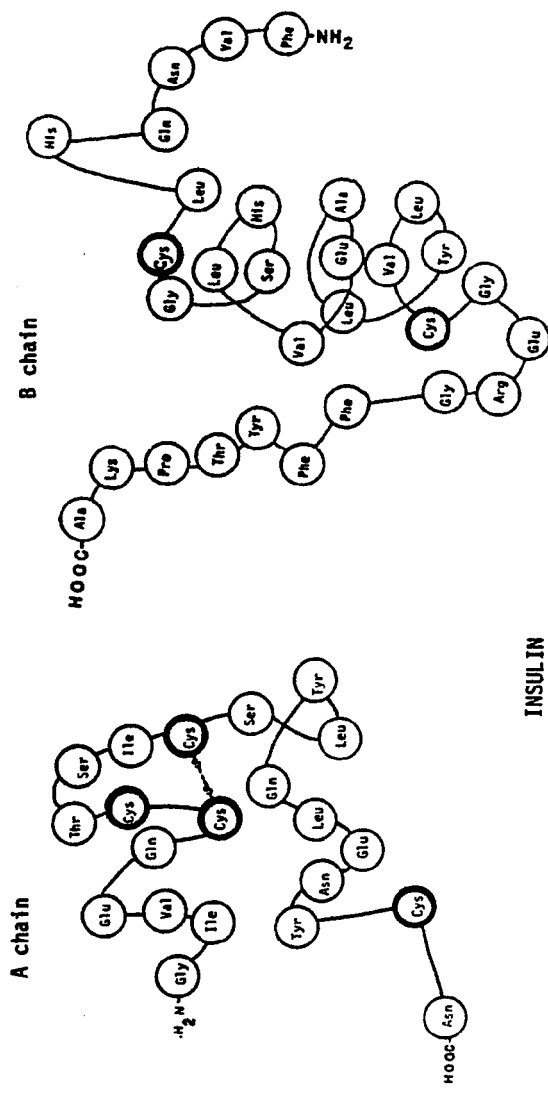
The beta cells of the islets of Langerhans located in the endocrine pancreas synthesize insulin as a single-chain peptide, proinsulin (118). Proinsulin has a molecular weight of 9000 daltons and consists of 81-86 amino acid residues. Proinsulin spontaneously folds, allowing the formation of the proper disulfide bridges present in the insulin molecule. In the Golgi apparatus, the proinsulin molecule is cleaved. In 1977, Steiner (118) mimicked this processing with trypsin, forming insulin, with 51 amino acid residues and a molecular weight of 6000 daltons, and C-peptide, with a molecular weight of 3000 daltons. The C-peptide, also named connecting peptide, contains acidic amino acid residues, and to date a physiologic role for the peptide hormone has not yet been elucidated. Insulin consists of two peptide chains connected by two disulfide bridges. A disulfide bridge also joins two cysteine residues within the A chain. Insulin has a well-defined three-dimensional structure, as depicted in Figure 1. Hodgkin (61) first reported the compact structure in 1972 using X-ray analysis. Blundell et al. (11) further elucidated the structure using circular dichroism. Interchain salt links and hydrogen bonds stabilize the molecule, in addition to the disulfide bridges.

The insulin molecule shows very few species differences. Most mammalian species differ only in the A-chain in the region of amino

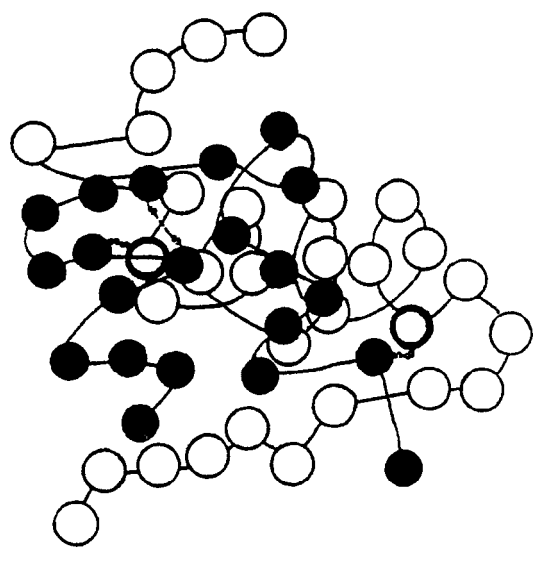
FIGURE 1

Structure of the Insulin Molecule

Drawing of the three-dimensional configuration of the amino acid residues of A chain, B chain, and insulin, based on the model of Blundell (11). Cysteine residues are highlighted in heavy circles; (-s-s) denotes sites of 2 interchain disulfide bridges and 1 intrachain disulfide bridge. Dark circles represent amino acid residues composing the A chain of insulin.



INSULIN



acid residues A₈-A₁₀ and in the carboxyl-terminal amino acid residue of the B-chain. These variations are not associated with any alteration in biological activity (118). Human, porcine and bovine insulin are virtually identical in their three-dimensional structure and their biological activity. The C-peptide differs considerably in length and amino acid composition from species to species. Insulin occurs in vivo as dimers and as hexameric complexes with zinc and protamine, a basic protein (14). The complex forms of insulin are more difficult to degrade than the monomer, with a half-life of 72 hours.

Blundell et al. (11) has identified the receptor binding regions of the insulin molecule to include amino acid residues A₁, A₄, A₂₁, B₁₂, B₁₃, B₂₁-26 and the tyrosine residues A-19, B₁₆, and B₂₆. By using insulin analogues, it has been found that biological potency is proportional to receptor binding. Proinsulin is only 20% as biologically active as insulin, presumably because the C-peptide masks the insulin receptor binding sites. The presence of arginine residues on the carboxyl terminal end of the B-chain diminishes biological activity by 70%. Serine and tyrosine residues in the insulin molecule are important for biological activity. No specific amino acid residue is absolutely required for insulin activity (118).

The most commonly utilized radioactive compounds are [¹²⁵I]- and [¹³¹I]-iodoinsulin (47,118,132). Insulin contains 4 tyrosyl residues. Roth (112) suggests that the desirable level of iodination yields 0.2 iodine atoms per tyrosyl residue, up to a maximum of 1.0 iodine atom per molecule (monoiodoinsulin). It is necessary to minimize the relative number of diiodotyrosyl groups produced by iodination to maintain biological activity (43,112). The Chloramine T method and, more

recently, lactoperoxidase method are routinely being used to [^{125}I]-radiolabel insulin. Unreacted iodide is removed from labeled insulin using dialysis, anion exchange columns, gel filtration columns and centrifugation of minicolumns packed with Sephadex G-25 resin (23,43,112). Monoiodoinsulin with the label primarily located on the A₁₉ tyrosyl residue is only half as potent as molecules with labeled A₁₄ tyrosyl residues, in respect to both biological potency and binding affinity, suggesting that A₁₉ is near the receptor binding region (47).

The normal human pancreas contains approximately 10 mg insulin. Daily, 1-2 mg of insulin are secreted into the blood stream via exocytosis (118). Using radioimmunoassay, normal serum levels (basal) range from 0.2 to 0.8 ng/ml, which is equivalent to 4.3 to 19.9 U/ml or 35 to $145 \times 10^{-12}\text{M}$ (14,132). The secretion of insulin in response to a carbohydrate-rich meal is rapid and closely parallels the elevation of blood glucose levels in normal patients (132).

In laboratory animals, plasma insulin levels range from 0.5 (basal) to 3.5 ng/ml (post-prandial). Several investigators have reported that peripheral tissues (brain, kidney) may contain insulin concentrations exceeding the plasma levels (35,55). Eng and Yalow (35) suggest that "insulin found in the brain is due in part to that in vascular spaces and perhaps also to that crossing the blood-brain barrier, diffusing through the brain and then concentrating on brain receptor sites." Havrankova et al. (55) have reported rat brain insulin concentrations 25 times higher than plasma levels, although this finding has been challenged by Eng and Yalow (35).

Clinically, highly purified pork or beef insulin is used to treat diabetics (14). Insulin is an acidic protein with an isoelectric point

of 5.3, and it is available in the crystalline form, prepared by precipitating insulin in the presence of zinc chloride to form zinc-insulin crystals. Regular crystalline insulin has a rapid onset of action (30 min-1 hr) and a duration of action of 5-7 hr. A wide variety of modified insulin conjugates are available with longer duration times and variable speed of onset. The 1982 standard of potency is based on an absolute dry weight of highly purified zinc-insulin and contains 24 units of activity per milligram (14). Not all diabetic patients require insulin injections, but approximately 3.0 million Americans are currently receiving daily injections of the hormone.

Biological Effects of Insulin

Insulin is an anabolic hormone which is extremely important in regulating the entire body's fuel metabolism. Purified insulin has been shown to stimulate anabolic processes and inhibit catabolic processes in the transport and utilization of glucose, fatty acids, and amino acids (18,25,69). The biological effects of insulin have been most intensively studied in adipose tissue, liver, and skeletal muscle. Currently, a large amount of research is being directed to determining 1) the exact metabolic enzymes and cellular processes affected by insulin and 2) which other tissues also respond to insulin (28). Processes affected by insulin may depend on the energy profile of the tissue and the level of key enzymes and substrates within the tissue (40, 104, 108). The biological effects of insulin appear very different in fed and fasted states (1,48), obese and nonobese states (52,79,90,92) and various disease states (14,22,32,107,117).

Insulin binds initially to the cell surface and generates a cascade of biological effects within the cell (25,43,67,69,80). Certain biological effects are immediate and require only a small percentage of binding sites to be occupied. These include glucose transport (and transport of specific nutrients) into fat cells and muscle cells. Freychet (43) has labeled these effects "metabolic", as opposed to "trophic" effects, which require a greater length of time and increased occupancy of receptor sites. Trophic effects include increased protein synthesis, increased DNA and RNA synthesis, and enzyme activation via phosphorylation or dephosphorylation. Enzymes that are activated by dephosphorylation by insulin include glycogen synthetase, pyruvate dehydrogenase, and acetyl-Co A carboxylase (16,41,77,78). Numerous enzymes involved in glucose metabolism and storage, lipid and sterol turnover, and protein and nucleic acid turnover have increased activity resulting from increased synthesis (45,48).

Generally, insulin increases glucose oxidation, glycogenesis, lipogenesis, proteogenesis and formation of ATP, DNA and RNA (25,67,80). Insulin maintains the cell in an anabolic state by concomitantly inhibiting glycogenolysis, lipolysis, proteolysis, ureogenesis, and ketogenesis. Lack of insulin depresses glucose utilization, drastically reduces protein synthesis and decreases fat synthesis, while promoting fat utilization. Blood glucose levels build up, ketone bodies are elevated, and blood levels of lipoproteins are increased five fold. These conditions combined with elevated levels of triglycerides, cholesterol, and phospholipids present excellent conditions for the development of atherosclerosis (22,34,59,119). At the other extreme, excess levels of insulin enhance glucose transport into fat and muscle cells, decrease blood levels of amino acids, increase protein stores in

body tissues, and inhibit fat utilization while promoting fat synthesis (18,21,26,39,41).

The effects of insulin are tissue-specific. Insulin effects are mediated by a specific receptor on the cell surface and require the presence of the appropriate enzyme system within the cell (64). Insulin stimulates fatty acid synthesis in adipose tissue and liver, but not in muscle since skeletal muscle does not contain enzymes for fatty acid synthesis. In liver, anti-gluconeogenesis and glycogenesis effects are principally observed; in adipose tissue, lipogenesis and antilipolytic effects are observed; and in muscle, protein synthesis and the anti-proteolytic effects of insulin are studied (25,43,48,80).

Insulin increases the rate of transport of glucose into skeletal muscle and adipose tissue. Transport is not rate-limiting in liver (80). D-glucose is transported into the cell by a stereospecific hexose transporter within the plasma membrane. The adipocyte transporter structure has been isolated and reconstituted using artificial phospholipid vesicles (18). It is a polypeptide distinct from the insulin receptor molecule, although it may be noncovalently associated with the cell surface (18,26,99,115). Inside the cell, D-glucose is phosphorylated and is metabolized through the glycolytic pathway with production of pyruvate (25,80). The pyruvate is converted to acetyl Co A in the liver by pyruvate dehydrogenase (66). This enzyme is similar to glycogen synthetase since it is also inactive when phosphorylated (78). In the presence of insulin, the enzyme is dephosphorylated and therefore more active, particularly in the liver. Seals and Jarett (114) have observed this effect of insulin on pyruvate dehydrogenase in vitro with a mixture of isolated adipocyte plasma membranes and mitochondria.

In many cases, insulin antagonizes effects of epinephrine and glucagon, both of which generate their effects by activation of adenylate cyclase and an increase in the level of 3'5'-adenosine monophosphate (cyclic-AMP) (80, 128). Some of the effects of insulin may result from decreasing cyclic-AMP levels within cells by inhibiting adenylate cyclase or stimulating the activity of the low K_m form of cyclic-AMP phosphodiesterase, the enzyme which converts cyclic-AMP to adenosine monophosphate. This causes less activation of protein kinase, which in turn causes less phosphorylation of enzymes, opposing the effect of epinephrine and glucagon on the cell metabolism.

Insulin's effects on phosphorylation/dephosphorylation appear to be caused by a specific rearrangement in which enzymes are phosphorylated within the cells, not net loss of total proteins phosphorylated (77). Several investigators, including Benjamin and Singer (4) have shown that insulin increases phosphorylation of some major peptides in both fat and liver, while decreasing the phosphorylation of others. Kasuga et al. (71) have shown that insulin stimulates phosphorylation of a protein subunit of its own receptor.

Insulin is involved in regulating nutrient supply and utilization at the tissue level in ruminants as well as in other mammalian species (104). Since little glucose is derived from the gastrointestinal tract in cows, due to microbial fermentation in the rumen, acetate is the primary substrate for energy storage and oxidation. Insulin has been demonstrated to have effects on glucose oxidation (15 to 45% increases) and acetate oxidation in isolated bovine fat cells (39). Studies of bovine diabetic fat yield differences, since acetyl Co A carboxylase may not require insulin. However, the effect of insulin on bovine fat cells

is similar to that in other mammals in that the overall effect is to increase triglyceride deposition in adipose tissue by increasing glucose uptake, increasing α -glycerophosphate availability, and increasing lipoprotein lipase activity. Gluconeogenic pathways utilize propionate, lactate, glycerol and amino acids to provide glucose. Insulin may not have many direct effects on bovine hepatic metabolism. Prior et al. (104) conclude that the primary effects of insulin are on nonhepatic carbohydrate, lipid, and amino acid metabolism in the ruminant.

Pillion et al. (100) have recently investigated the effect of insulin on isolated bovine cerebral microvessels. This laboratory has observed a direct effect of physiological doses of insulin on [^{14}C]-D-glucose oxidation to [$^{14}\text{CO}_2$] and neutral fats. Insulin also stimulates the low K_m form of cyclic 3'5' adenosine monophosphate phosphodiesterase. Similar results have since been obtained in isolated bovine retinal microvessels and cerebral microvessels from neonatal pigs (54).

Mechanism of Insulin Action

Despite numerous years of intensive investigation, the exact mechanism of insulin action is still unknown. Several possible mechanisms of action on the various tissues have been proposed. The currently favored hypothesis is that the insulin molecule exerts its effect primarily on the cell membrane and that a second messenger is released or activated which produces the intracellular effects of insulin. This hypothesis was first proposed by Sutherland (120) and is analogous to the adenylate cyclase-peptide hormone mechanism of action. To date, several investigators (66,77,114) have isolated chemical

mediators which have certain intracellular effects. It is as yet uncertain whether these chemical substances (peptides with molecular weights of approximately 1000 daltons) represent the true second messenger or just a specific activator of the particular enzyme studied, (i.e., glycogen synthase phosphoprotein phosphatase or mitochondrial pyruvate dehydrogenase). The second hypothesis is the "internalization" concept. For many years it was widely believed that insulin with a molecular weight of nearly 6000 did not enter the target cell. In this hypothesis, the insulin molecule may interact with the plasma membrane and enter the cell, perhaps via endocytosis, where it can bind with the various cell organelles directly (50,126). Several investigators (5,50,62,126) have presented evidence for the presence of insulin within the cell by means of autoradiography and fluorescein labeling.

Although recent evidence supports the internalization concept in that labeled insulin has been demonstrated to accumulate intracellularly within the lysosomes, Golgi regions, nuclei and the endoplasmic reticulum of fibroblasts, hepatocytes, adipocytes and lymphocytes (70), this hypothesis is still quite controversial. Intracellular high affinity sites may be distinct from those on the plasma membrane, and internalization of insulin may just be a step in the degradation process and not a requirement for insulin's action. Recently, Czech (26) has presented evidence that the plasma membrane may physically invaginate within adipocytes, masking binding sites, and these sites may appear to be associated with the Golgi apparatus rather than the plasma membrane, due to cell fractionation techniques.

A variation of the first hypothesis proposes that insulin reacts with the plasma membranes of the target cell via a receptor site and

activates a protease which releases a peptide which is either a part of the insulin molecule, the receptor-insulin complex, or an internal protein associated with the receptor molecule (26). This protein would then act as a "second messenger" to exert the actions of insulin on the target cell, resulting in the phosphorylation/dephosphorylation of key enzymes in the cytoplasm (80).

Insulin Receptor

Definition of Receptor

A receptor is a recognition site which selectively binds a ligand, in this case, the insulin molecule, and produces biological effects associated with the ligand. The receptor is a macromolecule associated with the membrane, cytoplasm or nucleus (23,69). Not all binding sites are true receptors. Insulin binds to a wide variety of substances, for example, glass and talc. Any cellular component may be referred to as a receptor if it meets several well-defined requirements (48). 1) There must be a finite, saturable number of binding sites per cell. 2) The ligand must bind reversibly through a specific molecular interaction. 3) The ligand must bind with high affinity, appropriate for the physiological concentrations of the ligand and 4) bind with a specificity proportional to the biological activity of the ligand. 5) Lastly, binding should be tissue specific and produce a specific biological effect.

Binding

Insulin binding has been observed in a wide variety of tissues, in many different species and under a wide variety of physiological conditions and disease states. The various tissues in which insulin binding has been studied include the three most recognized target tissues, fat, liver, and muscle. Other tissues investigated include mammary gland, placenta, kidney, central nervous system, blood, lung and heart. Insulin binding has been investigated in turkey erythrocytes, cultured chicken liver and embryonic heart cells, rat intestinal epithelial cells, human erythrocytes, mononuclear cells, IM-9 lymphocytes, 3T3-L1 fibroblasts, and cultured human colonic cancer cells. Among the various physiological states in which insulin binding has been studied are pregnancy, aging, embryonic, perinatal, physical exercise, fed, fasting, and obesity. Pathological states include hyperglycemia, hyperthyroid, hyperinsulinemia, uremia, acromegaly, ataxia telangiectasia, acanthosis nigricans, hyperlipemia, and of course diabetes (10,14, 22,31,32,63,82, 107,113,117).

Insulin receptor binding has been studied extensively with tissue homogenates (55,70,121,124), isolated cells (1,5,21,31,36,51,62 78, 81,92,93,117,122), cultured cells (6,10,44,103, 105,125,137) and cell membrane and particulate preparations (1,108,118,121,126). Intact cells can be obtained from cell culture or from isolation techniques involving mechanical disruption or enzymatic digestion. The hormone binding studies using intact cells are of primary importance since these cells may be metabolically active. Binding can, therefore, be correlated with hormonal biological response. Binding to whole cells has the

disadvantage of increased side reactions, heterogeneity of cell types and increased degradation of the ligand. Particulate fractions increase receptor concentration, but isolation procedures may disrupt receptors and may only be representative of plasma membranes. Receptors may have altered affinity of binding from intact cells. Hormone receptors have been shown to maintain their activity after solubilization with detergents such as dodecyl sulfate and Triton X-100 (3,46,49,53,101). Solubilization increases concentration of receptors, but detergents may also disrupt protein conformations, causing decreased specificity and affinity. Ligands may also associate with micelles, which may distort hormone-receptor interactions (46,49).

The hormone receptor interaction involves noncovalent binding, such as hydrogen bonding, hydrophobic interactions, and van der Waals forces. The circulation consists of a hydrophilic aqueous environment. The insulin receptor is embedded in the plasma membrane and has hydrophobic regions which attract the hydrophobic regions on the hormone's surface. These interactions drive the reaction. The receptor must have appropriate groups specifically placed to allow hydrogen bonds to form between the ligand and its receptor. These electrostatic interactions result in what is described in the literature as "affinity binding." The ratio of the rate of association to the rate of dissociation at equilibrium is called the equilibrium association constant (K_a). It is equivalent to the reciprocal of the equilibrium dissociation constant (K_d), which can be defined as the concentration of hormone required to saturate one half of the total number of receptors (the binding capacity) (43).

Conformational changes influence the sensitivity of the hormone-receptor interaction. Binding studies carried out in vitro with radiolabeled hormones illustrate that this interaction varies with pH, ionic strength, time, temperature and possibly occupancy (negative cooperativity or site-site interaction) (29,30,45,46,110).

The hormone-receptor interaction, also called affinity binding, is the result of weak, noncovalent bonding in a dynamic equilibrium (27,43,48). It is important that measurement procedures not interfere with the equilibrium. Numerous methods are used to separate bound insulin from free insulin, including centrifugation, centrifugation through an oil layer, various millipore filtrations, chromatography, gel filtration, and charcoal absorption (9,27,43,45,48,102,109). The residual, non-saturable binding of [^{125}I]-hormone that occurs in the presence of a large excess of unlabeled hormone is called non-specific binding. Specific binding is defined as total minus non-specific binding.

Insulin binding can be inhibited by insulin analogues, and the degree of inhibition of binding is related to the biological potency of the analogue. The insulin-receptor interaction results in a curvilinear Scatchard plot which has been interpreted two ways. The curvilinear plot can be resolved into two linear components—one representing a high affinity--low capacity binding site and the other a low affinity--high capacity binding site (21,26,40,93,106). In the two site model, the slope of a line tangent to the curvilinear line derived from Scatchard analysis of binding data (B/F versus Bound) corresponds to K_a or $1/K_d$. The intercept of the tangent line with the abscissa or x-axis is defined as the binding capacity. Alternatively, negative cooperativity explains

the curvilinear result (29,30,46,110). This hypothesis states that insulin binding to one receptor decreases the affinity of the surrounding receptors for insulin. In either case, the affinity should be in the range of the physiologically active concentrations in the blood to be a true reflection of insulin-receptor interactions (97,109,127).

Insulin Degradation

The liver is the primary site of insulin degradation and removes approximately 45% of the insulin that passes through the portal system. The second most important site of insulin metabolism is the kidney, which extracts 40% of the insulin molecules that transverse it via the systemic circulation (43). Until recently it was not recognized that degradation may be necessary for the biological action of insulin at the target cells (51,75,118).

Insulin degradation has been measured with a variety of different techniques. The most rapid method consists of precipitation of intact hormone in 5 % w/v trichloroacetic acid (TCA) (20). Radioimmunoassay is more reliable, but much more tedious. Fragments of the hormone which precipitate with TCA may have no biological activity. Degradation can also be measured by absorption to talc, rebinding to liver membranes and gel chromatography (43).

Several tissues have been reported to contain enzymatic activities that degrade insulin (51,75,118,124). Freychet has reported that insulin degradation appears to be independent of binding to the liver plasma membrane (43). He based this conclusion on the following experimental results. Labeled desalanine-desasparagine insulin (d-d-insulin) is

is degraded to the same extent as insulin, although it has an affinity only 2% that of intact insulin for the receptor. Freychet found no relationship between the bioactivity of insulin analogues and their ability to prevent degradation of insulin. Also, depending on the tissue studied, the ratio of binding to degradation differs greatly. He and other investigators (51) also found wide variation between the optimum pH, temperature and ionic strength for insulin binding as compared for insulin degradation.

Conversely, Steiner reported in 1977 that binding and degradation of insulin are closely related (118). He found that insulin binds rapidly to isolated rat hepatocytes and degradation products begin to appear linearly with time after a lag of 7-9 minutes. Increasing doses of unlabeled insulin depress the amount of labeled insulin degraded. He report that retention and degradation of labeled insulin is directly related to binding in both perfused liver and rat hepatocytes (122). In liver perfusion experiments he found that labeled proinsulin and labeled d-d-insulin are degraded to a very small extent. He report that d-d-insulin is degraded as well as insulin by an isolated insulin-degrading enzyme and by plasma membranes isolated from rat liver (118).

It is difficult to correlate degradation studies from different tissues and different laboratories, due to the many experimental variables that appear to influence degradation studies. To begin with, there is a difference in the sensitivity of the various methods used to measure degradation. Early studies measuring degradation overlooked the leakage of degradative activity from cells into the incubation media, resulting in non-receptor or non-bound hormone degradation. More

recently, numerous investigators have shown in various tissues that the rate of degradation is influenced by changes in pH, temperature, time, presence of albumin, and preincubation with insulin (43,124). Receptor-mediated degradation is changed under all conditions known to influence binding.

Isolation of the Insulin Receptor

Numerous investigators, including Cuatrecasas (23,24) Ginsberg et al. (46), Gould et al. (49), Harrison et al. (52), Lang et al. (75, 76) and Maturo and Hollenberg (85), have attempted to isolate the insulin receptor from crude soluble membrane preparations using affinity chromatography. They described physical characteristics of the receptor and determined that the insulin receptor is an ellipsoid globular glycoprotein. Cuatrecasas (23,24) used DEAE cellulose columns, insulin-agarose affinity columns and concanavalin A-agarose affinity columns to purify the receptor some 6,000-fold. Jacobs and Cuatrecasas (64), using affinity chromatography, found that the insulin receptor elutes as a single component, with Stokes radii of 38 Å and 72 Å and an isoelectric point of 4.0. Ginsberg et al. (46) and Gould et al. (49) in 1979 attempted reconstitution of the receptor into lipid vesicles. They found that the lipid environment is important in modifying the insulin-receptor interaction.

Recently, the physical structure of the insulin receptor has been elucidated by a number of groups using different experimental approaches, such as covalent cross-linking of [¹²⁵I]-insulin to its receptor (27,72,83,84,98,101,103), photoaffinity labeling (3,6,73,133-135) and immunoprecipitation of the insulin receptor (57,64,65,75,76).

Cuatrecasas and Jacobs (64) and Jacobs et al. (65) have successfully labeled a single band on SDS-PAGE in both placenta and liver using anti-receptor antibodies, estimating the molecular weight of the receptor at about 310,000 daltons. Investigators using all three methods have found that the insulin receptor is an integral membrane glycoprotein composed of two major subunits, with molecular weights of 90,000 and 130,000 daltons (27). A few reports (57,73) demonstrate the presence of high molecular weight species of 600,000 and 1,000,000 daltons in the absence of reducing agents and these presumably represent aggregates of the insulin receptor complexes.

Pilch and Czech (98) first reported the use of disuccinimidyl suberate to covalently attach [125 I]-insulin to its receptor in rat adipocytes and rat liver (98). This affinity labeling procedure has been applied to other tissues by several other investigators. Massague and Czech (83) and Massague et al. (84) characterized the insulin receptor in rat adipocytes and rat liver cells and extended this method to crosslink other related ligands (EGF, IGF, MSA) to their specific receptors. Recently, Kasuga et al. (71,72) characterized the insulin and insulin-like growth factor receptors in IM-9 human lymphocytes. Pollet et al. (101, 103) have also characterized the insulin receptor in IM-9 human lymphocytes. Basically, the method of Pilch and Czech consists of preparing plasma membranes from the various tissues, allowing the membranes to bind [125 I]-insulin, covalently crosslinking receptors in the membranes to the labeled insulin using disuccinimidyl suberate (DSS), quenching the reaction, and analyzing the results under reducing and nonreducing conditions using dodecyl sulfate-polyacrylamide gel electrophoresis.

Czech (27) has proposed the following model of the insulin receptor: the receptor consists of an $\alpha_2\beta_2$ composition, with the α subunit having a molecular weight of 125,000 daltons and the β subunit having a molecular weight of 90,000 daltons. The β subunit is very susceptible to proteolytic cleavage, forming a β_1 subunit with a molecular weight of 40,000 daltons. Massague et al. (83,84) have isolated three forms of nonreduced receptor complexes which they subsequently reduced and identified as $(\alpha\beta)_2$, $(\alpha\beta)(\alpha\beta_1)$ and $(\alpha\beta_1)_2$ in adipocyte plasma membranes. These data support the model and demonstrate the presence of disulfide bridges between the two α β subunits and between the α and β_1 subunits. They have also been able to reassociate the subunits following removal of reducing agents with dialysis and using oxidizing conditions. This demonstrates that the insulin receptor does not require any intermediate form for correct disulfide bridges to re-form (25).

Massague, Pilch and Czech (84) have discovered that most of the crosslinking occurs through the B chain of insulin. Since most [^{125}I]-label is on the A chain of insulin, it is crucial to use a reducing agent such as dithiothreitol in low concentrations to prevent reducing the interchain disulfide bonds holding the insulin molecule together. Using dithiothreitol, at two different concentrations, they have been able to selectively reduce disulfide bridges within the receptor molecule and dissociate the subunits.

The 130,000 dalton subunit may possess the principal insulin binding site since it is heavily labeled in affinity labeling experiments run under reducing conditions. Pollet et al. (103) have presented results demonstrating that two subunits are required for insulin binding.

Photoaffinity probes have been prepared which covalently bind to the receptor through different segments of the insulin molecule (135). The experimental results of Yip et al. (133-135) support Czech's model with a few modifications. Yip proposes that the binding site for one insulin molecule is composed of the α (130,000) subunit, the β (90,000, with a 40,000 distinct section) subunit and another β (40,000) subunit. In Czech's model, two different insulin binding sites are postulated, one binding site for each β subunit.

Numerous tissues have been studied using these various techniques. Investigators have isolated and characterized the insulin receptor in rat liver (4,23,24,27,65,83,84, 98,131,135), rat adipocytes (23,57,65, 83,84), human placenta (55,65) IM-9 human lymphocytes (6,71,72,75,76, 101,103), and several other tissues. Jacobs et al. (65) have also used photoaffinity labeling to isolate the receptor in turkey erythrocytes. Kuehn et al. (73) have similarly used photoaffinity labeling with porcine liver membranes. Im et al. (62) have isolated the insulin receptor in adult rat myocytes using column chromatography. Yip et al. (133) have reported two labeled insulin receptor subunits in rat adrenals, lungs, heart, and testes, using photoaffinity labeling techniques. They found only one intermediate size labeled subunit in brain membranes. With this exception, all investigators basically agree on the proposed structure of the insulin receptor and few species or tissue differences have been observed.

Microvascular Tissue

The Blood-Brain Barrier

The capillary endothelium of the brain functions as a selective barrier even for small molecules. This is in contrast to the characteristics of the capillary endothelium in the rest of the mammalian tissues, with the exception of the eye and the testis. In most tissues blood constituents freely diffuse into the interstitial space (7). The cerebral microvasculature is composed of a continuous endothelium with tight junctions between individual cells, which is responsible for maintaining the blood-brain barrier. The endothelial cells contain large numbers of mitochondria and are responsible for regulating brain metabolism (136). The neuronal microenvironment is regulated by the extraordinary capillary surface through specific transport systems, pinocytotic vesicles, and vascular permeability. There is some evidence that different transport systems exist on the luminal and the anti-luminal (abluminal) surfaces of the cerebral endothelium (8,33,95). Transport systems may operate at different rates and specificity on each side of the cell, resulting in the transport of substances through the blood-brain barrier.

The endothelial cells in the capillaries possess cylindrical forms with a diameter barely wide enough for a single erythrocyte to squeeze through. A viable, open lumen is maintained by the endothelial cells adhering tightly to the encircling basement membranes (16,137). The cells normally supply a nonthrombogenic surface on the luminal side so platelets and plasma proteins do not adhere. Investigators (6,86) have shown that these endothelial cells also secrete prostacyclin and other vasoactive agents which further prevent platelet aggregation. Maurer et

al. (87) have shown the bovine cerebral microvessels metabolize endogenous arachidonic acid to form prostaglandins and prostacyclin, which may be important for modulating the tone and reactivity of small cerebral blood vessels.

Isolated Microvessels

In 1974, Brendel et al. (13) and Meezan et al. (88) published a method for isolating metabolically active preparations of bovine brain and retinal microvessels using mild homogenization and selective sieving, as outlined in the methods section of this dissertation. They found that these preparations oxidize a variety of substrates under physiological conditions and can be maintained metabolically active for at least five hours. Vessels isolated according to their procedure range from 6 to 80 μm in diameter and generally remain associated with multiple branches and bifurcations. The isolated microvessels are described by Meezan et al. (88) to appear visually as a twisted aggregation of very fine thread-like tubules.

Carlson et al. (17) examined the ultrastructure and performed a biochemical analysis of basement membrane material isolated using Triton X-100 and deoxycholate both from brain and retinal microvessels. They found that the ultrastructure of the isolated basement membrane closely resembles the in vivo ultrastructure of the microvessels, with the exception that the cells are lacking.

The isolated bovine retinal and cerebral microvessels are not distinguishable from each other with a light microscope. Using the electron microscope, both types of microvessels appear to be composed of a central lumen enclosed by endothelial cells, which are in turn

enclosed by one or more layers of intramural pericytes surrounded by a 500-1000 Å thick sheath of basement membrane. This basement membrane serves as a support structure and permeability barrier. It is composed of equimolar amounts of glucose and galactose, with smaller amounts of other sugars and high contents of amino acids, such as glycine, proline, hydroxyproline, and glutamic acid (17). Bovine brain microvessels appear to have a basement membrane with a somewhat lower sugar content than other basement membrane preparations (17).

Since Meezan et al. (88) published their method in 1974, isolated brain microvessels have been studied by several investigators using a variety of isolation techniques and experimental animals. Hjelle et al. (60) isolated microvessels from rat, rabbit and bovine brains. Head et al. (56) have also examined brain microvessels in monkeys, chickens, guinea pigs and sheep. Head et al. (56,60) assayed the histamine and catecholamine contents in the various cerebral microvessel preparations. They found evidence for the presence of mast cells associated with isolated cerebral microvessels. The norepinephrine content in rat microvessels was found to be fourfold higher than normal rat plasma levels.

Drewes and Lidinsky (33) have studied the isolated canine brain capillary endothelial membrane. Endothelial cells have versatile substrate requirements and are very metabolically active. They conclude that these cells may play a key role in brain metabolism (33). Agreeing with Betz et al. (8), Drewes and Lidinsky used labeled membrane markers to show that the luminal and abluminal endothelial cell surfaces have a different biochemical composition (33). Mrsulja and Djuricic (91) have isolated the cerebral capillaries from gerbils and rats and found

them to have high levels of glutamyl transpeptidase and alkaline phosphatase. They have studied forty-four enzymes and found that many enzymes have different specific activities in the brain capillaries compared to those in the brain parenchyma. Hexokinase, lactate dehydrogenase, adenosine triphosphatase and guanosine triphosphatase are among the enzymes showing differences. Their findings (91) suggest that 1) gluconeogenesis occurs in cerebral capillaries, 2) that compared to brain parenchyma, endothelial cells are less oxygen dependent and do not produce much energy, 3) that the glycolytic pathway is active in endothelial cells, and 4) that the pentose phosphate shunt has a relatively high activity in capillaries. Endothelial cells possess both hexokinase and glucose 6-phosphatase and these enzymes may aid transport of glucose across the blood-brain barrier. Mrsulja and Djuricic (91) also noted that compared to the brain tissue itself, brain capillaries are less sensitive to direct ischemic injury.

Endothelial cells of the cerebral microvasculature contain enzymes which may be involved in permeability of the blood-brain barrier (95). Joo et al. (68) demonstrated the presence of adenylate cyclase and he discussed its significance as a hormonally sensitive enzyme which may be involved in the regulation of capillary permeability. Baca and Palmer (2) report a similar finding in a capillary-enriched fraction from rat cerebral cortex.

Several investigators (53,91) have described the neuronal and sympathetic innervation of cerebral microvessels. Mrsulja and Djuricic (91) detected large amounts of enzymes capable of degrading monoamines and norepinephrine and postulate that the microvasculature may play a role in preventing biogenic amines from entering the brain from the

blood. Alternatively, these enzymes in the microvessels may prevent leakage of neurotransmitter substances from the brain into the blood (91). Hartman et al. (53) have used histofluorescent and physical techniques to conclude that brain microvessels appear to be innervated by the central adrenergic system. Coupled with adenylate cyclase, α -adrenergic receptors have been demonstrated in isolated brain microvessels. Hartman et al. (53) support the concept of central adrenergic system control of capillary permeability and blood flow through direct innervation of capillary endothelial cells, pericytes or smooth muscle cells.

Betz et al. (7) have studied hexose transport and phosphorylation in isolated rat brain capillaries. They found that these capillaries have a glucose transport system with properties similar to those observed for the blood-brain barrier in vivo, and these investigators suggest that the isolated microvessels represent an excellent preparation in which to experimentally investigate sugar transport mechanisms. Under physiological conditions, Betz et al. (8) found a sizable pool of free glucose in the endothelial cells of isolated rat cerebral microvessels, indicating that phosphorylation is not required for glucose transport across capillaries. These investigators determined that glucose is transported across the cerebral microvessels by way of a Na^+ independent, facilitated diffusion system similar to that in erythrocytes.

Many researchers (2,7,8,13,17,33,53,56,60,68,87,91,95) agree that the isolated cerebral and retinal microvessels have all the characteristics of a functional blood-barrier and present an excellent opportunity to study the blood-brain barrier in vitro.

Insulin In Microvascular Tissue

Eng and Yalow (35) have measured the insulin concentrations of various mammalian tissues, such as brain, kidney, heart and plasma. These investigators found that insulin levels in the brains of large animals did not exceed plasma levels, whereas rat brains have an insulin concentration larger than that found in the plasma. These investigators have suggested that insulin found in the brain is due to plasma in brain vascular spaces and possibly from diffusion of insulin into the brain parenchyma.

Havrankova et al. (55) had originally reported rat brain insulin values of greater than 25 times the level in plasma. These investigators speculated that peripheral tissues may retain the ability to synthesize insulin, and this speculation led to many hypotheses, including that some cells may produce their own supply of insulin, which would down-regulate the plasma membrane insulin receptors. This hypothesis was particularly postulated for brain tissue since this tissue had the highest observed insulin levels and very few measurable insulin effects have been observed. In the past year Havrankova et al. (55) have revised their reported values for rat brain insulin levels so that their values are more in line with the results of Eng and Yalow (35). Whether there is actually a significant elevation in brain insulin levels in other mammalian species is currently unknown.

The role of insulin in the brain has been investigated in a number of different systems in recent years (94,,105,111,121,123,). It has been proposed that insulin may alter capillary permeability and blood flow through the brain (28,121), may alter amino acid transport (95,,96,111), may regulate levels of prostaglandins (87), or may regulate

brain development (94,105,111). Several researchers (26,58) have proposed that insulin increases the total amount of glucose taken up by the brain. Others have shown insulin directly affects brain metabolism (19,111). Roger and Fellows (111) have demonstrated a direct effect of insulin on ornithine decarboxylase activity in neonatal rat brains. Catalan et al. (19) recently showed that insulin increases acetylcholinesterase activity in rat brain. Verlangieri and Sestito (125) have demonstrated an effect of insulin on ascorbic acid uptake in heart endothelial cells and postulated that the same effect may be present in other tissues, such as cerebral and retinal capillary endothelial cells.

Insulin is not required for glucose uptake by cerebral cells, although Daniel et al. (28) have found that insulin does have an effect on the metabolism of glucose by the brain. The normal blood level of glucose is from 70 to 110 mg/dl. In one day, the brain uses 150 gm of glucose compared to 50 grams used by blood cells and 50 grams by the heart skeletal muscles and other tissues in a normal adult human male after an overnight fast (38). Daniel et al. (28) found that insulin apparently sustains the cerebral glucose uptake induced by high glucose levels, although not affecting the rate of glucose uptake. From their study in hypoglycemic rats, they concluded that insulin caused the brain cells to use glucose to form glycogen and other substances, such as non-essential amino acids. These investigators concluded that insulin stimulates brain glucose metabolism but not glucose transport across the blood brain barrier.

Hertz et al. (58) have demonstrated, using an indicator dilution method, that insulin may influence glucose transfer across the human

blood-brain barrier. This effect, which may be similar to the effect of insulin on the glucose carrier in heart muscle, is not demonstrable in isolated microvessels since both luminal and abluminal sides of the vessels are in contact with the solution and no net uptake is observed within the vascular cells. They found an increase in glucose extraction in vivo along with an increase in unidirectional glucose flux (58).

Several investigators have found insulin receptors in various regions of the brain. Szabo and Szabo (121) were among the first to demonstrate the presence of insulin receptors in the central nervous system. Havrankova et al. (55) and Pacold and Blackard (94) independently characterized the widespread distribution of insulin receptors in the rat brain. Pacold and Blackard (94) did not find any difference in insulin binding to brain homogenates from streptozotocin diabetic rats compared to normal rats. They measured insulin binding in cerebral homogenates composed of synaptosomes, myelin, and mitochondria. Raizada et al. (105) have cultured fetal rat brain cells and demonstrated the presence of insulin binding and biological response in these neuronal cells. Several investigators (55,94) have studied insulin's effect on the ventromedial hypothalamic nucleus and lateral hypothalamic area. These regions of the central nervous system are insulin-sensitive and appear to regulate systemic blood glucose levels. They may exert an effect on glucose metabolism in the liver. The evidence accumulated to date, therefore, suggests that insulin may also bind to sites in the brain other than the microvessels.

Van Houten and Posner (123) demonstrated insulin binding to pigeon and monkey brains in vivo and using autoradiography, presented the first clearcut evidence that insulin binds to cerebral microvessels.

They found that the majority of the specific insulin binding sites in the brain were localized around small blood vessels. These microvessels are composed of endothelial cells, intramural pericytes and basement membrane. Several investigators have measured insulin binding in endothelial cells. Bergeron et al. (5) demonstrated insulin binding to hepatocytes and liver endothelium by whole body perfusion with [^{125}I]-insulin and fixing the liver in situ. They used electron microscopic autoradiography to examine the hepatocyte plasma-membrane and determined the presence of 10^5 receptors per cell (5). With increased perfusion times, the label appears to be internalized. In control experiments, when excess unlabeled insulin was co-injected with the [^{125}I]-insulin, they found a localization of label primarily over endothelial cells and also inside vesicles and dense bodies within these hepatic endothelial cells. Bergeron et al. (5) suggest that this localization of labeled insulin does not represent nonspecific binding, but that the luminal surface of endothelial cells may contain a low affinity insulin receptor. Peacock, Bar and Goldsmith (96) found that bovine cultured endothelial cells from the pulmonary and systemic circulation have insulin receptors. Arterial endothelial cells bind more insulin per cell than cells prepared from pulmonary veins. These results suggest that insulin receptors in microvascular tissue may be located on the endothelial cells.

In 1981, Meezan and Pillion (89) presented findings directly demonstrating that cerebral and retinal microvessels respond to insulin. D-glucose oxidation and conversion to lipids were stimulated by the addition of physiological levels of insulin to isolated bovine cerebral and retinal microvessels. The low K_m form of cyclic-AMP

phosphodiesterase activity was also increased in a dose-dependent manner by the addition of insulin.

Frank and Pardridge (42) have confirmed the results presented in this dissertation that isolated bovine cerebral microvessels do specifically bind [125 I]-insulin and that Scatchard analysis of the binding data yields a curvilinear plot. In addition, insulin has been shown to dissociate from the cerebral microvessels more rapidly with dilution in the presence of excess unlabeled insulin than with dilution alone.

Yip et al. (133) have utilized photoaffinity probes to crosslink insulin to its receptor in brain tissue. They report only one labeled subunit of approximately 115,000 daltons in brain tissue, compared to two subunits for all other tissues they studied. They did not rigorously characterize the type of cells from which they prepared their brain membranes, so it is difficult to generalize from their results.

Despite recent controversy, it is widely accepted that insulin is present in the brain and insulin has a demonstrable effect on brain glucose metabolism. Insulin receptors have been identified throughout the central nervous system, particularly in the cerebral microvessels.

Vascular Complications in Diabetes Mellitus

Chronic vascular complications of diabetics can be subdivided into three classes: 1) hyperglycemia; 2) small vessel disease (microangiopathy); 3) large vessel disease (macroangiopathy).

Hyperglycemia is believed to be the cause of diabetic neuropathy. Generally, investigators support the hypothesis that better control of serum glucose levels will result in less neuropathy and will also ameliorate the vascular complications of diabetes. In spite of recent

advances with insulin pumps, no diabetic is as well controlled as the normal individual. Recently, hyperglycemia has been assessed by the measurement of hemoglobin A_{1c} to determine the degree of control of carbohydrate metabolism (34). Excess blood sugar results in abnormal glycosylation of hemoglobin and a wide variety of cellular components (32). Hyperglycemia has been linked to fibrotic changes in connective tissue and muscle, impaired phagocytosis and spread of infections. Hyperglycemia also increases edema in tissues, such as the eye and the nerves, and increases sorbitol levels from conversion of glucose by aldose reductase via the polyol pathway. These conditions lead to the various complications seen in diabetic patients: arthritis, infections, lens damage, and neuropathy. The impaired sensation in the extremities due to neuropathy, coupled with the increase in spread of infections, leads to gangrene with eventual amputation of the extremities (38,130).

Small vessel disease in diabetics includes diabetic retinopathy and nephropathy. Nephropathy involves glomerulosclerosis, atherosclerosis of efferent arterioles and pyelonephritis (34). The leading cause of death for juvenile onset diabetics is diabetic nephropathy.

Retinopathy is characterized by regional ischemia, sustained increased capillary permeability, edema, new vessel formation (neovascularization), hemorrhage, thickening of the basement membrane, and changes in the morphology of endothelial cells and pericytes (34,37). The visual ability is gradually impaired in the majority of diabetics, especially juvenile onset diabetics with a history of the disease for over twenty years. It has been found that good control with diet, exercise and appropriate drug therapy may slow down the progression of the microangiopathy, but a recent paper states that even the insulin pump is unable to reverse the condition (122).

Zetter (137) has observed differences in cultured endothelial cells from large and small blood vessels, particularly in regard "to their nutritional requirements and their responses to growth and migration stimuli." Endothelial cell damage or death is a common factor in both macro- and microangiopathy observed in diabetic patients.

Endothelial cell damage in large blood vessels is hypothesized to expose platelets to basement membrane material, releasing factors from the platelets and promoting formation of atherosclerotic plaques (119,136). Retinopathy and other diabetic microangiopathy is characterized by endothelial cell atrophy in microvessels, oily exudates, and abnormal neovascularization. Also, basement membranes appear thickened and permeability is altered in diabetic microangiopathy. Damage to the endothelial cell is highlighted as a major primary complication (34).

The earliest pathological changes observed in diabetic proliferative retinopathy are microaneurisms and breakdown in the blood retina barrier (14, 34). Ten percent of the 4 million diabetics in the United States today have proliferative retinopathy. Approximately 2 million have retinopathy.

In diabetic animals, there are high circulating levels of glucose and frequently during ketoacidotic states, high circulating levels of ketone bodies (92,130). The blood-brain barrier may require greater energy to prevent increased amounts of these substrates from passing from the blood to the brain, thus putting added stress on the level of metabolic activity of the endothelial cells. It is speculated that diabetic endothelial cells may contain fewer mitochondria than normal and this may be the primary defect that leads to endothelial cell damage

and death. The presence of exogenous insulin may stimulate angiogenesis, which leads to the state observed during diabetic retinopathy (117).

The third class of vascular complications is large vessel disease, or macroangiopathy, involving the brain, heart and the peripheral blood vessels. Diabetics have a much greater incidence and greater degree of atherosclerosis, of impaired brain and heart function and myocardial infarction. Both male and female diabetics are equally likely to develop heart disease at an early age (34,38).

It is postulated that high glucose levels may increase oxygen consumption and dilate vascular tissues. When patients with high glucose levels are treated with endogenous insulin, lipogenesis may result in the deposition of lipids in large vessels (119). In recent studies (34), it appears that atherosclerosis has no direct relationship to the degree of severity or duration of diabetes mellitus. Atherosclerosis does not appear to be directly caused by hyperglycemia alone. The concept of insulin having a direct effect on the vascular system may be very relevant to atherosclerosis (119) since there is experimental evidence that insulin plays an important role in regulation of plasma lipid transport. Since insulin has become available for treatment, frequency of atherosclerosis has become more prominent as a complication. It is currently not known whether this is directly due to insulin or just that other complications such as ketoacidosis and infection have been diminished and life-expectancy thereby increased.

Although water does not freely diffuse across brain capillaries, serum osmolality changes result in water movement into or out of brain tissue. Altered capillary permeability may result in cerebral edema. Hartman et al. (54) support the hypothesis that the central adrenergic

system may maintain brain fluid homeostasis by directly regulating blood flow and vascular permeability of the cerebral microvessels. Normal plasma osmolality is approximately 288 mosmol/L. Conscious behavior is directly altered by increased plasma osmolarity. Coma usually is observed in patients with plasma osmolarity levels above 400 mosmol/L (34,38,116,130).

In patients who died in diabetic coma, vascular ischaemic damage with deposits of lipid was prominent within the brain, suggesting abnormalities in the clotting system. Several investigators, including Colwell (22), have suggested that platelets are more adhesive in diabetes due to increased prostacyclin synthesis to aggregation stimuli. Diabetics also have a lower blood fibrinolytic activity and an increase in serum viscosity. Especially in older diabetics, a sudden change in mental status or evidence of dehydration may denote the onset of a hyperosmolar non-ketotic coma. Cerebral hyperosmotic coma may possibly result in cerebral edema (130), lactic acidosis, disseminated intravascular coagulation and infection, along with hypoglycemia and hypokalemia. Infusing a hypertonic solution through the brain for 20-30 sec may disrupt the blood-brain barrier by widening the endothelial cell tight junctions. Permeability is transiently increased and conscious behavior is temporarily altered along with brain edema and metabolic dysfunction.

The presence of insulin receptors in the cerebral microvascular system is of considerable interest, since there is a possibility that insulin has a direct effect on vascular permeability and responsiveness to osmotic changes. It is still uncertain whether diabetic coma results from hyperglycemia, hypoinsulemia or a combination of effects (38,130).

Abnormal vascular metabolism may result from too little as well as too much insulin. Since prior to insulin therapy, diabetics did not live long enough to manifest angiopathic complications, it is still problematic whether good control prevents diabetic complications in addition to its positive effects on longevity or whether good control, with its accompanying intermittent periods of hyperinsulinemia, actually promotes vascular complications (120).

III. MATERIALS AND METHODS

Animals

Brains and eyes of adult male and female cattle (Polar Meats and Lockers) were dissected within 15 minutes of slaughter and transported to the laboratory on ice. Adult male and female rats (Sprague Dawley, Southern Animal Farm) were housed in the U.A.B. Volker Hall animal care facility, three to a cage, with water and food available ad libitum. Neonatal male and female pigs (Bagwell Farm) were transported live to the laboratory where they were sacrificed by cardiac puncture and the brains removed within 20 min.

Chemicals

Chemicals used in these experiments included: [^{125}I]-monoiodinated insulin from New England Nuclear, purified porcine insulin (Iletin II) from Eli Lilly, A and B chain insulin from Sigma, prolactin from National Institute of Arthritis, Metabolism, and Digestive Diseases and human Chorionic Gonadotropin (A.P.L.) from Ayerst Laboratories. Bovine serum albumin, fraction V, was obtained from Sigma, dimethyl sulfoxide from Fisher, dinonylphthalate oil from Eastman Kodak Co. and Curtin Matheson Scientific, dibutylphthalate oil from Aldrich Chemical Co. and disuccinimidyl suberate from Pierce Chemical Co. PPO (2,5 diphenyloxazole) and POPOP (1,4 bis[2-(5-phenyloxazolyl)]-benzene) and dithiothreitol were obtained from Sigma Chemical Co.

Tissue Isolation

Bovine and porcine cerebral microvessels were isolated according to the procedure of Brendel et al. (13). First, the pial membrane and surface blood vessels were removed and the gray matter carefully scraped off with a metal spatula. The gray matter containing a minimal amount of white matter, from the cerebral cortex, was placed in ice cold Krebs-Ringer phosphate buffer (KRP), pH 7.4, with 0.01% bovine serum albumin (BSA). The tissue was then homogenized with a loose-fitting tapered Teflon pestle in a hand-held smooth glass homogenizer with 10 up-down strokes, filtered through a nylon sieve with openings of 153 μm , rehomogenized with 10 more strokes and refiltered through the 153 μm nylon sieve. The brain microvessels were then "combed" off the sieve with fine forceps and washed in a small amount of buffer before being minced with scissors and aliquoted into assay tubes.

Retinal microvessels were similarly prepared from cow eyes according to the procedure of Meezan et al. (88). After orbit was removed and retina exposed, a fine pair of forceps was used to gently scrape off the retina and place it into a plastic tube containing ice cold KRP buffer, pH 7.4, with 0.01% BSA. The tissue was rinsed several times in buffer to remove any dark pigment. The tissue was then homogenized in a glass homogenizer as above. Following homogenizing and filtering, the isolated microvessels were transferred to a small beaker and minced with scissors.

Membrane Preparation

A membrane preparation was made using the technique of Carter-Su et al. (18). Tissues were resuspended in 10 mM Tris-1 mM EDTA buffer, pH 8.0, containing 0.25 M sucrose and disrupted using a hand-held glass homogenizer with a tight fitting teflon pestle or a tissue sonicator. The solution was centrifuged at 2,000 xg to remove whole cells and vessels and the supernatant was then spun at 30,000 xg to pellet the crude plasma membrane fraction. The tissue pellet was resuspended in 10 mM Tris-1 mM EDTA, pH 8.0, and stored in the freezer at -20°C.

[¹²⁵I]-Insulin Binding Assay

[¹²⁵I]-insulin binding to vascular tissue was determined by centrifugation through oil. Isolated microvessels were centrifuged at 12,500 xg and resuspended in 0.2 ml of assay buffer consisting of KRP buffer, pH 7.76, containing 1% BSA and 1 mM D-glucose. [¹²⁵I]-insulin binding was measured in the presence of 1.0-2.0 ng/ml [¹²⁵I]-insulin and varying concentrations of unlabeled insulin (0.5-5000 ng/ml) at 22°C for 75 minutes with various isolated vascular tissues (100-200 µg protein per tube). Binding was terminated by adding 500 µl dinonylphthalate/dibutylphthalate oil (1:2) and immediately centrifuging at 12,500 xg in a Beckman microfuge for two minutes. An aliquot of 0.05 ml of the supernatant was counted to determine CPM Free [¹²⁵I]-insulin remaining in the medium and the percentage degradation was determined from a similar aliquot. The residual supernatant and oil was aspirated and the cut-off microfuge tube tip containing the tissue pellet was counted in order to determine CPM Bound [¹²⁵I]-insulin. Nonspecific binding, that

is, [^{125}I]-insulin binding to the tissue in the presence of excess unlabeled insulin (50-150 $\mu\text{g/ml}$), was subtracted for all tissues.

The pellet was resuspended in 0.5 ml of 0.1 N sodium hydroxide and digested for 2 hours at 55-60°C for protein and DNA determinations.

Degradation

Intact insulin was precipitated by 5% trichloroacetic acid (TCA) (18). The amount of [^{125}I]-insulin degraded by the various microvascular tissues was determined by adding a 50 μl aliquot of the supernatant from the binding assay to a microfuge tube with 250 μl of assay buffer containing 1% BSA. Following the addition of 300 μl of 10% TCA to precipitate intact peptide hormone, each tube was incubated at 4°C for at least 30 min. The tube was then centrifuged for 2 min at 12,500 $\times g$ and the supernatant immediately decanted into a counting tube. Both the pellet and supernatant were counted in a Beckman 9500 gamma counter for 2 min and the percentage of degradation of [^{125}I]-insulin was calculated by the following formula.

$$\% \text{ degradation} = \frac{\text{CPM (supernatant)}}{\text{total CPM (supernatant + pellet)}}$$

Protein Determination

The amount of protein per pellet was measured using the BioRad protein assay (12). An aliquot (20-100 μl) of the sodium hydroxide digest of the binding assay pellet was neutralized with 0.1 N hydrochloric acid. The volume was adjusted to 100 or 200 μl using

distilled water, and then 5 ml of diluted, filtered BioRad protein dye was added. The absorbance reading at 595 nm on a Bausch & Lomb, Spectronic 20 spectrophotometer was compared with a series of standards prepared using BSA.

Deoxyribonucleic Acid Determination

The amount of deoxyribonucleic acid (DNA) contained in various vascular tissue pellets was determined using a modification of a diphenylamine spectrophotometric method devised by Burton (15). An aliquot of 0.25 ml of the sodium hydroxide digest of the binding assay pellet was further extracted by addition of 0.25 ml of 1 N perchloric acid (PCA) for 45 min at 85°C. The sample was then diluted to 1.0 ml with 0.5 N PCA. Following the addition of 2 ml of a diphenylamine solution, containing glacial acetic acid, sulfuric acid, and aqueous acetaldehyde, the tubes containing a total of 3.0 ml were incubated for 18 hrs at 37°C. The absorbance at 595 nm was measured and compared to a series of standards prepared from perchloric acid-extracted calf thymus deoxyribonucleic acid ranging from 0-100 µg per tube.

[¹⁴C]-Inulin Space Determination

Microvessels were pelleted by centrifugation for 2 min at 12,500 xg and resuspended in KRP buffer, pH 7.76, with 1% BSA and 1 mM D-glucose. Binding was determined in a fashion identical to that used in the [¹²⁵I]-insulin binding assay, except that the radioligand used was [¹⁴C]-inulin, a non-metabolized polysaccharide which is commonly used to measure the amount of extracellular water trapped in tissue slices. The

assay was terminated with centrifugation of the microvessels through oil, as described in the [^{125}I]-insulin binding assay. An aliquot of the supernatant was dissolved in 3.0 ml of liquid scintillation fluid, containing 33% (v/v) Triton X-100 in toluene, 2.0 g/l PPO, and 0.025 g/l POPOP. Minivials were counted in a Beckman Beta Scintillation counter for 10 min. The cut-off microfuge tube tip containing the tissue pellet was likewise dissolved in the Triton-toluene-PPO-POPOP scintillation cocktail and counted. The amount of trapping was calculated by dividing the CPM of [^{14}C]-inulin in the pellet by the total counts of [^{14}C]-inulin per unit volume (CPM/ μl). The volume trapped (μl) was then used to correct for the amount of radioactivity specifically trapped in the [^{125}I]-insulin binding assay tissue pellets.

Dissociation Experiments

With insulin sensitive tissue, labeled insulin binding is a reversible reaction, and labeled insulin dissociates more rapidly on dilution in the presence of native insulin than with buffer alone. Tissue (200-300 μg) was centrifuged at 12,500 $\times g$ and resuspended in 0.25 ml of assay buffer, pH 7.76, containing 1% BSA and incubated with 4.5 ng [^{125}I]-insulin for 75 min at 22°C. Large plastic tubes were used for these experiments. At time 0, a 100-fold excess of ice cold assay buffer (25.0 ml) with and without 100 ng/ml unlabeled insulin was added to the incubation tubes. 5 ml aliquots were immediately removed and filtered using a Gelman filtration apparatus with 45 μm Millipore filters. A parallel experiment was conducted without tissue. At specified times, 5 ml aliquots were removed and filtered. Radioactivity

retained on the filter was measured in a gamma counter and the results were calculated as a percentage of the number of counts retained after initiation of dissociation.

Crosslinking Experiments

The insulin receptor in a variety of tissues can be covalently crosslinked using disuccinimidyl suberate (DSS) by a method devised by Pilch and Czech (98). Crude plasma membranes were prepared from the microvascular tissues by the procedure outlined previously. Tissue pellets containing 400-500 μ g protein were resuspended in 0.50 ml of KRP buffer, pH 7.76, containing 1% BSA and 1 mM D-glucose. Tissue was incubated with 6.6 nM (approx. 0.5 μ Ci) [125 I]-labeled insulin in 20 μ l for 60 min at 22°C with or without excess unlabeled insulin (50-100 μ g/ml) in 25 ml of assay buffer. Membranes were centrifuged at 30,000 xg for 15 min in glass centrifuge tubes, washed in ice-cold KRP buffer without BSA and then centrifuged at 30,000 xg for 15 min in glass centrifuge tubes.

Pellets were resuspended in 0.5 ml KRP, pH 7.4, and 10 μ l of 12.5 mM DSS dissolved in dimethyl sulfoxide was added. Following incubation at 4°C for 15 min, an excess (2.5 ml) of ice-cold 10 mM Tris-1 mM EDTA, pH 8.0, was added to quench the crosslinking reaction and the tissue was incubated an additional 20 min at 4°C. Membranes were centrifuged at 30,000 xg for 15 min, washed in 10 mM Tris-1 mM EDTA and recentrifuged at 30,000 xg for 15 min.

SDS-Polyacrylamide Gel Electrophoresis

Crosslinked membranes were dissolved in a modified Laemmli's sample buffer (74) containing 2% sodium dodecyl sulfate and 50 mM dithiothreitol, boiled 5 min, and centrifuged at 12,500 rpm for 2 min to precipitate any undissolved material. Each sample was subjected to polyacrylamide gel electrophoresis according to the procedure of Laemmli (74) for approximately five hours at 20-30 mA per gel, using a 4% acrylamide stacking gel and a 7.5% acrylamide separating gel. Following staining with Coomassie Brilliant blue dye and destaining, gels were dried on a BioRad gel drier using a cellophane cover.

Determination of Molecular Weight

High molecular weight standards were purchased from BioRad. A 1:200 dilution of standards with sample buffer was boiled for 5 min and a 50 μ l sample was applied to one lane on each slab gel. Molecular weights of unknowns were determined by comparing the R_f value with a standard line constructed using the R_f values for each standard (129).

Autoradiography

Autoradiography was performed on dried gels, using Kodak XAR-5 X-ray film with two Dupont Cronex Lightning Plus intensifying screens, in a freezer at -70°C for approximately one week. Autoradiographs were developed in an automatic X-ray film processor.

IV. RESULTS

Isolation of Microvessels

It has been previously shown by Meezan and colleagues (88) that cerebral and retinal microvessels can be isolated by gentle homogenization followed by selective sieving, as outlined in Fig. 2. This procedure is based upon the principle that nonvascular material is more susceptible to complete homogenization than is vascular tissue. Vascular tissue is retained on the nylon sieve and gently removed with a slow stream of buffer. After the first homogenization, a considerable amount of nonvascular material is retained on the sieve along with the vascular material. For this reason, several additional homogenizations were performed to eliminate contaminating material from the microvascular material. Contamination with nonvascular material is a more serious problem in the isolation of cerebral cortical microvessels since there is considerably more tissue to deal with and white matter resists complete homogenization and is retained on the sieve. This problem can be overcome with repeated homogenization. This procedure has the advantage of avoiding the use of collagenase and it produces adequate yield of viable microvessels for these experiments.

Brains and eyes from adult cattle were obtained from the slaughterhouse three times a week. Tissue was placed on ice ten to fifteen minutes following decapitation. The bovine brains and eyes were received in the laboratory between one and three hours later. The

FIGURE 2

Procedure for Isolation of Microvascular Tissue

The cerebral cortex of adult cattle or neonatal pigs was used for microvessel isolation. Bovine retinal microvessels are prepared in a like manner, with the use of a nylon sieve of a smaller pore size. Preparations were inspected using a light microscope for purity and rehomogenization was performed three to five times to minimize contamination with nonvascular material.

Cerebral Cortex

remove pia and surface vessels
(from cerebral cortex)

scrape off gray matter

place in glass homogenizer with loose fitting teflon pestle

homogenize with 10 up/down strokes in KRP-0.01% BSA on ice

filter non-microvascular components through
nylon sieve with 153 micron openings

wash vascular tissue off sieve

rehomogenize vascular material with 10 up/down strokes

filter on nylon sieve with 153 micron openings

rinse microvessels off sieve and suspend in ice cold KRP-0.1% BSA (approx. 5 ml)

Retina

gently remove retina

rinse off dark pigment

place in glass homogenizer with loose fitting teflon pestle

homogenize with 10 up/down strokes in KRP-0.01% BSA on ice

filter non-microvascular components through
nylon sieve with 86 micron openings

wash vascular tissue off sieve

rehomogenize vascular material with 10 up/down strokes

filter on nylon sieve with 86 micron openings

neonatal porcine brains were excised from the animal immediately after the animal was sacrificed in the laboratory. Therefore, the porcine tissue was not subjected to lengthy periods of anoxia prior to isolation.

Despite the differences in the tissues from which the microvessels were isolated, the three microvascular preparations are very similar upon visual inspection, as depicted in Fig. 3. It can be seen that the microvessels are composed primarily of small capillaries with luminal diameters of 8-10 microns. The appearance of these microvessels closely resembles the preparations characterized by Meezan and colleagues (88). The technique used to isolate microvessels does not exclude contamination by arterioles and venules. However, visual inspection of these preparations clearly shows that capillaries comprise greater than 90% of the material present. Electron microscopic examination of the microvascular preparations confirms the presence of red blood cells in the lumens of these vessels. It has been calculated by Meezan et al. (88) that the number of red blood cells present in an aliquot of these microvessels is sufficiently small to preclude any significant contribution to [125 I]-insulin binding by this preparation.

The quantity of microvessels which can be isolated from the various tissues is presented in Table 1. The wet weight of the gray matter and retinas was obtained by placing the tissues in a preweighed beaker. Microvessels were isolated and wet weights determined by centrifuging the microvessels at approximately 2250 xg for 5 min in a preweighed plastic tube. Approximately 1.7% of the weight of the retina can be recovered as microvessels by this isolation procedure. Between 0.5% and 0.8% of the gray matter can be isolated as microvessels. However, this

FIGURE 3**Phase Contrast Micrograph of Isolated Microvascular Tissue**

Microvessels from bovine brain, bovine retina and neonatal porcine brain closely resemble one another in size and the degree of branching. Dark Bar (—) in lower figure indicates 30 μm . (Magnification = 153x).



**BOVINE CEREBRAL
MICROVESSELS**



**BOVINE RETINAL
MICROVESSELS**



**PORCINE CEREBRAL
MICROVESSELS**

TABLE 1

Wet Weights of Isolated Microvascular Tissues

Tissue	Gray Matter/Retina	Microvessels
Bovine Brain (ADULT)	175.0 \pm 9.6 g	0.75 \pm 0.11 g
Porcine Brain (NEONATAL)	8.7 \pm 0.5 g	0.07 \pm 0.01 g
Bovine Eyes (10) (ADULT)	8.4 \pm 1.8 g	0.14 \pm 0.03 g

Microvessels were isolated by the method outlined in Fig. 2. Brains and eyes were obtained from adult male and female cattle weighing from 400 to 1100 pounds total body weight. They ranged from 8 months to 2 years of age. Wet weight of gray matter is approximately 40% of the wet weight of the cerebral cortex. Neonatal pigs were from 1 to 6 days of age and weighed approximately 5 to 10 pounds. Data represents the mean \pm standard deviation from three separate groups of animals.

technique is not designed to recover 100% of the microvessels which are present in the tissue. Therefore, these figures underestimate the total amount of microvessels present in the gray matter of the cerebral cortex and bovine retina.

Insulin Binding to Isolated Microvascular Tissue

[¹²⁵I]-Insulin Binding Assay

Specific binding of [¹²⁵I]-insulin was measured in isolated bovine cerebral and retinal microvessels and cerebral microvessels from neonatal pigs, according to the procedure outlined in Fig. 4. It was necessary to determine the protein content in each assay tube following centrifugation through the oil layer to verify that the amount of microvessels in each assay tube was sufficient for the insulin binding assay.

This method was used because it gives a better separation of bound from free [¹²⁵I]-insulin, due to the presence of a non-aqueous barrier between the [¹²⁵I]-insulin bound to the tissue and the radioactivity remaining in the supernatant layer. However, centrifugation through an oil layer can cause several problems. Most of the problems consist of incomplete pelleting of the entire tissue or incomplete separation of the supernatant layer from the oil layer. These problems were overcome by adjusting the ratio of dinonylphthalate and dibutylphthalate oil until good separation was achieved. The optimum ratio was found to consist of 1:2 dinonylphthalate:dibutylphthalate. It was also important to maintain the ratio of the volume of supernatant to oil so that the amount of oil was greater than twice the supernatant volume. This

FIGURE 4

Insulin Binding Assay

Insulin binding was measured by incubating [^{125}I]-insulin with isolated microvascular tissue according to the procedure described in the text. Following incubation in KRP buffer, pH 7.75, containing 1% BSA, [^{125}I]-insulin bound to the microvessels was separated from unbound (free) insulin by the addition of 1:2 dinonylphthalate/dibutylphthalate oil and centrifugation. An aliquot of the top layer was counted and also used to determine the percentage of degradation of [^{125}I]-insulin. The pellet was counted to determine bound [^{125}I]-insulin and digested in 0.5 ml of 0.1 N NaOH in order to determine the protein and DNA content.

Insulin Binding Assay

Tissue

 $[^{125}\text{I}]$ -insulin (0.25 ng, approx. 36,000 cpm)

+/- insulin (0.1 ng- 30 ug)



Incubate 75 min at 22°C

Add oil

Centrifuge 12,500 xg, 2 min

Free insulin

Oil

Bound insulin



prevents the supernatant layer from getting under the oil layer when transferring the tube from the microfuge to the microfuge tube holder. This is an important consideration when using a horizontal fixed angle microfuge, such as a Beckman B. It was also found that increasing the time of centrifugation from 1 min to 2 min or more facilitated complete separation of the tissue from the oil layer. Some preparations of bovine cerebral microvessels were difficult to sediment as a tightly packed pellet but this phenomenon was not observed consistently.

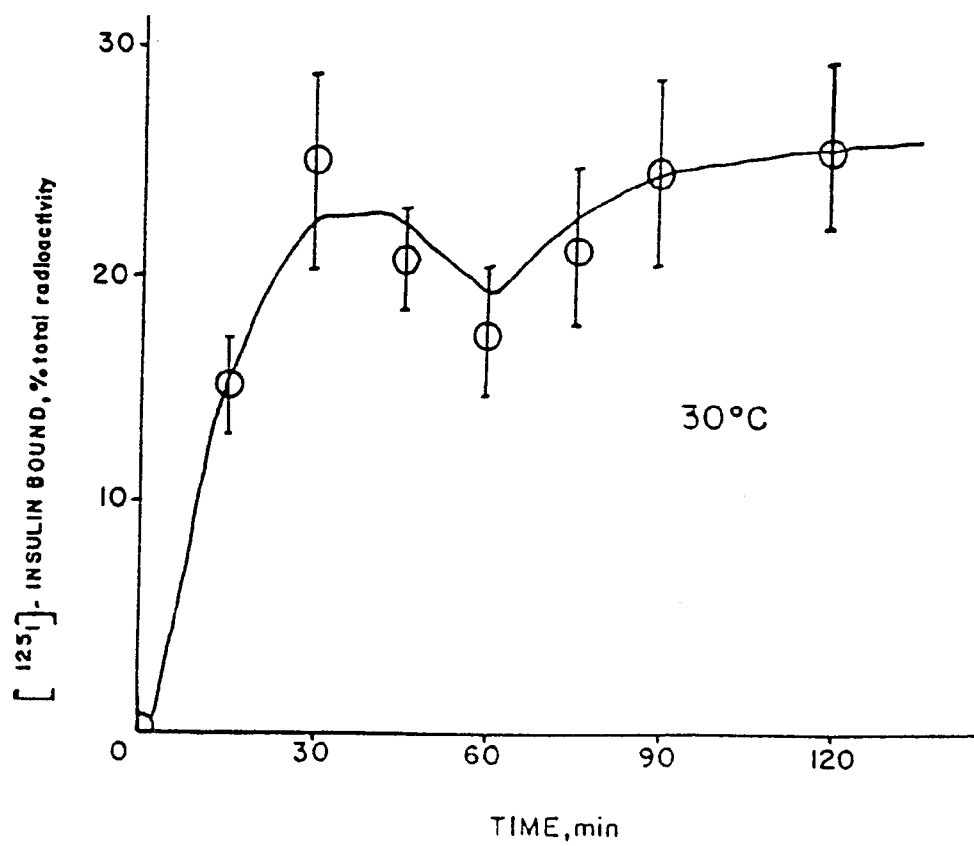
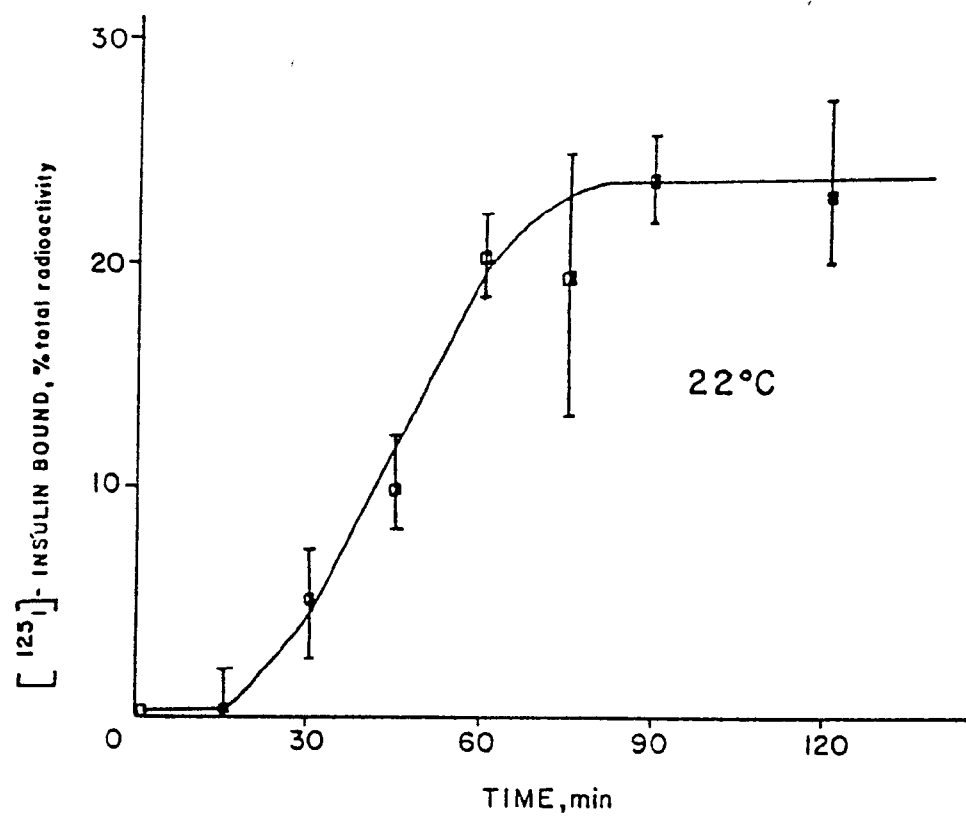
Effect of Protein Concentration

Nonspecific binding of insulin was measured in the presence of 50-150 g/ml unlabeled insulin and calculation of the difference in the total and nonspecific [^{125}I]-insulin was taken as the measure of the specific binding of [^{125}I]-insulin. As shown in Fig. 5, specific binding was found to be linear as a function of the concentration of protein in the sample of frozen retinal microvessels. Similar results were found for freshly isolated bovine retinal microvessels and porcine cerebral microvessels. The capacity of the microvessels to bind insulin was not destroyed by storing tissue frozen in KRP buffer for several days at -20°C . Therefore, frozen tissue can be used in binding studies. When using frozen preparations, following thawing, the microvessels were sedimented by centrifugation for 2 min at 12,500 xg and the supernatant discarded. Since results of binding experiments are expressed per mg protein and the intracellular protein lost from microvessel preparations during freezing and thawing contributes to the total protein but not to the binding activity, binding appears higher in frozen tissue than in fresh tissue. However, in parallel studies, the microvessels were not

FIGURE 5

[¹²⁵I]-Insulin Binding to Retinal Microvessels as a Function of Protein Concentration

Frozen retinal microvessels were thawed, centrifuged for 2 min at 12,500 xg and the supernatant discarded. Microvessels were resuspended in KRP buffer, pH 7.75, containing 1% BSA and 1 mM glucose. Tissue was incubated for 90 min at 22°C with 1.5 ng/ml [¹²⁵I]-insulin with and without excess unlabeled insulin (150 ug/ml). Specific binding was determined by subtracting nonspecific binding from the total binding, as described in the text. Data represent the mean of triplicate samples from two separate experiments (- o -) (- Δ -).



centrifuged prior to determination of binding, so protein concentrations were similar and the amount of total, nonspecific and specific [^{125}I]-insulin binding was not significantly different between the fresh and frozen preparations (data not shown).

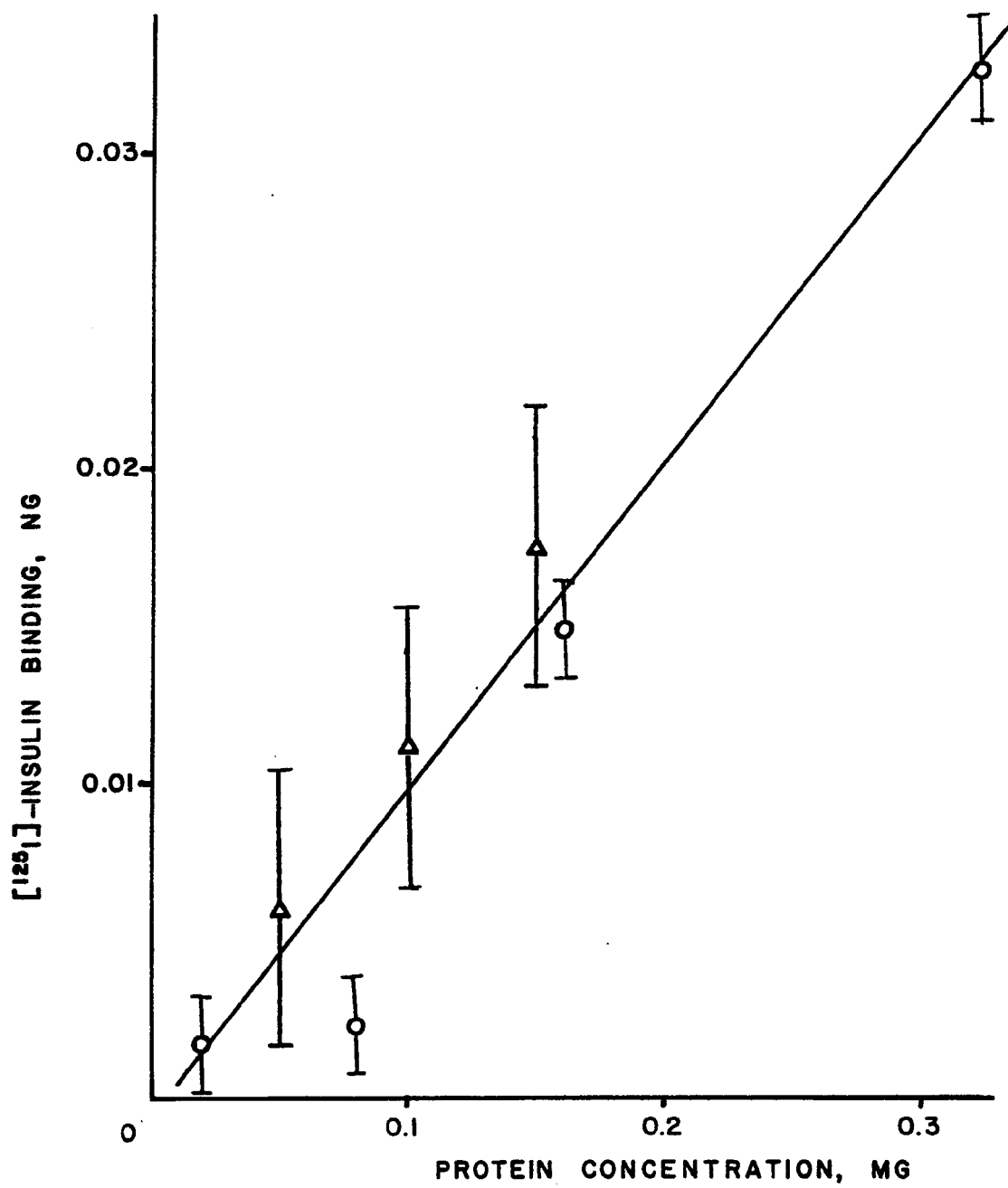
Effect of Time and Temperature

The effect of incubation time and temperature was examined with the microvascular tissue preparations. Fig. 6 demonstrates the effect of incubation time and temperature on specific [^{125}I]-insulin binding to frozen bovine cerebral microvessels. At 22°C, steady-state binding is achieved after 75 min. It was observed that one-half maximal insulin binding occurs in approximately 45 min. Binding is more rapid at 30°C and maximal binding has occurred by 20 min. Comparable results were found in isolated bovine retinal microvessels and porcine cerebral microvessels. The time course of insulin binding was found to be similar in all three tissues when comparing a 30 min incubation at 30°C or 75 min at 22°C. The time course of insulin binding was also measured in plasma membranes prepared from frozen bovine cerebral microvessels. At 20°C, maximal binding occurs after 60 min, with one-half maximal binding occurring after approximately 40 min. At 4°C, binding was very slow, with little measurable binding occurring after 150 min. After 4 hours, however, approximately 60% of maximal binding (that at 22°C for 60 min) could be measured. Binding at higher temperatures was more rapid for all microvascular preparations examined. A slight decrease in the amount of specific binding at 30°C was observed between 45 and 75 min. This phenomenon has also been reported in the literature for insulin binding in liver plasma membranes by Almira and Reddy (1).

FIGURE 6

Effect of Incubation Time and Temperature on Specific Binding of [125 I]-Insulin to Bovine Cerebral Microvessels

Frozen isolated bovine cerebral microvessels were incubated with 1.5 ng/ml [125 I]-insulin with and without 100 ug/ml unlabeled insulin at 22°C (- □ -) or 30°C (- O -), as indicated in the figure. The specific binding of [125 I]-insulin was determined at the time indicated. Each point represents the mean of triplicate determinations.



Characterization of Insulin Binding

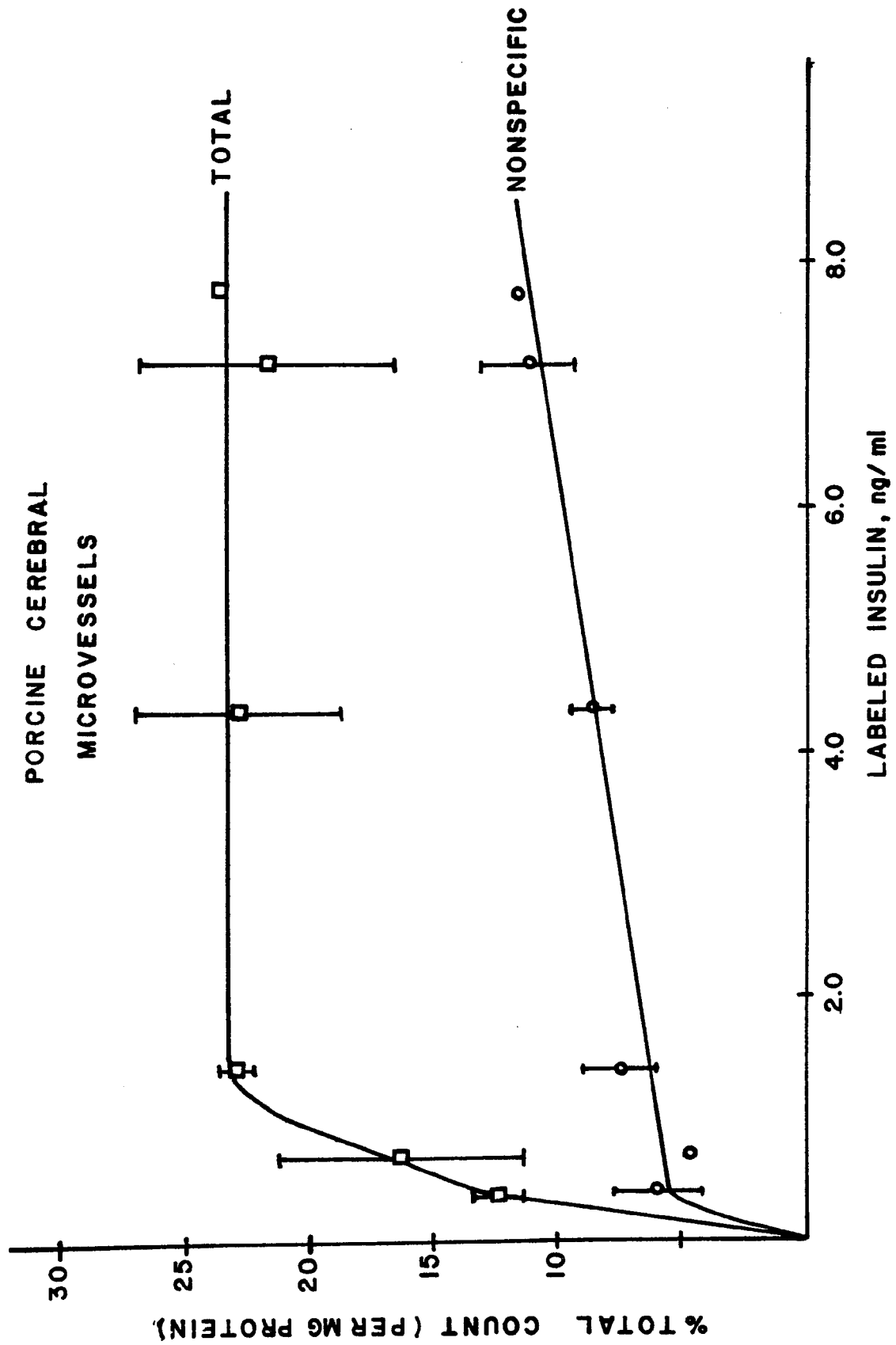
Saturation of [^{125}I]-insulin binding to cerebral microvessels isolated from neonatal pigs occurs at approximately 1.5 ng/ml [^{125}I]-insulin, as shown in Fig. 7. Nonspecific binding continues to increase in a linear fashion as increasing amounts of labeled insulin are incubated with freshly isolated porcine cerebral microvessels. This saturating concentration of labeled insulin corresponds to the amount chosen for the binding studies described in this dissertation. For this reason, as well as for economic considerations, higher levels of [^{125}I]-insulin were not used.

Several different assay buffers were investigated during the course of this study of insulin binding in microvascular tissue. [^{125}I]-Insulin binds equally well to bovine cerebral and retinal microvessels in KRP buffer described in the Methods section and in the assay buffer described by Olefsky and colleagues (92, 93) containing 35 mM Tris, 120 mM sodium chloride, 1.2 mM magnesium sulfate, 2.5 mM potassium chloride, 10 mM glucose, 1 mM ethylene diamine tetraacetic acid and 1% w/v bovine serum albumin. The effect of pH on insulin binding was also studied and results are comparable with those reported for other insulin receptors. [^{125}I]-Insulin binds poorly below pH 7.0 and the optimum pH for insulin binding in isolated microvessels appears to be between pH 7.6 and 8.0. Most of the binding studies reported in this dissertation were performed in KRP buffer, pH 7.75, containing 1% BSA and 1 mM glucose. Bovine serum albumin must be free of any insulin-like impurities. Radioimmunoassay confirmed the existence of an insulin-like impurity in one batch of BSA used in one experiment. Glucose was included in the assay media because the microvessels appear to bind labeled insulin with less

FIGURE 7

Effect of Variable Concentrations of [125 I]-Insulin on Insulin Binding to Neonatal Porcine Cerebral Microvessels

Cerebral microvessels from neonatal pigs were incubated in Krebs Ringer phosphate buffer, pH 7.75, containing 1% BSA and 1 mM glucose, with increasing amounts of [125 I]-insulin (0.75 to 8.0 ng/ml) with and without excess unlabeled insulin for 90 min at 22°C. Bound insulin was separated from free insulin, as described in the text, and the protein content determined in each pellet. Values were normalized per mg protein prior to calculating percentage of total radioactivity bound. Results represent the mean \pm standard deviation of triplicate determinations of each [125 I]-insulin concentration.



intraassay variation in the presence of a small amount of glucose. It is felt that any effect of glucose on insulin binding may possibly be an empirical requirement for this in vitro system, but a physiological role for glucose in the binding interaction has not been ruled out.

The binding of [^{125}I]-insulin to retinal and cerebral microvessels has been quantitated in several different ways. The data in Table 2 demonstrate the results of [^{125}I]-insulin binding to the three tissues, expressed as picograms insulin bound per milligram protein. Little significant variation was observed in the amount of labeled insulin bound to the two cerebral cortical microvascular preparations. Isolated retinal microvessels tended to have a slightly greater amount of displacement of [^{125}I]-insulin in the presence of small amounts of unlabeled insulin when compared with the cerebral microvessels from adult cattle and neonatal pigs ($p < 0.05$). When binding results were analyzed using the Student's t test, it was found that specific [^{125}I]-insulin binding in retinal microvessels is significantly different from brain microvessels at the 0.01 level. However, neither total nor nonspecific binding was significantly different at the 0.01 level. Following the binding assay, the microvessels were centrifuged and the pellets were digested in 0.1 N sodium hydroxide, for determination of protein and deoxyribonucleic acid content. The results of these experiments yielded a linear relationship between the amount of protein per pellet and the amount of DNA per pellet. The data in Table 3 were calculated from the data in Table 2, based on this linear function. Conversion from pg insulin bound/mg protein to pg insulin bound per mg DNA was based on the assumption that 0.135 mg DNA was present in 1 mg

TABLE 2

[¹²⁵I]-Insulin Binding to Isolated Microvessels per mg Protein

Tissue	Total Binding pg/mg protein	Nonspecific Binding pg/mg protein	Specific Binding Protein
Bovine Cerebral Microvessels	55.9 ± 14	30.8 ± 7.2	25.1 ± 7.4
Bovine Retinal Microvessels	65.4 ± 16.5	23.8 ± 5.2	42.6 ± 12.9
Porcine Cerebral Microvessels	44.7 ± 19.4	20.26	24.3 ± 12.0

Tissues were incubated for 75 min at 22°C in KRP buffer, pH 7.75, containing 1% BSA and 1 mM glucose, as previously described. Insulin binding was determined following centrifugation through oil. Pellets were counted for 2 min in a Beckman gamma counter and expressed as pg/mg progein. Total binding minus nonspecific binding equals specific binding. Nonspecific binding is defined as [¹²⁵I]-insulin binding per mg protein in tubes incubated in the presence of 100 µg/ml unlabeled insulin. Values are the mean ± standard deviation of triplicate determinations from three separate experiments.

TABLE 3

[¹²⁵I]-Insulin Binding to Isolated Microvessels per mg DNA

Tissue	Total pg/mg DNA	Nonspecific pg/mg DNA	Specific Binding pg/mg DNA	Specific Binding pg/10 ⁶ cell
Bovine Cerebral Microvessels	414	228	186	10.5
Bovine Retinal Microvessels	484	176	315	17.7
Porcine Cerebral Microvessels	331	150	180	9.9

Values from Table 2 were converted to per mg DNA, based on a linear relationship, $y = 0.135 - .002x$, $r = .993$, between protein and DNA content per 0.1 N NaOH digest of tissue pellets. Conversion was based on 0.135 mg DNA per mg protein. Assume: 6.2 μ g DNA per 10⁶ cells.

protein. If it is assumed that there are approximately 6.2 μg DNA per 10^6 cells, then specific binding ranged from 9-18 pg labeled insulin per 10^6 cells.

[^{14}C]-Inulin Trapping in Microvessels

The amount of [^{125}I]-insulin trapped in the extracellular water space of the microvessel pellet was calculated by measuring the amount of [^{14}C]-inulin retained by the different microvascular tissue preparations. A large proportion of the nonspecific [^{125}I]-insulin binding observed in Fig. 7 was found to be related to trapping, as shown in Table 4. Fresh microvessels appear to trap more radioactivity than microvessels which were frozen prior to incubation. The amount of trapping also increases with the protein content of the tissue pellet. Porcine cerebral microvessels appear to trap more radioactivity than bovine cerebral and retinal microvessels. Since nonspecific binding was subtracted from total insulin binding and the amount of trapping was less than the nonspecific binding, it was not necessary to correct specific binding for the amount of radioactivity trapped in the tissue pellet. The trapped radioactivity, however, does explain the large percentage of total binding that is not displaced by an excess amount of unlabeled insulin. A high percentage of nonspecific binding is normally present in most insulin binding assays involving whole tissues instead of isolated cells or membrane preparations.

TABLE 4

[¹⁴C]-Inulin Trapping in Tissue Pellets

Tissue		mg protein	% Total Counts trapped	Volume trapped (μ l)
Bovine Cerebral Microvessels	Fresh	0.2	3.3%	6.7 \pm 0.7
	Frozen	0.2	1.1%	2.2 \pm 0.4
Bovine Retinal Microvessels	Fresh	0.4	2.5%	4.9 \pm 1.1
	Frozen	0.2	1.7%	3.3 \pm 0.5
Porcine Cerebral Microvessels		0.1	2.3%	4.7 \pm 0.5
	Fresh	0.2	4.4%	8.7 \pm 0.7
		0.4	4.9%	9.7 \pm 0.4

Trapping was determined by incubating tissues at 22°C for 75 minutes using the same method as for determination of insulin binding. Results are from triplicate determinations of pellets dissolved in 1% Triton X-100-toluene-PPO-POP scintillation cocktail and counted 10.0 minutes in a Beckman B-counter.

Insulin Degradation in Microvessels

Degradation of insulin was measured by TCA precipitation of an aliquot (50 μ l) of the supernatant of the insulin binding samples. 5% TCA is sufficient to precipitate all intact insulin molecules. Proteolytic fragments of insulin and individual amino acids are not precipitated under these conditions. As shown in Tables 5 and 6, insulin degradation by retinal microvessels appears to increase as a function of protein concentration. Degradation is greater at 30°C than it is at 22°C (data not shown), and it increases with incubation time. Little degradation of [125 I]-insulin occurs in the presence of excess unlabeled insulin (50-150 μ g/ml). In most cases, degradation of [125 I]-insulin which occurred in assay tubes containing buffer and no tissue was equivalent to the amount of degradation in assay tubes containing microvessels and excess unlabeled insulin (50-150 μ g/ml). For most binding studies with bovine cerebral and retinal microvessels, degradation of [125 I]-insulin was less than 2.0% and thus the results were not corrected for degradation. Isolated cerebral microvessels from neonatal pigs appear to degrade [125 I]-insulin much more readily and caution is advised when incubating this tissue at 30°C for longer than 30 min. Degradation should be determined for each assay tube and binding results corrected for the amount of degradation when incubation time is in excess of 30 min at 30°C for all three preparations.

TABLE 5

[¹²⁵I]-Insulin Degradation in Bovine Retinal Microvessels:
Concentration Curve

Protein	% Degradation
0.08 mg	1.4 ± 0.5
0.15 mg	4.5 ± 0.6
0.32 mg	7.7 ± 0.5

Degradation of [¹²⁵I]-insulin was determined in fresh bovine retinal microvessels incubated at 30°C for 45 minutes in Krebs Ringer phosphate, pH 7.76, containing 1% BSA and 1 mM glucose. Degradation was determined in 50 µl aliquots of the supernate from triplicate samples by precipitation of intact protein in 5% TCA. Degradation in assay tubes containing an excess of unlabeled insulin were equivalent to degradation in assay tubes containing no microvessels. This background was subtracted from values presented.

TABLE 6

[¹²⁵I]-Insulin Degradation in Bovine Retinal Microvessels: Time Response

Time, min	% Degradation	[¹²⁵ I]-Insulin Degradation	
		Femtamoles per pellet	Femtamoles per mg protein
15	0	0	0
30	1.8 ± 0.4	1.0	2.3
60	5.3 ± 0.8	3.0	6.6
90	9.2 ± 0.5	5.1	12.2

Degradation was measured by TCA precipitation of degraded [¹²⁵I]-insulin in assay tubes incubated with fresh bovine retinal microvessels, as described in Table 5. Data represent mean of triplicate determinations. Background was subtracted from values presented.

Competitive Displacement Experiments

As shown in Tables 7, 8 and 9, isolated microvessels bind [^{125}I]-Insulin specifically and this binding can be displaced in a dose-dependent manner with unlabeled porcine insulin. In general, both bovine and porcine cerebral microvascular tissue preparations behaved similarly with respect to labeled insulin binding studies and competitive displacement experiments. [^{125}I]-Insulin binding to isolated bovine retinal microvessels tends to be more easily displaced with slightly lower unlabeled insulin concentrations. The results in Table 7 represent [^{125}I]-insulin binding to bovine cerebral microvessels which were stored frozen after isolation, and prior to assay for binding activity, thawed, centrifuged at 12,500 xg for 2 min and the supernatant discarded. Insulin binding to this preparation appears substantially higher, when expressed as pg insulin bound per mg protein, than the binding reported in Table 2 for freshly isolated bovine cerebral microvessels. This is due to a lower protein concentration in the frozen tissue pellets due to loss of intracellular protein.

Bovine cerebral microvessels were incubated with 1.5 ng/ml [^{125}I]-insulin and various concentrations of unlabeled porcine insulin for 75 min at 22°C. As shown in Fig. 8, the inhibition of [^{125}I]-insulin binding was expressed as a percentage of the initial labeled insulin binding. Binding is clearly shown to be inhibited by the unlabeled insulin in a dose-dependent manner. A 50% decrease in binding is achieved at approximately 4.0 nM unlabeled insulin. When Scatchard analysis was performed on this data, a curvilinear plot was obtained, as shown in Fig. 9. Using graphical

TABLE 7

[¹²⁵I]-Insulin Binding to Isolated Bovine Cerebral Microvessels

Unlabeled insulin (ng/ml)	Specific Bound (ng [¹²⁵ I]-insulin/mg protein)	% Maximum Binding
0	.151	100
9	.104	68.9
100	.036	23.8
1,000	.017	11.3

Frozen cerebral cortical microvessels (0.1-0.2 mg protein) were incubated with 2.5 ng/ml [¹²⁵I]-insulin and various concentrations of unlabeled insulin for 75 min at 22°C. Nonspecific binding was determined in the presence of 10 µg/ml unlabeled insulin and subtracted from all binding values to yield specific binding.

TABLE 8

[¹²⁵I]-Insulin Binding to Isolated Bovine Retinal Microvessels

Unlabeled Insulin (ng/ml)	Specific Bound (ng [¹²⁵ I]-insulin/mg protein)	% Maximum Binding
0	.053	100
0.5	.041	78.3
5	.025	48.4
50	.004	8.4
500	.001	2.5

Freshly isolated retinal microvessels (0.1 to 0.2 mg protein/sample) were incubated with 2.5 ng/ml [¹²⁵I]-insulin (0.1 μ Ci) for 75 min at 22°C in the presence of various concentrations of unlabeled insulin. Nonspecific binding was subtracted from all values. The data represent the mean values from triplicate determinations.

TABLE 9

[¹²⁵I]-Insulin Binding to Isolated Porcine Cerebral Microvessels

Unlabeled Insulin (ng/ml)	Specific Bound (ng [¹²⁵ I]-insulin/mg protein)	% Maximum Binding
0	.0225	100
5	.018	78.8
50	.011	47.7
500	.008	37.1
5000	.003	19.5

Freshly isolated cerebral microvessels from neonatal pigs (0.1-0.2 mg protein per sample) were incubated for 30 min at 30°C with 1.5 ng/ml [¹²⁵I]-insulin in the presence of various concentrations of unlabeled insulin. Nonspecific binding was determined in the presence of 100 µg/ml labeled insulin and subtracted from each value. The data represent the mean values of triplicate determinations from two separate assays.

FIGURE 8

**Inhibition of Specific [125 I]-Insulin Binding
to Bovine Cerebral Microvessels**

Isolated bovine cerebral microvessels were incubated for 75 min at 22°C with 1.5 ng/ml [125 I]-insulin, as described in the text. Binding was determined in the presence of various concentrations of unlabeled insulin. Nonspecific binding was defined as the amount of binding present when tissue was incubated with 100 μ g/ml of unlabeled insulin and subtracted from all values. Results represent means of triplicate determinations from three separate experiments and the binding values are expressed as a percentage of the maximal [125 I]-insulin binding.

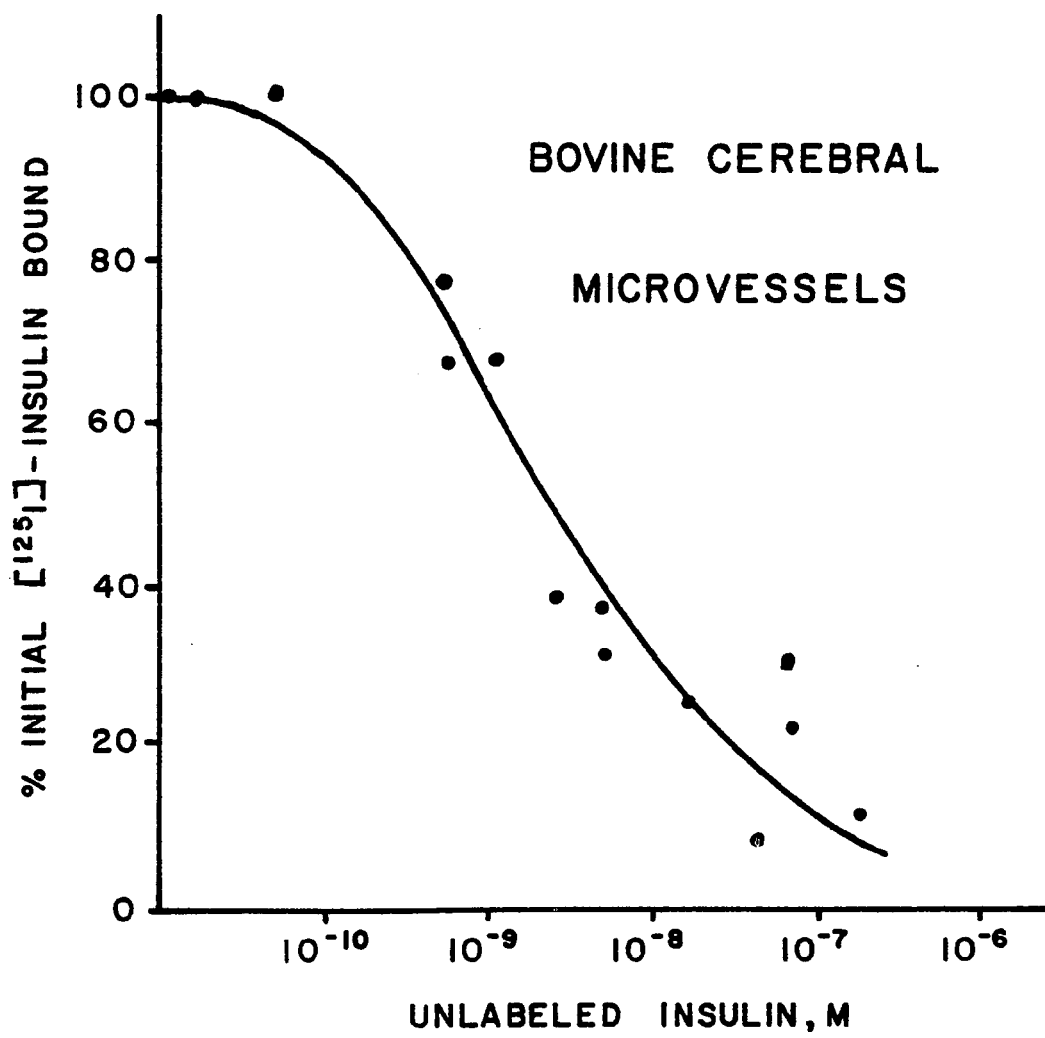
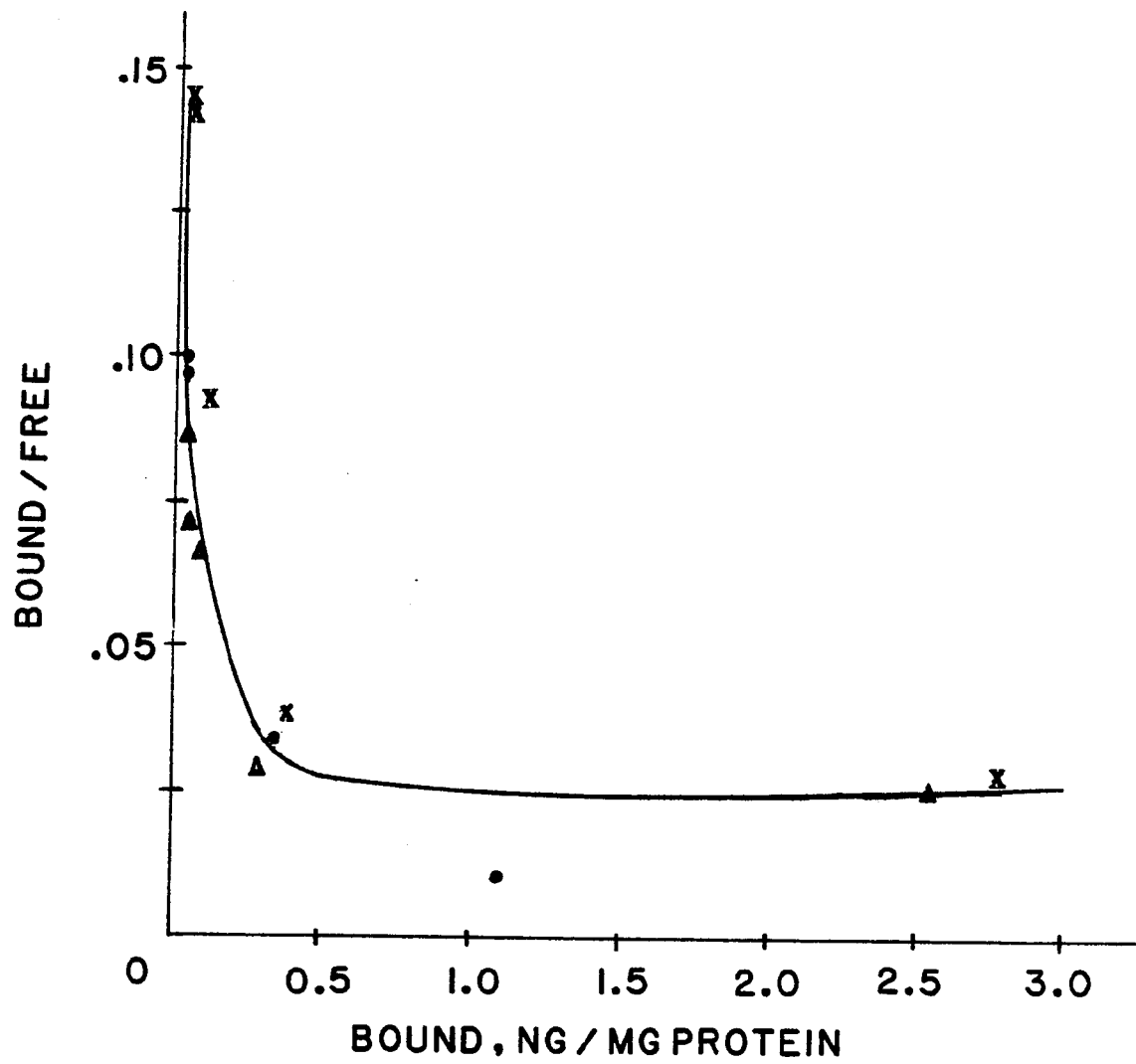


FIGURE 9

Scatchard Analysis of [125 I]-Insulin Binding to
Bovine Cerebral Microvessels

[125 I]-Insulin binding was carried out as described in the text. Bovine cerebral microvessels (0.1 - 0.2 mg protein) were incubated with 1.5 ng/ml [125 I]-insulin for 75 min at 22°C in the presence of varying concentrations of unlabeled insulin. Nonspecific binding was determined in the presence of 100 μ g/ml unlabeled insulin and subtracted from all binding values. Results are expressed as means of triplicate determinations from three separate assays.



in IM-9 Lymphocytes, a dissociation constant of 0.33 nM was calculated for the high affinity receptor. The binding capacity corresponds to 0.027 pmoles [125 I]-insulin per mg protein.

Competitive displacement experiments were similarly performed with freshly isolated bovine retinal microvessels and freshly isolated cerebral microvessels from neonatal pigs. Results of experiments in which [125 I]-insulin was incubated with bovine retinal microvessels and various concentrations of unlabeled insulin are presented in Table 8 and Figs. 10 and 11. A 50% decrease in [125 I]-insulin binding is achieved at approximately 0.8 nM. Scatchard analysis of this data is shown in Fig. 11. Assuming the two site hypothesis, the high affinity site was calculated to have a dissociation constant of 0.33 nM and a binding capacity of 0.039 pmoles per mg protein. Results of competitive binding experiments with porcine cerebral microvessels are shown in Table 9 and Figs. 12 and 13. A 50% decrease in binding is achieved at approximately 5.0 nM unlabeled insulin. The shape of the inhibition curve for porcine cerebral microvessels (Fig. 12) is more similar to that seen with bovine cerebral microvessels (Fig. 10). The Scatchard analysis, shown in Fig. 13, yields a curvilinear plot with a dissociation curve for the high affinity site of 0.34 nM and a binding capacity of 0.066 pmoles per mg protein. [125 I]-Insulin binding capacities and dissociation constants for the high affinity, low capacity site are summarized in Table 10. Dissociation constants were calculated using linear regression analysis based on at least five points with ordinate values between 0.05 and 0.10 (Bound/Free ratio).

FIGURE 10

**Inhibition of Specific [125 I]-Insulin Binding to
Bovine Retinal Microvessels**

Isolated bovine retinal microvessels were incubated for 30 min at 30°C with 1.5 ng/ml [125 I]-insulin, as described in the text. Binding was determined in the presence of various concentrations of unlabeled insulin. Nonspecific binding was defined as the amount of binding present when the tissue was incubated with 100 μ g/ml of unlabeled insulin and the nonspecific binding thus determined subtracted from all values. Results represent means of triplicate determinations from three separate experiments. Binding values are expressed as percentage of the maximal [125 I]-insulin binding.

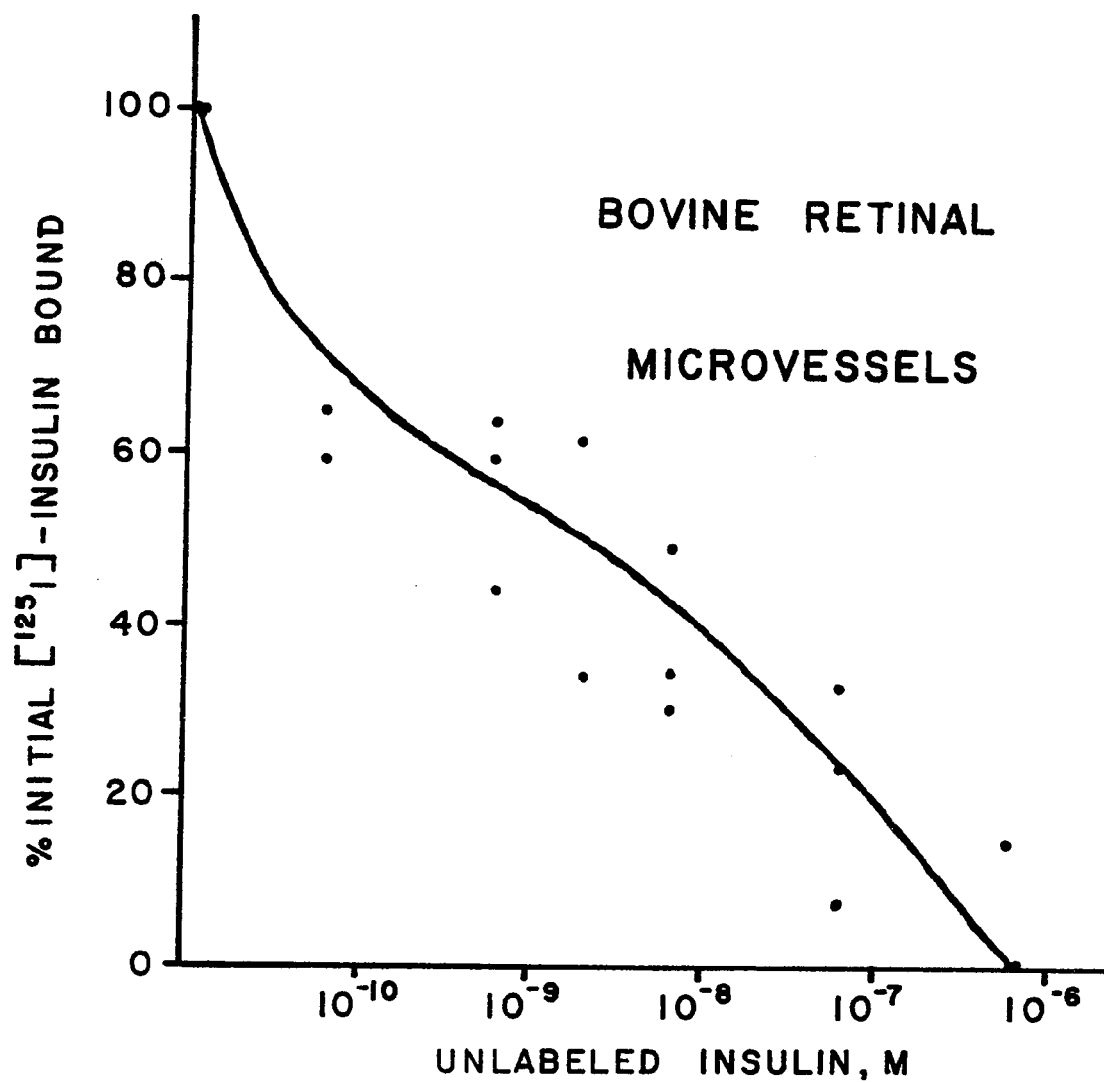


FIGURE 11

Scatchard Analysis of [^{125}I]-Insulin Binding to
Bovine Retinal Microvessels.

Bovine retinal microvessels were incubated for 30 min at 30°C with 1.5 ng/ml [^{125}I]-insulin, as described previously. [^{125}I]-Insulin binding was determined in the presence of various concentrations of unlabeled insulin. Nonspecific binding was subtracted from each point. Results represent pooled data from five experiments.

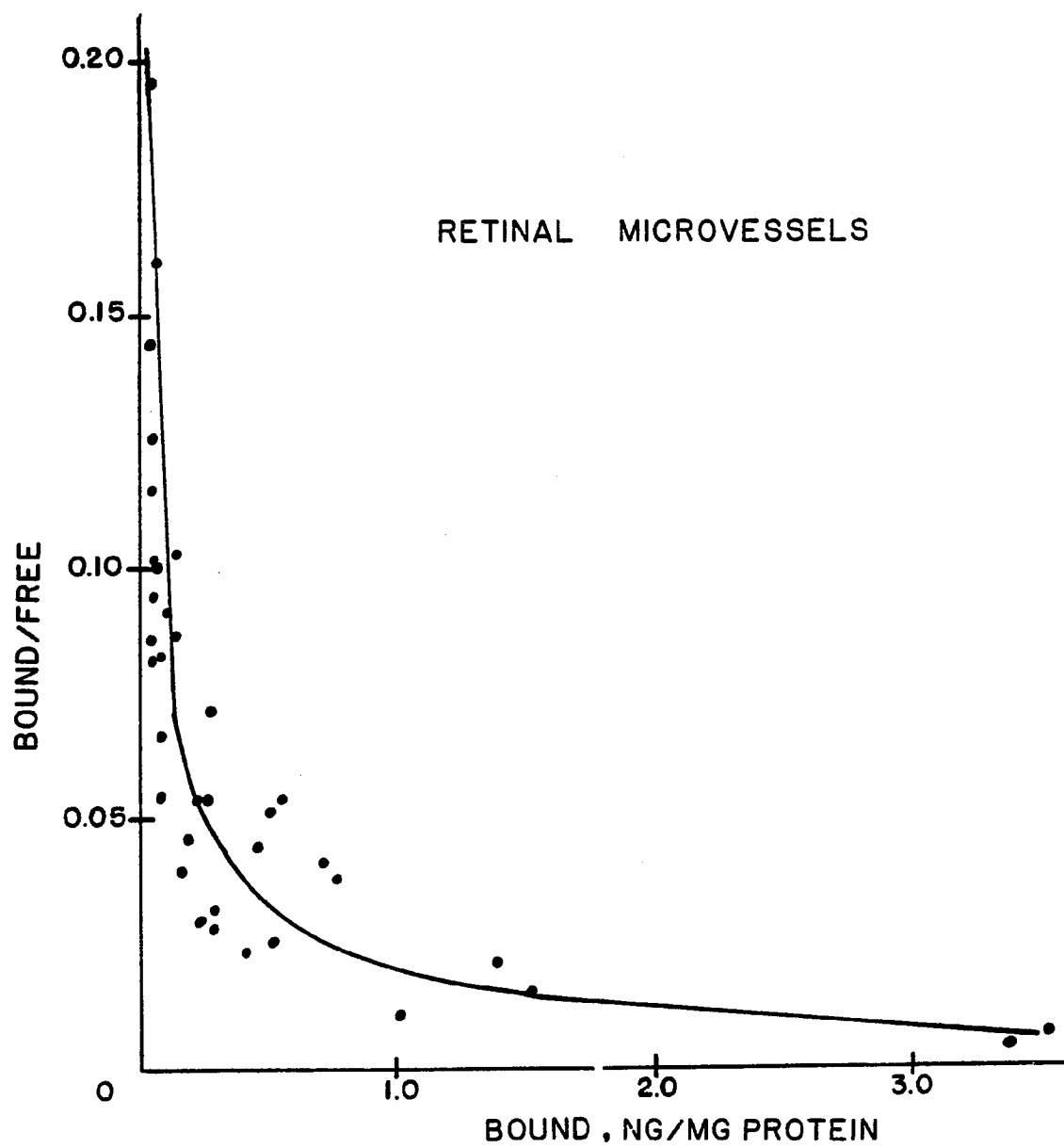


FIGURE 12

**Inhibition of Specific [^{125}I]-Insulin Binding
to Porcine Cerebral Microvessels**

Isolated cerebral microvessels from neonatal pigs were incubated for 30 min at 30°C with 1.5 ng/ml [^{125}I]-insulin, as described in the text. Binding was determined in the presence of various concentrations of unlabeled insulin and nonspecific binding in the presence of 100 µg/ml unlabeled insulin was subtracted from each point. Results represent means of triplicate determinations from two separate experiments. Binding values are expressed as a percentage of the maximal [^{125}I]-insulin binding.

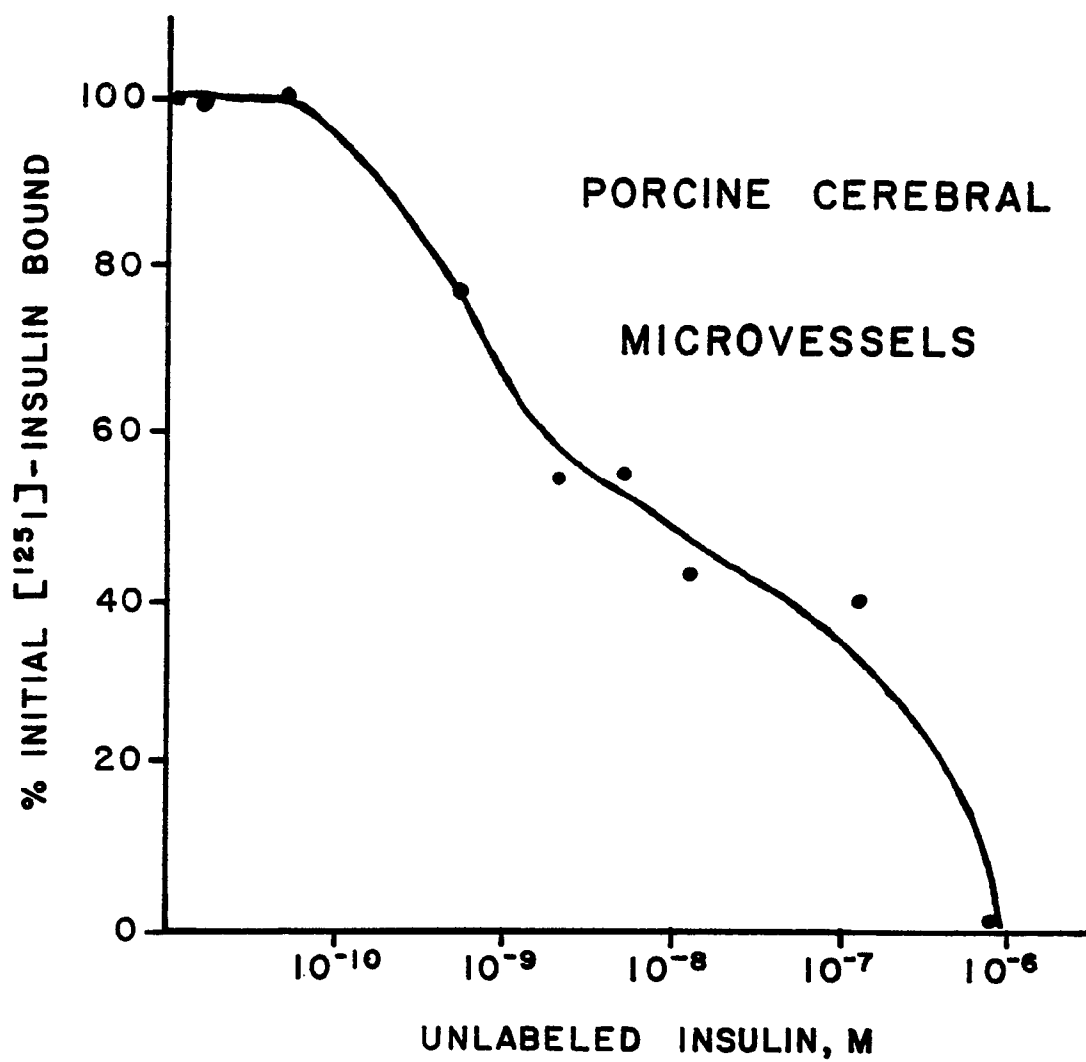


FIGURE 13

Scatchard Analysis of [^{125}I]-Insulin Binding to
Porcine Cerebral Microvessels

Cerebral microvessels from neonatal pigs were incubated for 30 min at 30°C with 1.5 ng/ml [^{125}I]-insulin, as described previously. Binding was determined in the presence of various concentrations of unlabeled insulin. Nonspecific binding was determined in the presence of 100 $\mu\text{g/ml}$ unlabeled insulin and subtracted from each point. Results are expressed as the mean of triplicate determinations from two separate assays.

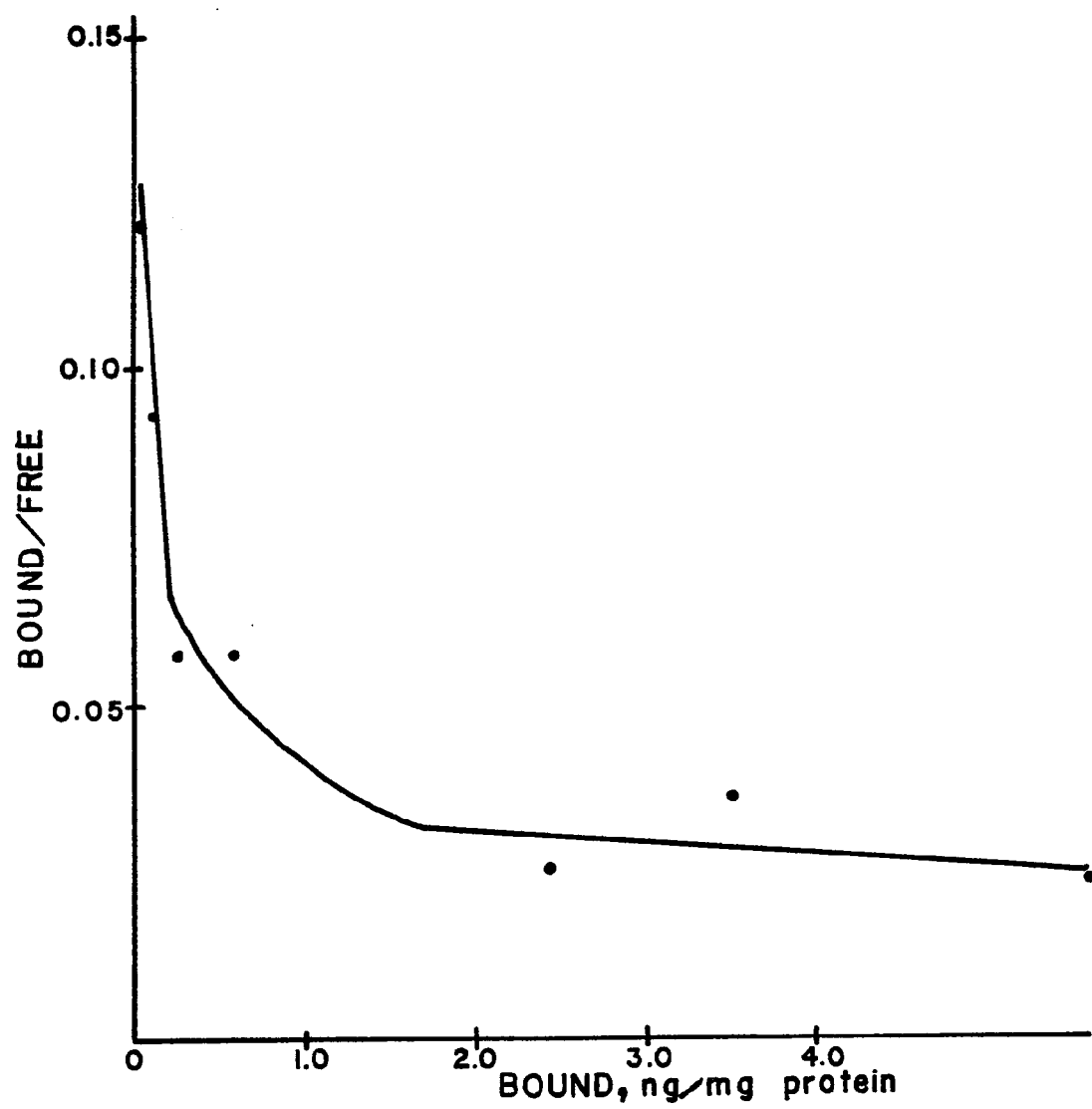


TABLE 10

[¹²⁵I]-Insulin Binding Constants and Binding Capacities

Tissue	Binding Capacity	Dissociation Constant	Reference
	(pmoles/mg protein)	(nM)	
Bovine Cerebral Microvessels	0.027	0.33	Haskell et al. (54)
Bovine Retinal Microvessels	0.039	0.33	Haskell et al. (54)
Porcine Cerebral Microvessels	0.066	0.34	Haskell et al. (54)
Liver		0.5	Almira et al. (1)
Adipose	0.20	0.77	Cuatrecasas (23)
		1.7	Pillion and Czech (99)
Muscle (Heart)	0.38	1.7	Freychet (43)
Lymphocyte (IM-9)		0.1-1.0	DeMeyts et al. (30)

The effect of various analogues of insulin and other polypeptides on [^{125}I]-insulin binding to freshly isolated bovine retinal microvessels are presented in Table 11. It can be seen that porcine insulin effectively inhibits the binding of [^{125}I]-insulin to retinal microvessels. A and B chain insulin are devoid of biological activity and have only a small effect on binding. Prolactin and human chorionic gonadotropin have virtually no effect on binding, even in greater than physiological concentrations.

Dissociation of [^{125}I]-Insulin

Bovine Cerebral Microvessels

Fig. 14 shows the results of experiments designed to test whether steady-state [^{125}I]-insulin binding is reversible. The freshly isolated bovine cerebral microvessels were incubated with 4.5 ng/ml [^{125}I]-insulin for 75 min at 22°C before being washed rapidly at 4°C and were allowed to dissociate upon dilution with a 100-fold volume of ice cold assay buffer with and without 100 ng/ml unlabeled insulin. The presence of unlabeled insulin greatly enhances the initial rate of dissociation of [^{125}I]-insulin initially bound to the cerebral microvessels. The curve for dissociation in the presence of unlabeled insulin appears to level off after 30 min, with both lines becoming parallel. This result is obtained whether tissue is separated from unbound insulin by centrifugation or by filtration. When the two methods of separating bound and dissociated [^{125}I]-insulin are compared, it appears that the filtration method indicates a greater amount of

TABLE 11

Effect of Insulin Analogues on [^{125}I]-Insulin Binding

<u>Analogues</u>	<u>Concentration</u>	<u>% Inhibition</u>	<u>% Maximal Bound</u>
Porcine Insulin	50 ng/ml	81.6%	8.4%
	50 ug/ml	100.0%	0
A Chain Insulin	50 ng/ml	10%	90%
	50 ug/ml	24%	76%
B Chain Insulin	--	--	--
	50 ug/ml	22%	78%
Prolactin	5 ug/ml	1.5%	98.5%
HCG	0.3 U/ml	1.4%	98.6%
	75 U/ml	18%	82%

Fresh bovine retinal microvessels were incubated for 30 min at 30°C with 1.5 ng/ml [^{125}I]-insulin in the presence of various concentrations of the peptides listed above. Data represent means of triplicate determinations.

dissociation in the presence of unlabeled insulin. In the case of dissociation due to dilution in buffer only, both methods (filtration = triangles; centrifugation through oil = circles) are very similar. The majority of dissociation appears to occur within the first 30 min with dilution alone and with dilution with buffer containing 100 ng/ml unlabeled insulin.

Bovine Retinal Microvessels

The filtration method of separating bound [125]-insulin from dissociated insulin was used with freshly isolated bovine retinal microvessels, as shown in Fig. 15. Dilution with buffer containing 100 ng/ml unlabeled insulin greatly enhanced the rate of dissociation from these vessels, compared with dilution with assay buffer alone. As in the case of bovine cerebral microvessels, both lines appear parallel after 30 min. Results were corrected for the amount of [125 I]-insulin binding to the filters themselves and expressed as a percentage of the insulin binding at time 0.

FIGURE 14

Dissociation of [125 I]-Insulin from Bovine Cerebral Microvessels

[125 I]-insulin (4.5 ng/ml) was incubated for 75 min at 22°C with bovine cerebral microvessels (1.2-1.4 mg protein). At time 0, microvessels were diluted with 100 volumes of ice-cold assay buffer with and without 100 ng/ml unlabeled insulin. At the time indicated, aliquots were removed and bound [125 I]-insulin separated from dissociated [125 I]-insulin by centrifuging an aliquot through oil, as described in the Methods section [without unlabeled insulin = open circles (-○-); with unlabeled insulin = closed circles (-●-)]. A duplicate experiment was performed using the filtration method described in the text [without unlabeled insulin = open triangles (-△-); with unlabeled insulin = closed triangles (-▲-)]. Results are expressed as percentage of [125 I]-insulin bound at time 0.

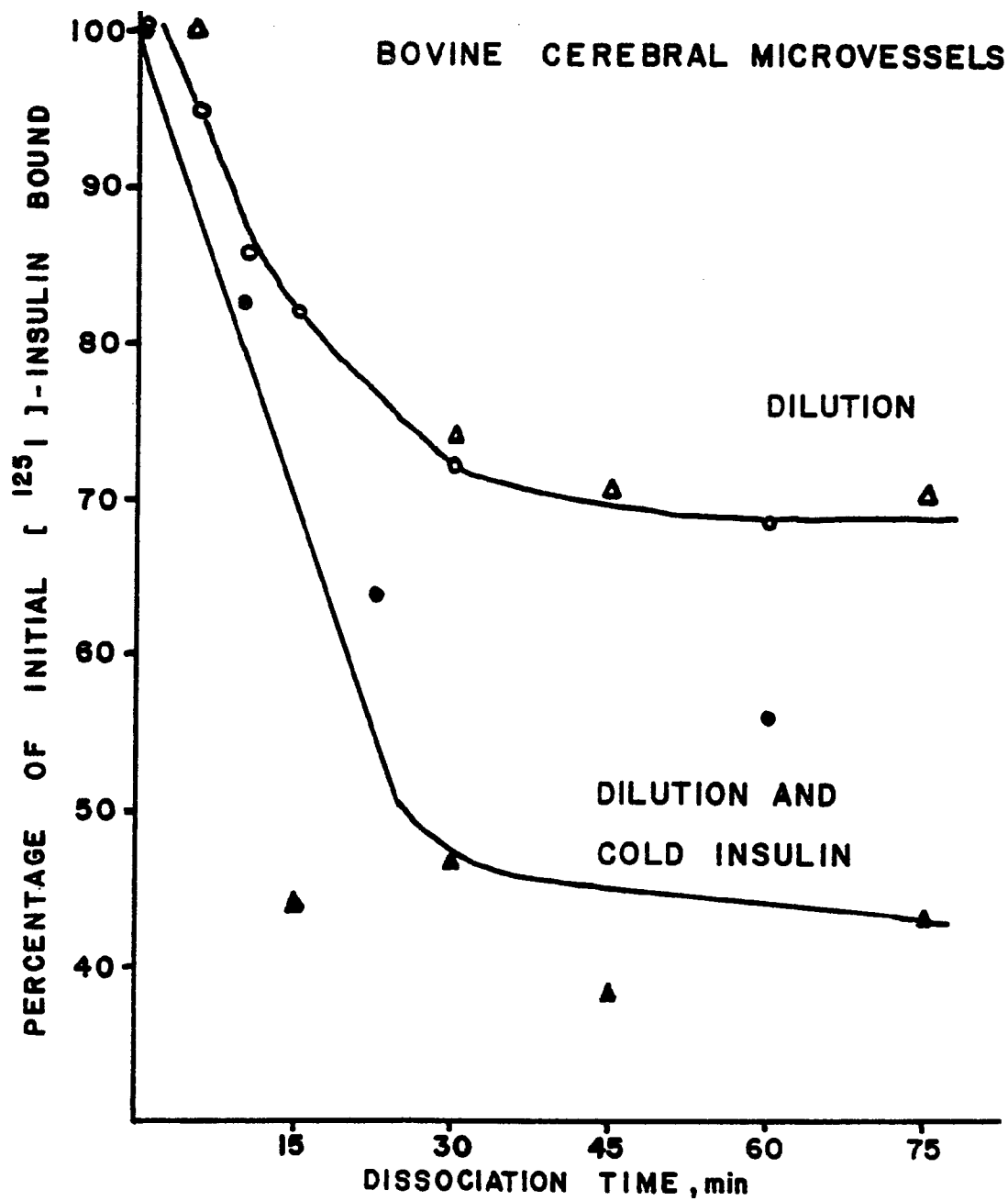
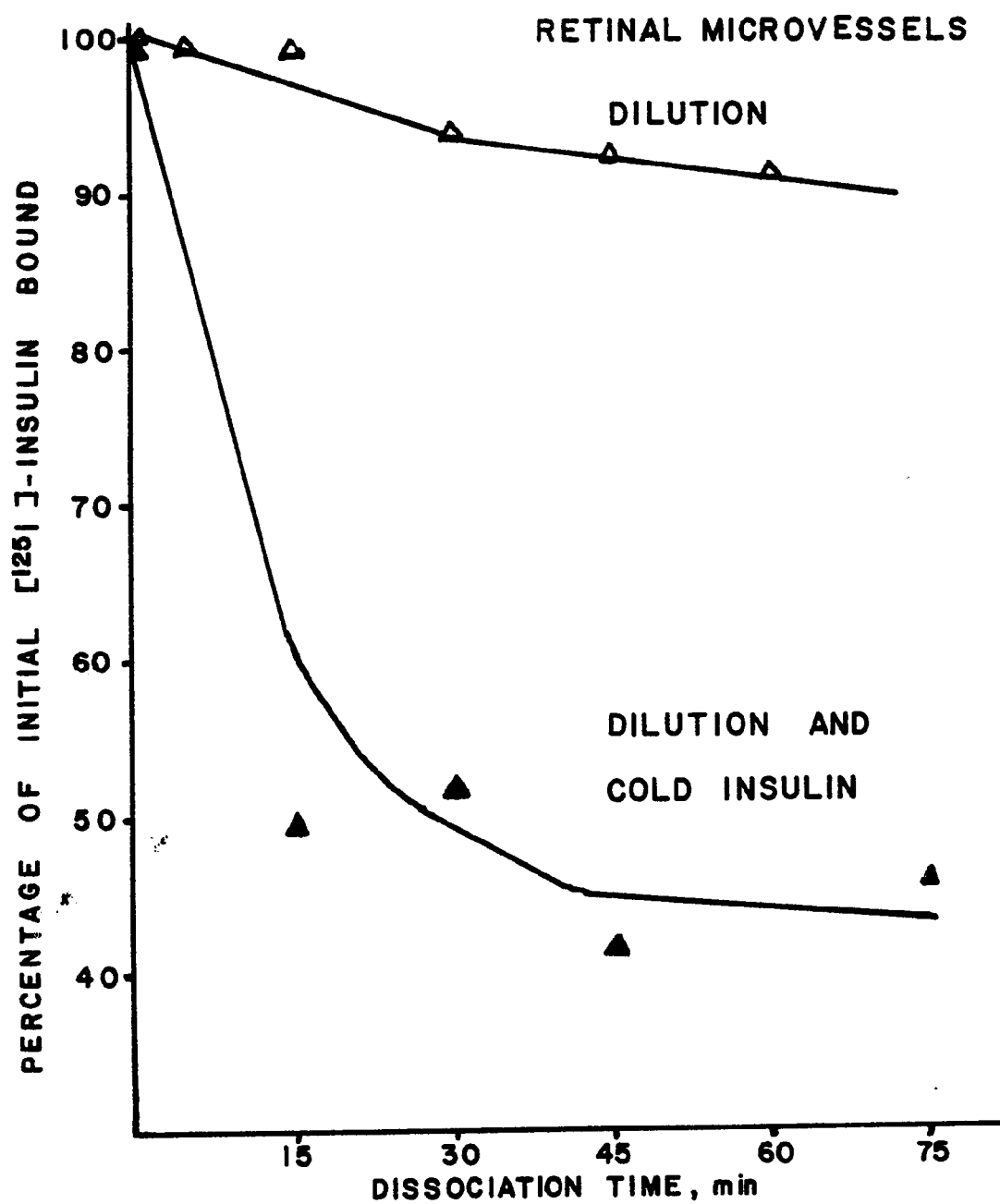


FIGURE 15

Dissociation of [125 I]-Insulin from Bovine Retinal Microvessels

Retinal microvessels were incubated with 4.5 ng/ml [125 I]-insulin for 75 min at 22°C. At time 0, microvessels were diluted with 100 volumes of ice-cold assay buffer with and without 100 ng/ml unlabeled insulin. At the time indicated, aliquots (5 ml) were removed and filtered through prewashed filters, as described in the text. Results are the average of duplicate determinations and are expressed as a percentage of [125 I]-insulin bound at time 0 [diluted without unlabeled insulin = open triangles (- Δ -); diluted with unlabeled insulin = closed triangles (- \blacktriangle -)].



Identification of the Microvascular Insulin Receptor

Crosslinking Procedure

The procedure for covalently crosslinking [^{125}I]-insulin to its plasma membrane receptor according to the method of Pilch and Czech (98) is outlined in Fig. 16. Membranes were prepared as described in the Materials and Methods section. Tissue pellets containing 400-500 μg protein were incubated with 0.5 μCi [^{125}I]-insulin with and without excess unlabeled insulin (100 $\mu\text{g}/\text{ml}$) for 60 min at 22°C in KRP buffer, pH 7.75, containing 1% BSA and 1 mM glucose. Microvessels were incubated in a volume of 250-500 μl during the insulin binding portion of this experiment. Binding to microvessels which were centrifuged through oil is shown in Table 12 and was found to consist of between 3-4% of the total radioactivity. Binding to liver plasma membranes was found in this experiment to be approximately 9.1% of the total [^{125}I]-insulin.

Following insulin binding, the membranes were centrifuged and washed rapidly at 4°C in KRP buffer, pH 7.4, without BSA. It is absolutely critical to remove bovine serum albumin from the membrane supernatant at this step in order to prevent crosslinking of [^{125}I]-insulin to this protein.

Membranes were centrifuged, resuspended in BSA-free phosphate buffer and 0.25 mM disuccinimidyl suberate added. The tissue was incubated for 15 min at 4°C before being quenched with a fivefold excess of Tris-EDTA buffer and incubated 20 min at 4°C, as depicted in Fig. 16.

FIGURE 16

Crosslinking Procedure

Procedure for covalently crosslinking [^{125}I]-insulin to its plasma membrane receptor using disuccinimidyl suberate, according to the methods of Pilch and Czech (98), is outlined here and described in the text.

Crosslinking Procedure

Membrane Preparation

↓
[¹²⁵I]-insulin Binding (75 min, 22°C)

↓
Wash (1 min, 4°C)

↓
Crosslinking with .25 mM DSS (15 min, 4°C)

↓
Quenching with Tris-EDTA (20 min, 4°C)

↓
Wash (1 min, 4°C)

↓
SDS-PAGE

↓
Autoradiography

TABLE 12

[¹²⁵I]-Insulin Binding in Crosslinking Experiments[¹²⁵I]-Insulin Binding

<u>Membrane Preparations</u>	<u>Total (% Total Count)</u>	<u>Nonspecific (% Total Count)</u>	<u>Specific (% Total Count)</u>
Bovine Brain Microvessels	7.6	4.7	2.9
Bovine Retinal Microvessels	7.8	4.0	3.8
Porcine Brain Microvessels	6.3	3.3	3.0
Rat Liver	13.3	4.2	9.1

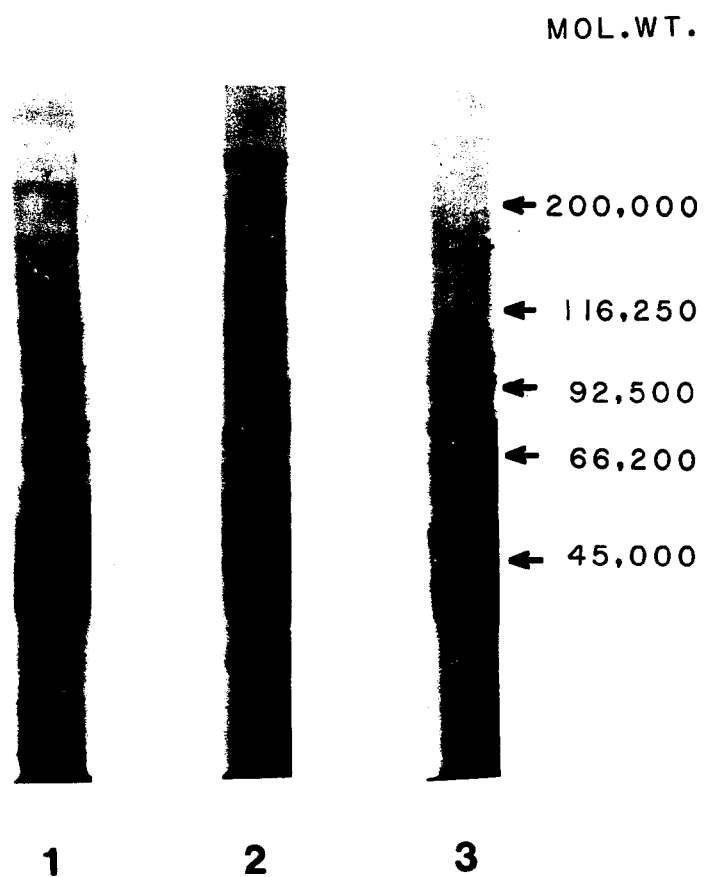
Tissue pellets containing 0.4-0.5 mg protein were incubated with 0.5 μ C [¹²⁵I]-insulin with and without excess unlabeled insulin (100 μ g/ml) for 60 min at 22°C. Incubation was carried out in 0.25 ml Krebs-Ringer phosphate buffer, pH 7.75, containing 1% BSA and 1 mM glucose. Following incubation, 50 μ l aliquots were removed and centrifuged through oil. The remaining 200 μ l of sample was crosslinked using disuccinimidyl suberate. Protein content was determined by digesting the pellet in 0.1 N NaOH. Pellets were counted in a gamma counter and the counts were normalized per mg protein. Results are expressed as percentage of total radioactivity.

Microvascular and liver membranes were rapidly washed with Tris-EDTA buffer. The membranes were then centrifuged and the supernatant discarded. After this final wash, pellets were dissolved in sample buffer and boiled 5 min before being applied to the dodecyl sulfate polyacrylamide slab gel. Fig. 17 shows the electrophoretic patterns of bovine retinal microvascular membrane preparations, porcine cerebral microvascular membrane preparations and liver membranes used in covalent crosslinking experiments. Coomassie Brilliant Blue R was used to stain the protein bands seen in Fig. 17. It can easily be seen that the two microvascular preparations closely resemble each other and share many common electrophoretic protein bands. They have several distinct features, mainly the presence of different high molecular weight protein bands. Molecular weight markers from Bio-Rad were used and the position of the standards are depicted in the figure. Microvascular membranes have a tendency to smear when applied to the dodecyl sulfate polyacrylamide gels. This is possibly due to the contamination of basement membrane proteins which are not readily solubilized in the sample buffer. This problem was overcome by changing the method by which the membranes were prepared. Better gel patterns have resulted from the use of a small (5 ml) smooth glass homogenizer with a tight fitting teflon pestle. Frozen microvessels were washed several times in cold distilled water and centrifuged prior to homogenization. Centrifuging the sample after it was solubilized in sample buffer or filtering it was not particularly helpful. Conducting the multiple wash steps in the crosslinking procedure in Corex glass centrifuge tubes in rubber adapters and centrifuging at 30,000 xg was found to greatly improve the yield of crosslinked protein and improve the appearance of the Coomassie blue stained gel.

FIGURE 17

Electrophoretic Patterns of Membrane Proteins

Membranes were prepared as described in the text from microvessels isolated from bovine retina and porcine cerebral cortex. These membranes were dissolved in sample buffer, boiled for 5 min and applied to a dodecyl sulfate polyacrylamide gel. Following electrophoresis, the gel was stained with Coomassie brilliant blue and dried on a Bio-Rad gel drier. Liver membranes were also applied to the gel.



1. BOVINE RETINAL MICROVESSELS

2. PORCINE CEREBRAL MICROVESSELS

3. RAT LIVER

Isolation of the Insulin Receptor

Rat liver membranes were used to repeat the experiments of Massague and Czech (83) and Massague et al. (84). Membranes were incubated with [^{125}I]-insulin for 60 min at 22°C, as described in the Materials and Methods section. The autoradiograph shown in Fig. 18 demonstrates that the insulin receptor isolated under non-reducing conditions has a molecular weight of approximately 300,000 daltons. When liver membranes are solubilized under reducing conditions, the [^{125}I]-insulin is crosslinked to a protein of approximately 125,000 daltons. These results agree with the results reported by Pilch and Czech (98) and Massague et al. (84) for the insulin receptor in rat liver adipocytes.

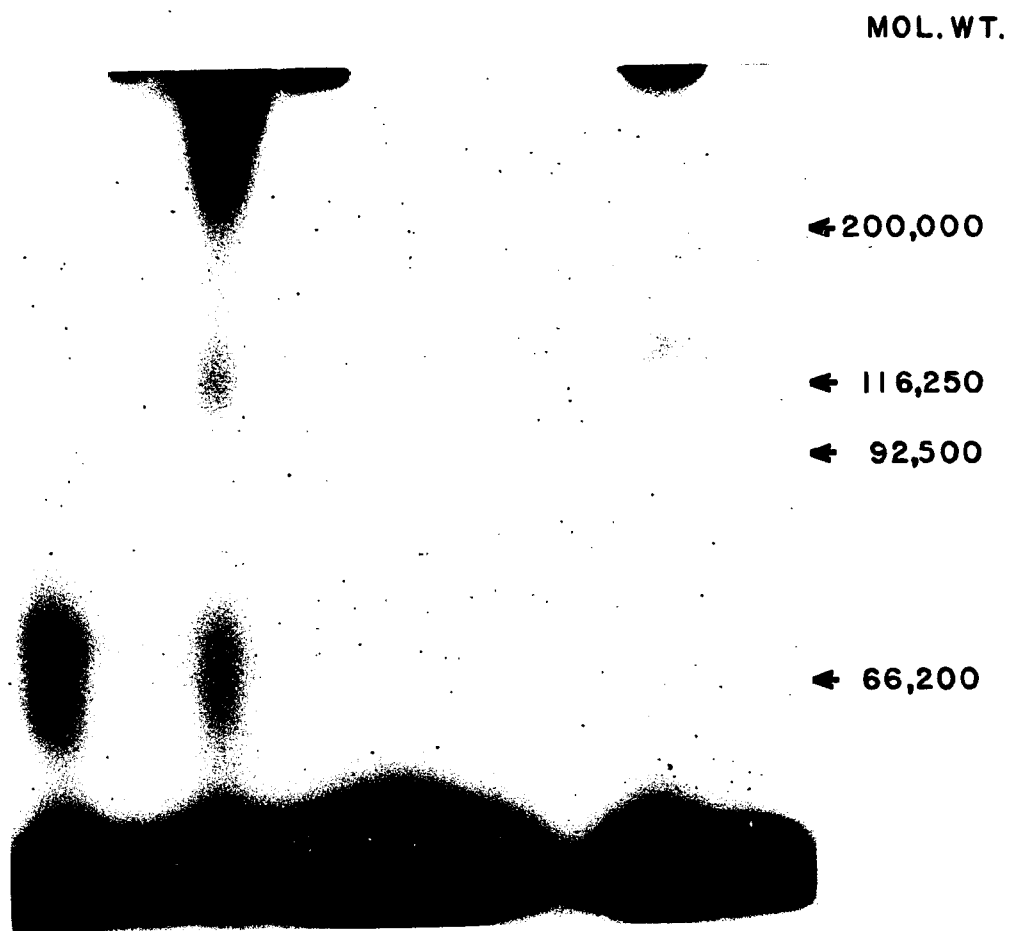
Plasma membranes from rat liver and bovine retinal microvessels were incubated with 0.5 μCi [^{125}C]-insulin for 60 min at 22°C, and then crosslinking of [^{125}I]-insulin to the receptor was achieved by the addition of 0.25 mM disuccinimidyl suberate. Membranes were boiled in sample buffer containing 50 mM DTT and 2% SDS and applied to an SDS-polyacrylamide gel. Following electrophoresis, the gel was dried with a Bio-Rad gel drier and autoradiography performed. Fig. 19 demonstrates that [^{125}I]-insulin is crosslinked to a protein of 125,000 dalton molecular weight in both the retinal microvessel membranes and the liver membranes which were not incubated with excess unlabeled insulin. The band at 66,200 daltons apparently represents nonspecific binding to bovine serum albumin which was not completely removed from the sample. The 125,000 dalton molecular weight band was not observed in the samples incubated with excess unlabeled insulin, indicating that this protein is specifically bound to [^{125}I]-insulin. These results

indicate that the insulin receptor in bovine retinal microvessels closely resembles the insulin receptor in rat liver, with respect to its subunit structure.

FIGURE 18

Isolation of the Insulin Receptor in Liver Using
Disuccinimidyl Suberate and Reducing and Nonreducing
Conditions

Plasma membranes from rat liver cells were incubated with [125]-insulin for 60 min at 22°C in the presence and absence of excess unlabeled insulin (100 μ g/ml). Membranes in lanes 3,4,7 and 8 were covalently crosslinked with 0.25 mM disuccinimidyl suberate, while membranes in lanes 1,2,5 and 6 were incubated without disuccinimidyl suberate. Samples in lanes 1,2,3 and 4 were solubilized with sample buffer without dithiothreitol; samples in lanes 5,6,7 and 8 were solubilized in sample buffer containing 50 mM dithiothreitol. Even-numbered lanes contain samples incubated in the presence of excess unlabeled insulin, while odd-numbered lanes contain samples incubated in the absence of unlabeled insulin. Dodecyl sulfate polyacrylamide gels were electrophoresed, stained with Coomassie blue and dried on a Bio-Rad gel drier. Autoradiographic visualization of the gels yielded the pattern presented.

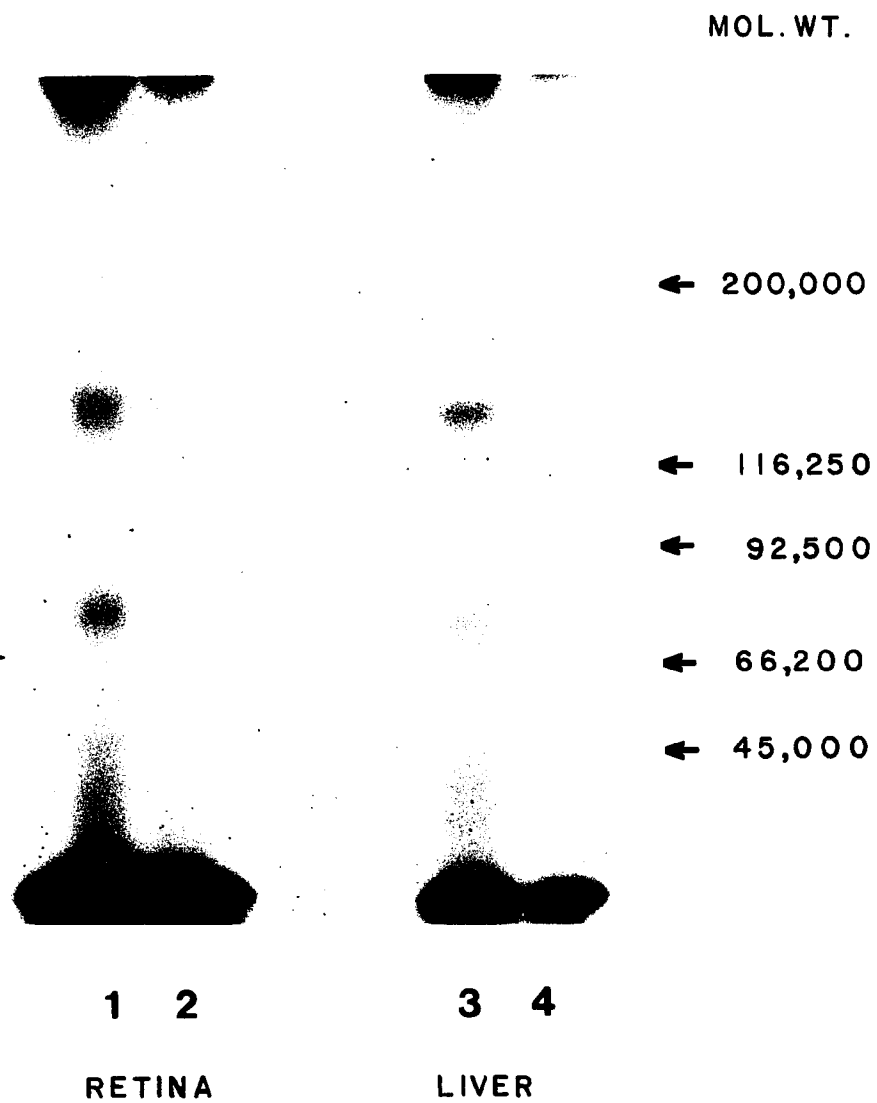


1	2	3	4	5	6	7	8
-	c	-	c	-	c	-	c
—		DSS		—		DSS	
—without DTT—				—with DTT—			

FIGURE 19

Isolation of the Insulin Receptor of Retinal Microvessels and Liver

Plasma membranes from rat liver and bovine retinal microvessels were incubated with 0.5 μ C [125 I]-insulin for 60 min at 22°C and then crosslinked using 0.25 mM disuccinimidyl suberate. Isolation of the resulting [125 I]-insulin-receptor complex was achieved by solubilizing the membranes in buffer containing 50 mM dithiothreitol and 2% SDS and applying the samples to a dodecylsulfate polyacrylamide gel in the following order: (1) retinal microvessel membranes plus [125 I]-insulin, (2) retinal microvessel membranes plus [125 I]-insulin and 100 μ g/ml unlabeled insulin, (3) liver membranes plus [125 I]-insulin, (4) liver membranes plus [125 I]-insulin and 100 μ g/ml unlabeled insulin. Following electrophoresis, the gels were dried with a Bio-Rad gel drier and autoradiography performed. The band at 66,200 daltons molecular weight corresponds to nonspecific binding of [125 I]-insulin to BSA not completely removed from the sample.



V. DISCUSSION

Tissue Isolation

Cerebral and retinal microvessels are unique since they comprise the blood-tissue barrier in the brain and eye, respectively. Contrary to the endothelium in other tissues throughout the body, the cerebral and retinal microvascular endothelium consists of a continuous layer of endothelial cells with tight junctions. Recent studies have indicated that the function of this barrier is disturbed in disease states, such as diabetes mellitus. In fact, diabetics are often diagnosed from the appearance of microangiopathy and microvascular disturbances in the retina prior to the discovery of poor carbohydrate tolerance and increased blood glucose levels. Diabetics of long duration have been found to have thickened basement membranes and impaired permeability of their microvessels. It is now well established (2,7,8,13,17,33,53,56,60,68,87,91,95) that cerebral and retinal microvessels isolated according to the procedure described in Fig. 2 have characteristics of the blood-brain barrier and are representative of the microvessels in which microangiopathy is known to occur in diabetics.

These microvessels have been shown to have intact metabolic activity (7,13,60,87,88,95) and they respond to various hormonal stimulation (2,53,68,89). Preparations of isolated bovine cerebral and retinal microvessels and cerebral microvessels isolated from neonatal pigs, (89,100) which are analogous to the preparations used here,

exhibit an increase in glucose metabolism with physiological doses of insulin, as measured by conversion of ^{14}C -glucose to $^{14}\text{CO}_2$ and radio-labeled lipids. Insulin also has been shown to increase the activity of the low K_m form of cAMP-phosphodiesterase in these same vessels (100).

Insulin Binding

Insulin is secreted by the B cells of the endocrine pancreas into the blood stream where it is carried throughout the body until it is cleared by the kidney or the liver or degraded by peripheral tissue enzymes. Before it is degraded, the insulin molecule can bind to specific receptors on target cells in insulin-sensitive tissues where insulin causes physiological effects. This hypothesis was first proposed by Sutherland (20) as the mechanism of action for peptide and polypeptide hormones and is widely accepted as the mechanism of insulin action (25,43,50). It is currently unknown exactly how the insulin molecule manages to generate its well-established physiological effects. Although it has been well known that microvascular complications are prevalent in diabetics, a direct effect of insulin on blood vessel walls has been hypothesized recently. Several years ago insulin receptors were demonstrated in red blood cells, monocytes and various blood-borne cells. More recently, receptors for insulin were found throughout the central nervous system, although it is controversial whether increased levels of insulin cross the blood-tissue barrier and are available to these binding sites.

Van Houten and Posner (123) have shown that large amounts of insulin bind to cerebral microvessels under in vivo conditions. Bergeron et al. (5) have noted that a larger number of insulin molecules bind to liver endothelium even in the presence of excess unlabeled insulin, which may possibly not be due to nonspecific binding. This work has generated interest in the presence of insulin receptors in the microvascular system along with speculation as to the physiological role of these receptors. It is not currently known whether insulin has "trophic" as well as "metabolic" effects on these vessels, as discussed by Freychet (43). The results of Meezan and Pillion (89) and Pillion et al. (89,100) suggest a metabolic effect of insulin on microvascular tissue, but a trophic effect (protein synthesis, DNA replication, etc.) has not yet been demonstrated.

In this dissertation, the binding and degradation of [^{125}I]-insulin in microvessels isolated from bovine cerebral and retinal tissue and neonatal porcine cerebral cortex has been characterized. The results show the effects of increasing protein concentration, increasing concentration of labeled insulin, varying time of incubation, increasing temperature, and increasing concentration of unlabeled insulin on the binding of [^{125}I]-insulin to the microvascular receptors.

Binding is affected by pH, temperature and other physiological conditions under which insulin binding has been shown to vary in liver, adipose tissue and muscle. Binding is specific for insulin and not displaceable by insulin analogues such as A chain or B chain, which do not have physiological activity. Other protein hormones, such as prolactin and human chorionic gonadotropin, have no effect on [^{125}I]-insulin binding, even when high, non-physiological concentrations were used.

Scatchard Analysis

Unlabeled insulin inhibited [^{125}I]-insulin binding to microvascular tissue in a dose-dependent manner. Approximately 2-9 ng/ml unlabeled insulin was required to inhibit 50% of [^{125}I]-insulin binding. Scatchard analysis of the binding data yielded a curvilinear plot resembling that exhibited by liver or adipocyte receptors. The insulin receptor in cerebral and retinal microvessels resembled the insulin receptor in other well-characterized insulin sensitive tissues. It exhibited binding characteristics which were specific, saturable, finite, readily reversible, and which showed affinity constants in the physiological range of insulin concentrations in plasma. Graphical analysis of the binding data yielded similar high affinity binding constants in all three microvascular preparations, as shown in Table 10. The binding constants of other insulin sensitive tissues are also presented in Table 10. The binding capacity is clearly lower in isolated microvascular tissue than in liver, fat or muscle. Two possible explanations would account for this low binding capacity. The first hypothesis is that since the microvessels are constantly exposed to insulin, at least on the luminal surface of the endothelium, any receptors might possibly be down-regulated to prevent an overload of the insulin stimulation on the cells of the vessels. To test this hypothesis, it would be very interesting to examine binding in microvessels from diabetic animals in which circulating insulin levels are minimal, thus eliminating the possibility of down-regulation of receptor sites. The second hypothesis is that although insulin binding capacity is low per cell, the microvascular system is composed of a relatively vast number of endothelial cells. Binding to these cells

could in effect bind many molecules of insulin and maintain a reservoir of insulin molecules which could be released to increase available insulin supplies to liver, adipose tissue, and muscle cells under varying physiological and pathological conditions. In essence, insulin binding to microvascular insulin receptors could protect other insulin-sensitive cells from an exposure to excess amounts of insulin during periods of hyperinsulinemia and could release intact insulin during periods of normoinsulinemia. In this hypothesis, the thickening of the basement membrane in maturity-onset diabetes might result from increased exposure of the microvascular insulin receptors to the high circulating levels of insulin even prior to systemic imbalance of carbohydrate metabolism.

Dissociation of [125 I]-Insulin

Dissociation of [125 I]-insulin from its binding sites was accelerated in the presence of unlabeled insulin. The dissociation of labeled insulin is shown in Fig. 14 for isolated bovine cerebral microvessels and in Fig. 15 for isolated bovine retinal microvessels. Dissociation was rapid and similar in both tissues, suggesting that the binding interaction between insulin and its microvascular receptor is a reversible interaction. These results are compatible with either negative cooperativity as proposed by DeMeyts et al. (30) or the two site hypothesis as described by Pollet and Levey (102). The finding that the presence of unlabeled insulin increases dissociation has been demonstrated in most insulin-sensitive tissues and the significance of this finding is still controversial.

Isolation of the Insulin Receptor

Using dodecyl sulfate polyacrylamide gel electrophoresis, the insulin receptor was isolated under reducing conditions yielding a labeled subunit which was visualized using autoradiography. The subunit structure of the microvascular insulin receptor highly resembled the insulin receptor subunit structure described in liver. Table 13 summarizes the results obtained by various investigators using either the photoaffinity labeling method or the affinity crosslinking method. It can readily be seen that the affinity crosslinking method results in isolation of the insulin receptor, giving a molecular weight of 300,000 δ under non-reducing conditions and 125,000-170,000 δ under reducing conditions.

These results are consistent with the $\alpha_2\beta_2$ model proposed by Pilch and Czech (98) for the insulin receptor and discussed in the Review section of this dissertation. The α subunit (125,000 δ) is readily visualized by autoradiography of [^{125}I]-insulin crosslinked to its membrane receptor using disuccinimidyl suberate. The B subunit (90,000 δ) and B_1 subunit (40,000 δ) are less well isolated using this method. Bovine serum albumin (66,200 δ) was nonspecifically bound to [^{125}I]-insulin and produced bands in all four columns of the autoradiograph shown in Fig. 19. It is also demonstrated in Fig. 19 that the insulin receptor in isolated bovine retinal microvessel membranes exactly corresponded to the insulin receptor isolated under reducing conditions (50 mM DTT) in rat liver membranes.

In the future, it would be interesting to use this technique to isolate the insulin receptor in other tissues, such as bovine and porcine cerebral microvessels which have similar affinity constants for

TABLE 13

Summary of Insulin Receptor Characterization

Tissue	Molecular Weight		Reference
	Native	Reduced	
Photoaffinity Labeling Method			
Rat liver	310,000	135,000 45,000 90,000	Jacobs et al. (65)
Rat adipocytes (rodent liver)	380,000 300,000 230,000	130,000 90,000 40,000	Yip et al (133-135)
Rat brain		115,000	Yip et al (133)
Rat liver		130,000 100,000	Wisher et al (131)
Affinity Crosslinking Method			
Rat liver Rat adipocytes	300,000	125,000	Pilch and Czech (98)
Cultured human lymphocytes	310,000	170,000 (120,000) (50,000)	Pollet et al (103)
Bovine retinal microvessels		125,000	Haskell et al. (54)
Rat myocytes	370,000	130,000 82,000 47,000	Im et al. (62)

[¹²⁵I]-insulin, and renal preparations (glomeruli and tubules) which have two different affinity constants for [¹²⁵I]-insulin. It would also be interesting to attempt to isolate other polypeptide hormone receptors using the affinity crosslinking method and to identify their subunit composition.

VI. SUMMARY

Isolated microvessels from bovine cerebral cortex, bovine retina and porcine cerebral cortex bind [^{125}I]-insulin in a specific manner. Binding was examined using different protein concentrations, various incubation time and temperature conditions and at various concentrations of [^{125}I]-insulin. Unlabeled insulin displaces bound [^{125}I]-insulin in a dose-dependent fashion. A and B chains of insulin did not displace bound; certain other protein hormones (prolactin and human chorionic gonadotropin) at physiological concentrations did not displace bound [^{125}I]-insulin. Scatchard analysis yielded a curvilinear plot for all three microvascular preparations. The presence of a high affinity binding site in microvascular tissue resembles the results obtained with other insulin-sensitive tissues. Dissociation of bound [^{125}I]-insulin was rapid and was accelerated in the presence of unlabeled insulin. These results confirmed the presence of an insulin receptor in isolated cerebral and retinal microvessels. The insulin receptor in isolated bovine retinal microvessels was crosslinked to [^{125}I]-insulin using 0.25 mM disuccinimidyl suberate. Using dodecylsulfate-polyacrylamide gel electrophoresis, the insulin receptor was isolated under reducing conditions, with a labeled subunit visible using autoradiography. An approximately 125,000 dalton molecular weight band was obtained which coincided with that of the B subunit of the insulin receptor isolated on the same gel from rat liver.

VII. BIBLIOGRAPHY

1. Almira, E. and Reddy, W.: Effect of fasting on insulin binding to hepatocytes and liver plasma membranes from rats. *Endocrinology* 104:205-211, 1979.
2. Baca, G. M. and Palmer, G. C.: Presence of hormonally-sensitive adenylate cyclase receptors in capillary-enriched fraction from rat cerebral cortex. *Blood Vessels* 15:286-298, 1978.
3. Baron, M. D., Wisher, M. H., Thamm, P. M., Saunders, D. J., Brandenburg, D. and Sonksen, P. H.: Hydrodynamic characterization of the photoaffinity-labeled insulin receptor solubilized in Triton X-100. *Biochemistry* 20:4156-4161, 1981.
4. Benjamin, W. B. and Singer, I.: Effect of insulin on the phosphorylation of adipose tissue protein. *Biochim. Biophys. Acta.* 351:28-41, 1974.
5. Bergeron, J. M. M., Sikstrom, R., Hand, A. R. and Posner, B. I.: Binding and uptake of [¹²⁵I]-insulin into rat liver hepatocytes and endothelium. *J. Cell Biol.* 80:427-443, 1979.
6. Berhanu, P. and Olefsky, J. M.: Photoaffinity labeling of insulin receptors in viable cultured human lymphocytes. *Diabetes* 31:410-417, 1982.
7. Betz, A. L., Csejtei, J. and Goldstein, G. W.: Hexose transport and phosphorylation by capillaries isolated from rat brain. *Am. J. Physiol.* 236:C96-C102, 1979.
8. Betz, A. L., Firth, J. A. and Goldstein, G. W.: Polarity of the blood-brain barrier. *Brain Res.* 192:17-28, 1980.
9. Bhalla, V., Haskell, J., Grier, H. and Mahesh, V.: Gonadotropin binding factor(s) - Extraction of high affinity gonadotropin binding sites from rat testis and partial characterization of their interaction with hFSH, hLH, and hCG. *J. Biol. Chem.* 251:4947-4957, 1976.
10. Blackard, W., Guzelian, P. and Small, M.: Down regulation of insulin receptors in primary cultures of adult rat hepatocytes in monolayer. *Endocrinology* 103:548-553, 1978.

11. Blundell, T., Dodson, G., Hodgkin, D. and Mercola, D.: Insulin: the structure in the crystal and its reflection in chemistry and biology. *Adv. Protein Chem.* 26:279-394, 1972.
12. Bradford, M.: A rapid and sensitive method for the quantitation of microgram quantities of protein utilizing the principle of protein-dye binding. *Anal. Biochem.* 72:248-254, 1976.
13. Brendel, K., Meezan, E. and Carlson, E. C.: Isolated brain microvessels: A purified, metabolically active preparation from bovine cerebral cortex. *Science* 185:953-954, 1974.
14. Bressler, R.: Insulin Therapy. Management of diabetes mellitus. Bressler, R. and Johnson, D. G., Eds., Boston, John Wright PSG Inc., 1982, pp. 51-90.
15. Burton, K.: A study of the conditions and mechanism of the diphenylamine reaction for the colorimetric estimations of deoxy-ribonucleic acid. *Biochem. J.* 62:315-319, 1956.
16. Carlson, C. and Kim, K.: Regulation of hepatic acetyl coenzyme A carboxylase by phosphorylation and dephosphorylation. *J. Biol. Chem.* 248:378-380, 1973.
17. Carlson, E. C., Brendel, K., Hjelle, J. T. and Meezan, E.: Ultrastructural and biochemical analyses of isolated basement membranes from kidney glomeruli and tubules and brain and retinal microvessels. *J. Ultrastructural Res.* 62:26-53, 1978.
18. Carter-Su, C., Pillion, D. J., and Czech, M. P.: Reconstituted D-glucose transport from the adipocyte plasma membrane chromatographic resolution of transport activity from membrane glycoproteins using immobilized Con A. *Biochem.* 19:2374-2375, 1980.
19. Catalan, R. E., Martinez, A. M., Mata, F. and Aragones, B.: Effects of insulin on acetylcholinesterase activity. *Biochem. Biophys. Res. Commun.* 101:1216-1220, 1981.
20. Chisolm, A.: Measurement of the degradation products of radioiodinated proteins. *Anal. Biochem.* 111:212-219, 1981.
21. Ciaraldi, T. and Olefsky, J. M.: Relationship between deactivation of insulin-stimulated glucose transport and insulin dissociation in isolated rat adipocytes. *J. Biol. Chem.* 253:327-330, 1980.
22. Colwell, J. A., Lopes-Virella, M. and Halushka, P.V.: Pathogenesis of atherosclerosis in diabetes mellitus. *Diabetes Care* 4:121-131, 1981.
23. Cuatrecasas, P.: Properties of the insulin receptor isolated from liver and Fat Cell Membranes. *J. Biol. Chem.* 247:1980-1991, 1972.

24. Cuatrecasas, P.: Affinity chromatography and purification of the insulin receptor in liver cell membrane. *Proc. Natl. Acad. Sci. USA* 69:1277-1281, 1972.
25. Czech, M. P.: Molecular basis for insulin action. *Ann. Rev. Biochem.* 46:359-384, 1977.
26. Czech, M.: Review - Insulin action and the regulation of hexose transport. *Diabetes* 29:399-409, 1980.
27. Czech, M.: The insulin receptor: structural features. *Trends in Biochem. Sci.* 6:222-225, 1981.
28. Daniel, P. M., Love, E. R. and Pratt, O. E.: The influence of insulin upon the metabolism of glucose by the brain. *Proc. R. Soc. Lond. B.* 196:85-104, 1977.
29. DeLean, D. and Rodbard, D.: Kinetic analysis of cooperative ligand binding application to the insulin receptor. *Fed. Proc.* 39:116-120, 1980.
30. DeMeyts, P., Bianca, A. and Roth, J.: Site-site interactions among insulin receptors. *J. Biol. Chem.* 251(7):1877-1888, 1976.
31. DePirro, R., Fusco, A., Lauro, R., Testa, I., Fibrete, F. and DeMartinis, D.: Erythrocyte insulin receptors in non-insulin-dependent diabetes mellitus. *Diabetes* 29:96-99, 1980.
32. Dolhofer, R., and Weiland, R.: Increased glycosylation of serum albumin in diabetes mellitus. *Diabetes* 29:417-422, 1980.
33. Drewes, L. D. and W. A. Lidinsky: Studies of cerebral capillary endothelial membrane. *Adv. Exp. Med. and Biol.* 216:17-27, 1980.
34. Ellenberg, M.: Chronic complications of diabetes. In *Diabetes in theory and in practice*. New York, Biomedical Information Corporation, 1978, pp. 20-27.
35. Eng, J. and Yalow, R.: Insulin recoverable from tissues. *Diabetes* 29:105-109, 1980.
36. Eng, J., Lee, L. and Yalow, R.: Influence of the age of erythrocytes on their insulin receptors. *Diabetes* 29:164-166, 1980.
37. Engerman, R. and Wallow, I.: Retinopathy in nonhereditary diabetes. In *Secondary diabetes: The spectrum of the diabetic syndromes*, Podolsky, S. and Viswanathan, M., Eds., New York Raven Press, New York, 1980, pp. 503-519.
38. Felig, P.: *Pathophysiology of diabetes mellitus*. Pfizer, Inc. New York, Biochemical International Corp., 1978, pp. 6-16.

39. Flatt, J. P. and Ball, E. G.: Studies on the metabolism of adipose tissue XIX. An evaluation of the major pathways of glucose catabolism as influenced by acetate in presence of insulin. *J. Biol. Chem.* 241:2862-2869, 1966.
40. Flier, J. S., Kahn, C. R. and Roth, J.: Receptors, antireceptor antibodies and mechanisms of insulin resistance. *N. Engl. J. Med.* 300:413-419, 1979.
41. Foulkes, J. and Cohen, P.: The hormonal control of glycogen metabolism-phosphorylation of protein phosphatase inhibitor - in vivo in response to adrenaline. *Eur. J. Biochem.* 97:251-256, 1979.
42. Frank, H. J. L. and Pardridge, W. M.: A direct in vitro demonstration of insulin binding to isolated brain microvessels. *Diabetes* 30:757-761, 1981.
43. Freychet, P.: Review: Interactions of polypeptide hormones with cell membrane specific receptors: studies with insulin and glucagon. *Diabetologia* 12:83-100, 1976.
44. Gavin, J., Roth, J., Neville, D., DeMeyts, P. and Buell, D.: Insulin-dependent regulation of insulin receptor concentrations: a direct demonstration in cell culture. *Proc. Natl. Acad. Sci. USA* 71:84-88, 1974.
45. Ginsberg, B. H.: The Insulin Receptor: Properties and regulation. *biochemical mech. of hormone action*, Litwack, G., Ed. New York, Academic Press, 1977, pp. 313-349.
46. Ginsberg, B. H., Cohen, R. M., Kahn, C. R. and Roth, J.: Properties and partial purification of the detergent-solubilized insulin receptor-A demonstration of negative cooperativity in micellar solution. *Biochim. Biophys. Acta* 542:88-100, 1978.
47. Glieman, J., Sonne, O., Linde, S. and Hansen, B.: Biological potency and binding affinity of monoiodoinsulin with iodine in Tyrosine A14 or Tyrosine A19. *Biochem. Biophys. Res. Commun.* 87:1183-1190, 1979.
48. Gordon, P.: Hormone receptor interaction. *Diabetes* 28:8-12, 1979.
49. Gould, R. J., Ginsberg, B. and Spector, A.: Reconstitution of the solubilized insulin receptor in phospholipid vesicles. *Endocrine Res. Commun.* 6:279-290, 1979.
50. Goldfine, I. D.: The insulin receptor. In *Methods in receptor research*, Vol. 9, M. Blecher, Ed., New York, Marcel Dekker, Inc., 1977, pp. 335-337.

51. Hammons, G. and Jarett, L.: Lysosomal Degradation of receptor-bound [125 I]-labeled insulin by rat adipocytes - its characterization and dissociation from short-term biologic effects of insulin. *Diabetes* 29:475-486, 1980.
52. Harrison, L., Billington, T., East, I., Nichols, R. and Clark, S.: The effect of solubilization on the properties of the insulin receptor of human placental membranes. *Endocrinology*. 102:1485-1495, 1978.
53. Hartman, B. K., Swanson, L. W., Raichle, M. E., Preskorn, S. H., Clark, H. B.: Central adrenergic regulation of cerebral microvascular permeability and blood flow: anatomic and physiologic evidence. In *The Cerebral Microvascular Investigation of the Blood-Brain Barrier*, Eisenberg, H.M. and Suddith, R. L., Eds. New York, Plenum Press, 1979, pp. 113-127.
54. Haskell, J. F., Meezan, E. and Pillion, D. J.: Retinal microvascular insulin receptor: structure and function. Submitted for publication.
55. Havrankova, J., Roth, J. and Brownstein, N.: Insulin receptors are widely distributed in the central nervous system of the rat. *Nature* 272:827-829, 1978.
56. Head, R. J., Hjelle, J., Jarrott, B., Berkowitz, B., Cardinale, G. and Spector, S. Isolated brain microvessels: preparation, morphology, histamine and catecholamine contents. *Blood Vessels* 17:173-186, 1980.
57. Heinrich, J., Pilch, P. and Czech, M.: Purification of the adipocyte insulin receptor by immunoaffinity chromatography. *J. Biol. Chem.* 255:1732-1737, 1980.
58. Hertz, M. M., Paulson, D. B., Barry, D. I., Christiansen, J. S. and Swendsen, P. A.: Insulin increases glucose transfer across the blood-brain barrier in man. *J. Clin. Invest.* 67:597-604, 1981.
59. Hill, D. E., Herzberg, V. L., Boughter, J. M., Szisak, T. J. and Carlisle, S. K.: The nature of the insulin receptor: implications for diabetes mellitus. In *Etiology and Pathogenesis of Insulin-Dependent Diabetes Mellitus*, Martin, J. M., Ehrlich, R. M. and Holland, F. J., Eds., New York, Raven Press, 1981, pp. 87-98.
60. Hjelle, J. T., Baird-Lambert, J., Cardinale, G., Spector, S. and Udenfriend, S.: Isolated microvessels: the blood-brain barrier in vitro. *Proc. Natl. Acad. Sci. USA* 75:4544-4548, 1978.
61. Hodgkins, D. C.: The structure of insulin. *Diabetes* 21:1131-1137, 1972.

62. Im, J. H., Frangakis, C., Meezan, E., DiBona, D. R. and Kim, H. D.: Isolation and partial characterization of insulin receptors from adult rat myocytes. *J. Biol. Chem.* 257:11128-11134, 1982.
63. Insel, J., Kolterman, O. G., Saekow, M. and Olefsky, J. M.: Short-term regulation of insulin receptor affinity in man. *Diabetes* 29:132-138, 1980.
64. Jacobs, S. and Cuatrecasas, P.: Insulin receptor: structure and function. *Endocrine Reviews* 2:251-263, 1981.
65. Jacobs, S., Hazum, E., Shechter, Y. and Cuatrecasas, P.: Insulin receptor: covalent labeling and identification of subunits. *Proc. Natl. Acad. Sci. USA* 76:4918-4921, 1979.
66. Jarett, L. and Seals, J. R.: Pyruvate dehydrogenase activation in adipocyte mitochondria by an insulin-generated mediator from muscle. *Science* 206:1407-1408, 1979.
67. Jefferson, L.: Role of insulin in the regulation of protein synthesis. *Diabetes* 29:487-495, 1980.
68. Joo, F., Rakonczay, Z. and Wollemann, M.: cAMP-mediated regulation of the permeability in the brain capillaries. *Experientia* 15:582-584, 1975.
69. Kahn, C. R., Baird, K. L., Flier, J. S. and Van Obberghen, E.: Insulin receptors, receptor antibodies and the mechanism of insulin action. *Recent Progress in Hormone Research* 37:477-529, 1981.
70. Kahn, C. R., Goldfine, I., Neville, D. and DeMeyts, P.: Alterations in insulin binding induced by changes in vivo in the levels of glucocorticoids and growth hormone. *Endocrinology* 103:1054-1066, 1978.
71. Kasuga, M., Karlson, F. A. and Kahn, C. R.: Insulin stimulates the phosphorylation of the 95,000-dalton subunit of its own receptor. *Science* 215:185-186, 1981.
72. Kasuga, M., Van Obberghen, E., Yamada, K. M. and Harrison, L. C.: Autoantibodies against the insulin receptor recognize the insulin binding subunits of an oligomeric receptor. *Diabetes* 30:354-357, 1981.
73. Kuehn, L., Meyer, H., Rutschmann, M. and Thamm, P.: Identification of photoaffinity labeled insulin receptor proteins by linear polyacrylamide gradient gel electrophoresis under non-denaturing conditions. *FEBS Letters* 113:189-192, 1980.
74. Laemmli, U. K.: Cleavage of structural proteins during assembly of the head of bacteriophage T4. *Nature (London)* 227:680-685, 1970.

75. Lang, U., Kahn, C. R. and Chrambach, A.: Characterization of the insulin receptor and insulin-degrading activity from human lymphocytes by quantitative polyacrylamide gel electrophoresis. *Endocrinology* 106:40-49, 1980.
76. Lang, U., Kahn, C. R. and Harrison, L.: Subunit structure of the insulin receptor of the human lymphocyte. *Biochem.* 19:64-70, 1980.
77. Larner, J., Galasko, G., Cheung, K., DePaoli-Roach, A. Huang, L., Daggy, P. and Kellogg, J.: Generation by insulin of a chemical mediator that controls protein phosphorylation and dephosphorylation. *Science* 206:1408-1410, 1979.
78. Lawrence, J. and Larner, J.: Activation of glycogen synthase in rat adipocytes by insulin and glucagon involves glucose transport and phosphorylation. *J. Biol. Chem.* 253:2104-2113, 1979.
79. LeMarchand-Brustel, Y., Jeanrenaud, B. and Freychet, P.: Insulin binding and effects in isolated soleus muscle of lean and obese mice. *Am. J. Physiol.* 234:E348-E358, 1978.
80. Levine, R.: Insulin action: 1948-1980. *Diabetes Care* 4:38-44, 1981.
81. Livingston, J., Purvis, B. and Lockwood, D.: Insulin-dependent regulation of insulin-sensitivity of adipocytes. *Nature* 273:394-396, 1978.
82. Loh, H. and Law, P. Y.: The Role of membrane lipids in receptor mechanisms. *Ann. Rev. Pharmacol. Toxicol.* 20:201-234, 1980.
83. Massague, J. and Czech, M. P.: Role of disulfides in the subunit structure of insulin receptor. *J. Biol. Chem.* 257:6729-6738, 1980.
84. Massague, J., Pilch, P. F. and Czech, M. P.: Electrophoretic resolution of three major insulin receptor structures with unique subunit stoichiometries. *Proc. Natl. Acad. Sci. USA* 77:7137-7141, 1980.
85. Maturo, J. and Hollenberg, M. D.: Insulin receptor: interaction with nonreceptor glycoprotein from liver cell membrane. *Proc. Nat. Acad. Sci. USA* 75:3070-3074, 1978.
86. Maugh, T. H.: Hormone receptors: new clues to the cause of diabetes. *Science* 193: 220-223, 1976.
87. Maurer, P., Moskowitz, M. A., Levine, L. and Melamed, E.: The synthesis of prostaglandins by bovine microvessels. *Prostaglandins and Med.* 4:153-161, 1980.
88. Meezan, E., Brendel, K. and Carlson, E. C.: Isolation of a purified preparation of metabolically active retinal blood vessels. *Nature* 251:65-67, 1974.

89. Meezan, E. and Pillion, D. J.: Direct demonstration that cerebral and retinal microvessels respond to insulin. *Fed. Proc.* 40:366, 1981.
90. Misbin, R., O'Leary, J. P. and Pulkkinen, A.: Insulin receptor binding in obesity: A Reassessment. *Science* 205:1003-1004, 1979.
91. Mrsulja, B. B. and Djuricic, B. M.: Biochemical characteristics of cerebral capillaries. *Adv. Exp. Med. Biol.* 216:29-43, 1980.
92. Olefsky, J. M.: Decreased insulin binding to adipocytes and circulating monocytes from obese subjects. *J. Clin. Invest.* 57:1165-1172, 1976.
93. Olefsky, J. M. and Chang, H.: Further evidence for functional heterogeneity of adipocyte insulin receptors. *Endocrinology* 104: 462-466, 1979.
94. Pacold, S. T. and Blackard, W. G.: Central nervous system insulin receptors in normal and diabetic rats. *Endocrinology* 105:1452-1457, 1980.
95. Pardridge, W. M.: Tryptophan transport through the blood-brain barrier. *Life Sci.* 25, 1519-1528, 1979.
96. Peacock, M. L., Bar, R. S. and Goldsmith, J.: Interactions of insulin with bovine endothelium. *Metabolism* 31: 52-56, 1982.
97. Peters, F. and Pingaud, A.: Numerical analysis of binding studies: a direct procedure avoiding the pitfalls of a Scatchard analysis of equilibrium data for unknown binding models. *Int. J. Biomed.* 10: 401-415, 1979.
98. Pilch, P. and Czech, M.: The subunit structure of the high affinity insulin receptor - evidence for a disulfide-linked receptor complex in fat cell and liver plasma membrane. *J. Biol. Chem.* 255:1722-1731, 1980.
99. Pillion, D. J. and Czech, M.: Antibodies against intrinsic adipocyte plasma membrane proteins activate D-glucose transport independent of interaction with insulin binding sites. *J. Biol. Chem.* 253:3761-3764, 1978.
100. Pillion, D. J., Haskell, J. F. and Meezan, E.: Cerebral cortical microvessels: An insulin-sensitive tissue. *Biochem. Biophys. Res. Commun.* 104:686-692, 1982.
101. Pollet, R. J., Haase, B. and Standaert, M.: Characterization of detergent-solubilized membrane proteins. *J. Biol. Chem.* 256:12128-12126, 1981.
102. Pollet, R. J. and Levey, G.: Principles of membrane receptor physiology and their application to clinical medicine. *Annal. Intern. Med.* 92:63-680, 1980.

103. Pollet, R. J., Kempner, E. S., Standaert, M. L. and Haase, B. A.: Structure of the insulin receptor of the cultured human lymphoblastoid cell IM-9. *J. Biol. Chem.* 257:894-898, 1982.
104. Prior, R. L. and Smith, S. B.: Hormonal effects on partitioning of nutrients for tissue growth: Role of insulin. *Fed. Proc.* 41: 2545-2549, 1982.
105. Raizada, M. K., J. W. Yang and Fellows, R. F.: Binding of [¹²⁵I]-insulin to specific receptors and stimulation of nucleotide incorporation in cells cultured from rat brain. *Brain Research* 200:389-400, 1980.
106. Reaven, G. M. and Olefsky, J. M.: Role of insulin resistance in the pathogenesis of hyperglycemia. In *Diabetes, obesity and vascular disease Vol. 2.* Katzen, H. M. and Mahler, R. J., Eds., Washington, Hemisphere Pub. Corp., 1978, 230-331.
107. Rechler, M., Schilling, E., King, G., Fioroli, F., Rosenberg, A., Higa, O., Podskalny, J., Greenfeld, C., Nissley, S. P., and Kahn, C. R.: Receptors for insulin and insulin-like growth factors in disease. In *Receptors for neurotransmitters and peptide hormones*, Pepeu, G., Kuhar, M. J., and Enna, S. J., Eds., New York, Raven Press, 1980, 489-497.
108. Robinson, C. A., Boshell, B. and Reddy, W.: Insulin binding to plasma membranes. *Biochim. Biophys. Acta* 290:84-91, 1972.
109. Rodbard, D.: Mathematics of hormone receptor interaction. In *Receptors for reproductive hormones.* O'Malley, B. and Means, A. P., Eds., New York, Plenum Press, 1973, pp. 289-326.
110. Rodbard, D.: Editorial-Negative cooperativity: A positive finding. *Am. J. Physiol.*, 6:E203-E205, 1979.
111. Roger, L. S. and Fellows, R. E.: Stimulation of ornithine decarboxylase activity by insulin in developing rat brain. *Endocrinology* 106:619-625, 1980.
112. Roth, J.: Insulin receptors in diabetes. *Hospital Practice*, 94-103, 1980.
113. Roth, G. S.: Receptor changes and the control of hormone action during Aging. *Adv. in Pathobiol.* 7:228-237, 1980.
114. Seals, J. and Jarett, L.: Activation of pyruvate dehydrogenase by direct addition of insulin to an isolated plasma membrane mitochondria mixture: Evidence for generation of insulin's second messenger in a subcellular system. *Proc. Natl. Acad. Sci. USA* 77:77-81, 1980.

115. Shanahan, M. and M. Czech, Partial purification of the d-glucose transport system in rat adipocyte plasma membrane. *J. Biol. Chem.* 252:6554-6561, 1977.
116. Sokoloff, L.: Mapping of local cerebral functional activity of measurement of local cerebral glucose utilization with [^{14}C]-deoxyglucose. *Brain* 102:653-668, 1979.
117. Soman, O. and DeFronzo, R.: Direct evidence for down regulation of insulin receptors by physiologic hyperinsulinemia in man. *Diabetes* 29:159-163, 1980.
118. Steiner, D. F.: Insulin today. *Diabetes* 26:322-340, 1977.
119. Stout, R. W.: Diabetes and atherosclerosis - the role of insulin. *Diabetolog.* 16:141-150, 1979.
120. Sutherland, E. W.: Studies on the mechanism of hormone action. *Science* 177:401-403, 1972.
121. Szabo, O. and Szabo, A. J.: Evidence for an insulin-sensitive receptor in the central nervous system. *Am. J. Physiol.* 223:1349-1353, 1972.
122. Tamborlane, W. K., Puklin, J. E., Bergman, M., Verdonk, C., Rudolf, M. C., Felig, P., Genel, M. and Sherwin R: Long term improvement of metabolic control with insulin pump does not reverse diabetic microangiopathy. *Diabetes Care* 5:58-64, 1982.
123. Van Houten, M. and Posner, B. I.: Insulin binds to brain vessels in vivo. *Nature* 282:623-628, 1979.
124. Varandani, P. T., Organisciak, D. T. and Nafz, M. A.: The occurrence of glutathione-insulin transhydrogenase in the retina. *Invest. Ophthalmol. Visual. Sci.* 22:715-719, 1982.
125. Verlangieri, A. J. and Sestito, J.: Effect of insulin on ascorbic acid uptake by heart endothelial cells: Possible relationship to Retinal Atherogenesis. *Life Sciences* 29:5-9, 1981.
126. Vigneri, R., Pezzino, V., Cohen, D., Pliano, N. B., Wong, K. Y., Headek, G., Jones, A. and Goldfine, I. D. Regulation of rat liver plasma membrane and intracellular insulin binding sites during diabetes, liver regeneration and hyperinsulinism: radiolabeled hormone binding and electron microscopic autoradiography studies. In *Receptors for neurotransmitters and peptide hormones*. Pepeu, G., Kuhar, M. J., and Enna, S. J., Eds., New York, Raven Press, 1980, pp. 499-506.
127. Waelbroeck, M, Obberghen, E. V. and DeMeyts, P.: Thermodynamics of the interaction of insulin with its receptor~ *J. Biol. Chem.* 254:7736-7740, 1979.

128. Wang, J. H. and Desai, R.: Modulator binding protein: bovine brain protein exhibiting the Ca^{++} dependent association with the protein modulator of cyclic nucleotide phosphodiesterase. *J. Biol. Chem.* 252:4175-4184, 1977.
129. Weber, K. and Osborn, M.: The reliability of molecular weight determination by dodecyl sulfate polyacrylamide gel electrophoresis. *J. Biol. Chem.* 244:4406-4412, 1969.
130. Williams, T. F.: Diabetes mellitus. *Clinics in Endocrinol. and Metab.* 10:179-194, 1981.
131. Wisher, M., Baron, M., Jones, R. and Sonksen, P.: Photoreactive insulin analogues used to characterize the insulin receptor. *Biochem. Biophys. Res. Commun.* 92:492-498, 1980.
132. Yalow, R. S. and Berson, S. A.: Immunoassay of endogenous plasma insulin in man. *J. Clin. Invest.* 39:1157, 1960.
133. Yip, C. C., Moule, M. L. and Yeung, C. W. T.: Characterization of insulin receptor subunits in brain and other tissues by photoaffinity labeling. *Biochem. Biophys. Res. Commun.* 96:1671-1678, 1980.
134. Yip, C. C., Moule, M. L. and Yeung, C. W. T.: Characterization of the functional insulin receptor. In *Etiology and pathogenesis of insulin-dependent diabetes mellitus*, Martin, J. M. and Holland, F. J., Eds. Raven Press, New York, 1981, pp. 79-86.
135. Yip, C., C. Yeung and Moule, M.: Photoaffinity labeling of insulin receptor proteins of liver plasma membrane preparations. *Biochem.* 19:70-76, 1980.
136. Zeleznik, A. J. and Roth, J.: Plasma membrane receptors for peptide hormones: *in vivo* role as reservoir for the circulating hormone. Abstract No. 27, 58th Endocrine Society Meeting, 1976.
137. Zetter, B. R.: The Endothelial Cells of large and small blood vessels. *Diabetes* 30:24-28, 1981.

GRADUATE SCHOOL
UNIVERSITY OF ALABAMA IN BIRMINGHAM
DISSERTATION APPROVAL FORM



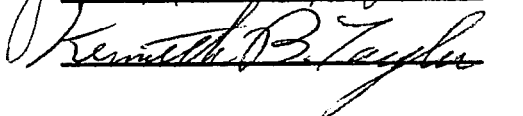
Name of Candidate Joyce Fehl Haskell


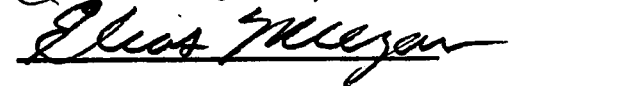
Major Subject Biochemistry

Title of Dissertation Characterization of the Insulin Receptor in
Isolated Bovine Cerebral and Retinal Microvessels

Dissertation Committee:

 Chairman

Director of Graduate Program 

Dean, UAB Graduate School 

Date 12/3/82